



5-2010

Computational Circle Packing: Geometry and Discrete Analytic Function Theory

Gerald Lee Orick
orick@math.utk.edu

Recommended Citation

Orick, Gerald Lee, "Computational Circle Packing: Geometry and Discrete Analytic Function Theory." PhD diss., University of Tennessee, 2010.
http://trace.tennessee.edu/utk_graddiss/731

To the Graduate Council:

I am submitting herewith a dissertation written by Gerald Lee Orick entitled "Computational Circle Packing: Geometry and Discrete Analytic Function Theory." I have examined the final electronic copy of this dissertation for form and content and recommend that it be accepted in partial fulfillment of the requirements for the degree of Doctor of Philosophy, with a major in Mathematics.

Kenneth Stephenson, Major Professor

We have read this dissertation and recommend its acceptance:

Charles Collins, Stefan Richter, Thomas Papenbrock

Accepted for the Council:
Carolyn R. Hodges

Vice Provost and Dean of the Graduate School

(Original signatures are on file with official student records.)

To the Graduate Council:

I am submitting herewith a dissertation written by Gerald Lee Orick Jr. entitled "Computational Circle Packing: Geometry and Discrete Analytic Function Theory." I have examined the final electronic copy of this dissertation for form and content and recommend that it be accepted in partial fulfillment of the requirements for the degree of Doctor of Philosophy, with a major in Mathematics.

Kenneth Stephenson

Major Professor

We have read this dissertation
and recommend its acceptance:

Charles Collins

Stefan Richter

Thomas Papenbrock

Accepted for the Council:

Carolyn R. Hodges

Vice Provost and Dean of the Graduate School

(Original signatures are on file with official student records.)

Computational Circle Packing: Geometry and Discrete Analytic Function Theory

A Dissertation
Presented for the
Doctor of Philosophy
Degree
The University of Tennessee, Knoxville

Gerald Lee Orick Jr.
May 2010

Abstract

Geometric Circle Packings are of interest not only for their aesthetic appeal but also their relation to discrete analytic function theory. This thesis presents new computational methods which enable additional practical applications for circle packing geometry along with providing a new discrete analytic interpretation of the classical Schwarzian derivative and traditional univalence criterion of classical analytic function theory. To this end I present a new method of computing the maximal packing and solving the circle packing layout problem for a simplicial 2-complex along with additional geometric variants and applications. This thesis also presents a geometric *discrete Schwarzian* quantity whose value is associated with the classical Schwarzian derivative. Following Hille, I present a characterization of circle packings as the ratio of two linearly independent solutions of a discrete difference equation taking the *discrete Schwarzian* as a parameter. This characterization then gives a discrete interpretation of the classical univalence criterion of Nehari in the circle packing setting.

Contents

1	Introduction	1
1.1	Circle Packings	1
1.2	Computational Challenges	2
1.3	An Alternate View	3
1.4	New Circle Packing Results	4
2	Geometry of Circle Packings	5
2.1	Preliminary Triangle Geometry	5
2.2	Circle Packings	6
2.3	Dual Packings	8
2.4	Circle Packing Quadrilaterals	8
2.5	Face Paths	9
2.6	Interior Triangulations	10
2.7	Circle Packing Maps	11
2.8	Matrix Representations of Möbius Maps and Circles	13
2.9	Directed Möbius Edge Derivative	15
2.10	Harmonic Functions and Circle Packing Weights	16
2.11	Tutte's Theorem for Planar Graph Embeddings	19
2.12	General Triangulations and Circle Packing Geometries	20
3	Functions on Circle Packings	22
3.1	Convergence on Compact Sets	22
3.2	Linear Derivative	24
3.3	Schwarzian Derivative	24
3.4	Face Linear Systems	30
3.5	Path Mappings and Deformation Metrics	32
3.6	Functions with Specified Schwarzian Derivative	33
3.7	Circle Packing Quotient Theorem	35
3.8	A Discrete Hille Condition	37

4 Univalence Results	41
4.1 Zeros of Circle Packing Maps	41
4.2 Zeros and Univalence	42
4.3 Some Results on Zeros of Circle Packing Maps	44
4.4 The Results of Nehari	46
4.5 Some Notes on Schlicht Circle Packing Maps	49
5 Linearized Circle Packing Algorithm	51
5.1 Abstract	51
5.2 Introduction	51
5.3 Fundamental Global Maximal Packing Geometry	57
5.4 Linearized Circle Packing Algorithm	59
5.4.1 STEP 1: Boundary Layout	60
5.4.2 STEP 2: Interior Layout	60
5.4.3 STEP 3: Effective Radii	61
5.4.4 Discussion of Convergence	61
5.4.5 Error Estimation	62
5.5 Geometry and Weights	63
5.6 Conclusion	64
6 Experiments	69
6.1 Circle Packing Function Approximation	69
6.2 Schwarzian Derivative	69
6.3 Alternate Schwarzian Approximation	71
6.4 The Sine Function	72
6.5 The Koebe Function	72
7 Maximal Packing Convergence	78
7.1 Measures of Convergence	78
7.2 Example Packings	79
7.3 Convergence Data	79
Bibliography	81
Vita	84

List of Figures

1.1	The Apollonian Gasket	2
1.2	Gramazio & Kohler Circle Packing Facade	4
2.1	Fundamental Triangle Geometry	6
2.2	Circle Packing Flower or Cycle of Circles.	8
2.3	A Circle Packing and its Dual	9
2.4	Circle Packing Quadrilateral	9
2.5	Circle Packing Quadrilateral Edge Intersection Circle.	10
2.6	Circle Packing Minimal Paths.	11
2.7	A Circle Packing Interior Triangulation.	12
2.8	Quadrilateral Skew Error	21
3.1	Example face linear Systems.	32
3.2	Example Interior Face Linear Systems.	40
5.1	Triangulation and Circle Packings.	52
5.2	Spherical circle packing image of MRI data.	53
5.3	Maximal packings of the disc and the sphere.	54
5.4	Triangular Face Matching.	56
5.5	Circular Sector Centroids.	57
5.6	Puncturing a Spherical Maximal Packing.	58
5.7	Maximal Packing Geometry.	59
5.8	Modification of Disc Packing Combinatorics.	65
5.9	Circle Packing Algorithm.	65
5.10	Example Maximal Packing Sequence.	66
5.11	Inscribing Boundary Circles.	66
5.12	Effective Radii Computation.	66
5.13	Fixed Boundary Conditions for Three Boundary Vertices.	67
5.14	Circle Packing Error Measurement.	67
5.15	Alternate Circle Packing Weight Construction.	67
5.16	Packings with Generic Boundary.	68

6.1	Function Approximation for the Exponential function	73
6.2	Function Approximation for the Sine function	73
6.3	Function Approximation for the Koebe function	73
6.4	Function Approximation over a maximal packing	74
6.5	Edge Schwarzian Approximation for Exponential Map	74
6.6	Exponential Map over Disc Domain	75
6.7	Face Averaged Schwarzian Approximation for the Sine Function.	76
6.8	Koebe Map Range over Hexagonal Domain.	77
6.9	Face Averaged Schwarzian Approximation for the Koebe Function.	77
7.1	Example Three Boundary Conversion.	78
7.2	Example Circle Packings for Convergence Test.	79
7.3	Convergence Data for Example Packings	80
7.4	Convergence Data for Modified Example Packings	80

Chapter 1

Introduction

Circle patterns have been a subject of aesthetic interest and mathematical study from the time of ancient Greece. The Greek mathematician Apollonius of Perga considered the geometric problem of finding a solution circle mutually tangent to three given circles, a problem which became known as the *Apollonian Circle Problem*. These patterns form the basis of the *Leibniz packing* or *Apollonian Gasket*, an infinitely recursive collection of mutually tangent triples of circles contained in a bounding disc which serves as our first example of a *circle packing*(figure 1.1). The geometry of circle patterns has been prominent in the study of classical geometry through the centuries. Modern texts such as Schwerdtfeger's *Geometry of Complex Numbers* (Schwerdtfeger, 1979) provide a mechanism for expressing many such relations in terms of projective geometric matrix expressions. We will focus on *circle packings* which are patterns of circles whose interiors are locally disjoint and which obey a well defined tangency pattern defined by a simply connected triangulation, more specifically a simply connected simplicial 2-complex.

1.1 Circle Packings

Circle packing geometry provides a tool to both visualize and study the nature of classical analytic functions. In the 1980's Thurston observed that circle packings would converge uniformly over compact set to classical analytic functions under successively refined domain packings, a result which was quickly proven by Rodin and Sullivan (Rodin and Sullivan, 1987). This initial success coupled with the observation that the magnitude of the derivative was related to the ratio of associated radii in a circle packing map lead to further extensions of discrete analytic function theory in the context of circle packings. To this end corresponding circle packing statements for several fundamental concepts of analytic function theory were discovered. These advances included a *Discrete Riemann mapping Theorem*, a *Discrete Schwarz Lemma* and natural definitions of *Discrete Blaschke Products*

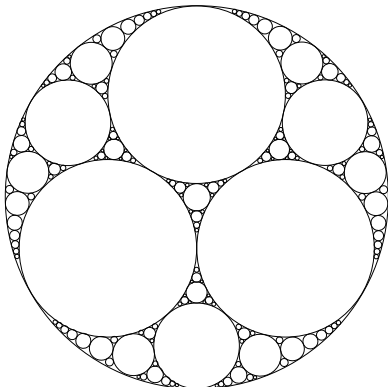


Figure 1.1: The Apollonian Gasket

for example (Dubejko, 1993). This thesis presents a new method for computing circle packing geometries and further extends the discrete analytic foundation in the circle packing setting by introducing a *discrete Schwarzian derivative* quantity which has many properties similar to the traditional Schwarzian derivative. The discrete Schwarzian derivative leads to new results concerning the zeros for our discrete analytic (circle packing) functions and opens the door to a circle packing interpretation univalence criterion of Nehari which will be more fully studied in future work.

1.2 Computational Challenges

Advances in circle packing and discrete analytic function theory lead to interest in applications such as medical cortical imaging (Hurdal et al., 1999) and graph representation schemes but implementations were limited by computational considerations. Thurston's original algorithm of iterating radii to match the desired tangency conditions effectively gave solution radii for finite packings. However geometrically realizing the resulting circle packing layout remained a challenge due to severe sensitivity of the layout schemes to the accuracy of the computed radii (Stephenson, 2005b). These difficulties were especially evident in the complex combinatorics met in practice such as those produced from medical MRI brain imaging.

This thesis presents a new approach to circle packing computations and procedures which effectively solves the layout problem while simultaneously providing a significantly improved method for radii computation. This new computational method is iterative and employs repeated solutions to a discrete harmonic Dirichlet problem to simultaneously estimate euclidean circle centers and circle radii. The appropriate harmonic weights end up being locally equivalent to the random walk edge conductances in Dubejko's work (Dubejko and Stephenson, 1995).

The principal algorithm applies in the maximal packing case and can be empirically

demonstrated to converge in nominal cases, though no complete characterization of convergence conditions is available. It is possible that a physics based interpretation may lead to a physics/harmonic function based convergence condition, especially in the simplified fixed three vertex boundary case. This thesis presents some initial steps toward a convergence proof as well as a physical interpretation in terms of physical film tension on a triangulated surface which may also lead to a convergence proof.

This new approach opens the door to many applications including further advances in brain scan imaging (Hurdal and Stephenson, 2004) and image processing applications presented in the appendix. This image processing algorithm has been used in an architectural setting by Gramazio & Kohler *Architecture and Digital Fabrication*, Switzerland, to develop geometric circle packing facades for the proposed building complex shown in figure 1.2.

1.3 An Alternate View

Previous circle packing research has focused on expanding the foundations of discrete analytic function theory in parallel with classical theory. This thesis aims to exploit the geometric nature of circle patterns to further extend the notion of a discrete analytic function theory and presents a significant step forward by introducing the circle packing *discrete Schwarzian* which serves as a discrete quantity similar to the classical Schwarzian derivative.

Traditional circle packing research has emphasized the combinatorics and the associated circle radii. This paper presents an alternate view for discrete analytic function aspects. The ratio of associated radii for a circle packing map has been shown to correspond to the magnitude of the local derivative – one goal is to obtain a quantity related to the true complex valued derivative associated with the map. A complex valued derivative quantity can be obtained by considering the dual packing formed by the face incircles. An interesting open problem is to quantify the nature of the convergence of these first derivatives to the traditional derivative under suitably refined packings, especially in light of previous results by He and Schramm. In our study we are most interested in the invariant properties of the Schwarzian derivative, a quantity that can be developed in the circle packing setting by considering the dual circle packing.

The dual packing representation also allows for a circle packing map to be described in terms of a *face Möbius system* which maps the domain face circles onto the range face circles, appropriately mapping the edge intersection points. These face Möbius mappings allow for the definition of a *circle packing Möbius edge derivative* which is invariant under post composition by an automorphism of the plane, one of the original motivations for the definition of the Schwarzian derivative (Nehari, 1949), and serves as the basis for the circle packing *discrete Schwarzian*.

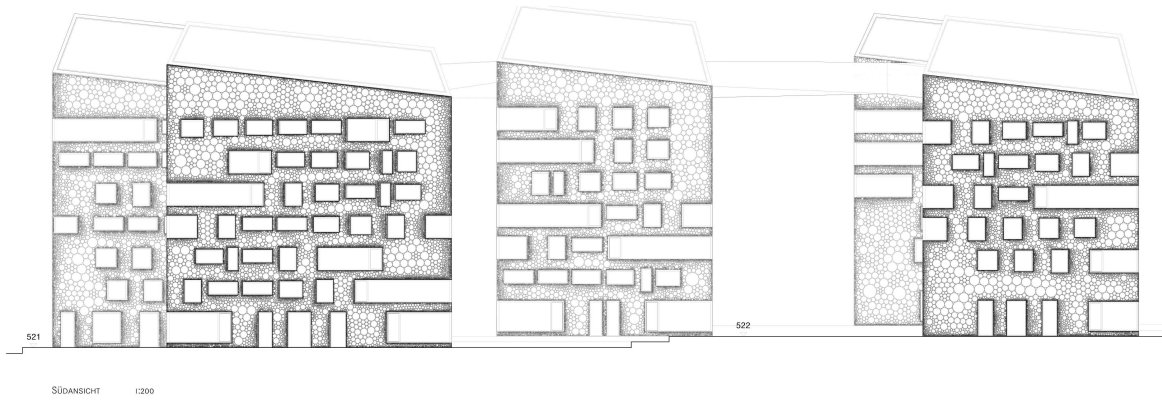


Figure 1.2: Gramazio & Kohler Circle Packing Facade

1.4 New Circle Packing Results

The circle packing *discrete Schwarzian* parallels the traditional Schwarzian derivative in more than just a superficial manner. This thesis presents a new characterization theorem for circle packings which is the discrete circle packing analogue of Hillie's decomposition of an analytic function as the ratio of two linearly independent solutions to the second order differential equation

$$y'' + p(z)y = 0 \quad (1.1)$$

where $p(z)$ is half the Schwarzian derivative at the specified point. This fundamental circle packing result is then employed to translate the traditional univalence criteria of Nehari into their circle packing equivalents (Hille, 1922)(Nehari, 1949).

This translation of Nehari's univalence criteria leads to local circle packing expressions which describe the discrete quantization differences between the circle packing and traditional cases.

Chapter 2

Geometry of Circle Packings

2.1 Preliminary Triangle Geometry

Circle packings can be decomposed into a tiling of triangles, ordered triples of points in \mathbb{C} , which are joined to form an oriented triangulation belonging to one of the the disc \mathbb{D} , the plane \mathbb{C} or the Riemann sphere \mathbb{P} . The orientation convention for triangles takes a counter-clockwise ordering of the vertexes. Each triangle is uniquely determined by a triple of real radii as specified in the following elementary remark.

Remark 2.1.1. For any triangle T in \mathbb{C} given as an oriented triple (z_1, z_2, z_3) there is a corresponding unique triple of positive real valued radii, (r_1, r_2, r_3) , such that the edge lengths of T are determined by the sums of the respective vertex radii; and conversely any such triple of positive real valued radii (r_1, r_2, r_3) determines a unique triangle T up to rotation and translation.

Triangle mensuration formulas have been widely tabulated, a few useful in the context of circle packings are recorded here (Beyer, 1987) (figure 2.1).

Remark 2.1.2. In the following let \mathbb{A} = area, ρ = radius of the inscribed circle, R = the radius of the circumscribed circle. Let a, b and c be the triangle side lengths and A, B and C the corresponding vertex angles for a triangle and let s be the semi-perimeter $\frac{1}{2}(a+b+c)$.

- *Law of cosines:*

$$c^2 = a^2 + b^2 - 2ab \cos C \quad (2.1)$$

- *Area (Huron's formula):*

$$\mathbb{A} = \sqrt{s(s-a)(s-b)(s-c)} \quad (2.2)$$

- *Inscribed circle radius:*

$$\rho = \mathbb{A}/s \quad (2.3)$$

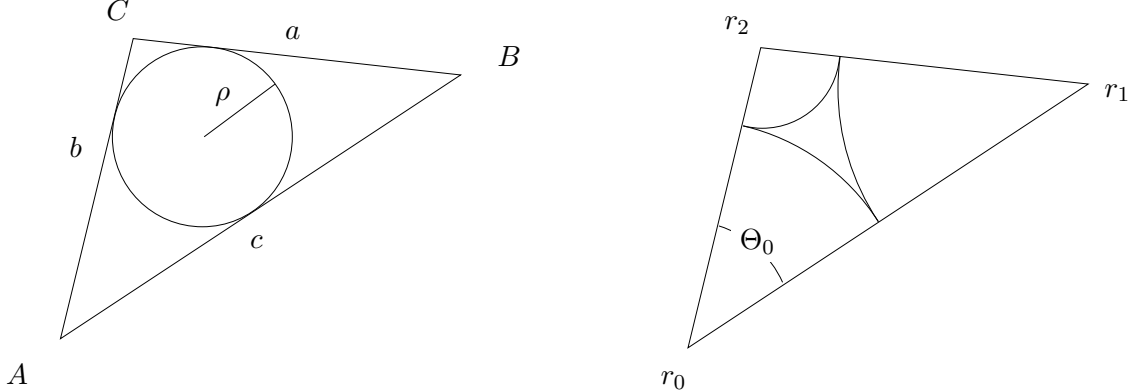


Figure 2.1: Fundamental Triangle Geometry

- *Circumscribed circle Radius:*

$$R = \frac{abc}{4\mathbb{A}} \quad (2.4)$$

There are convenient forms of the above equations when the triangle side lengths are specified by vertex radii.

Remark 2.1.3. Let T be a triangle specified by the triple of radii (r_0, r_1, r_2) then the interior angle at the initial vertex corresponding to r_0 is

$$\Theta_0 = \cos^{-1} \left(1 - \frac{2r_1 r_2}{(r_0 + r_1)(r_0 + r_2)} \right), \quad (2.5)$$

the triangle area by

$$\mathbb{A} = \sqrt{(r_0 + r_1 + r_2) r_0 r_1 r_2} = \sqrt{\sum r_j \prod r_j}, \quad (2.6)$$

and the incircle radius as

$$\rho = \sqrt{\frac{r_0 r_1 r_2}{r_0 + r_1 + r_2}} = \sqrt{\frac{\prod r_j}{\sum r_j}}. \quad (2.7)$$

2.2 Circle Packings

A *circle packing*, \mathcal{P} , is a configuration of circles with a specified pattern of tangencies. The tangency graph for a Circle Packing is usually specified as the simplicial 2-complex, $K = (\mathcal{V}, \mathcal{E}, \mathcal{F})$, serving as the triangulation of an oriented and simply connected surface. A *circle packing geometry* for a specified complex K is denoted \mathbf{P} when the combinatoric structure is clear by context and is then a collection of circles in the appropriate geometry (euclidean, hyperbolic or spherical) each corresponding to a single vertex of K , having a specified radius and center and satisfying the tangency requirements. We will let ∂V and V_o denote the boundary and interior vertexes of K respectively, and let ∂v will denote the

cycle of vertexes about an interior vertex $v \in V_o$ or the chain of neighboring vertexes about a boundary vertex $v \in \partial V$, taking the conventional counter clockwise ordering.

Circle packings are comprised of triples of circles which determine triangles on centers. The converse is also present, namely that each triangle is uniquely specified by a triple of circles, with radii determining the triangle up to translation and rotation. Triples of circles are then arranged to form *flowers* or *cycles* of circles about a central circle which locally meet the specified tangency conditions (figure 2.2).

A *radii label* for a given combinatoric structure K is an assignment $\mathbf{R} : \mathcal{V} \rightarrow \mathbb{R}^+$ of circle radii which potentially determine a circle packing. A circle packing is specified (up to rotations and translations) by a radii label which satisfy the *angle sum* condition about each interior vertex, namely that the radius for each vertex v is chosen so that the neighboring cycle of vertex circles, ∂v , extend through an angle which is an integer multiple of 2π , with the multiple determined by the branching about the central vertex v . The angle sum Θ_v about an interior vertex is the sum of the individual neighboring interior face angles θ_f about the central vertex and can be computed simply by the law of cosines:

$$\Theta_v = \sum_{1 \leq k \leq |\partial v|} \theta_k = \sum_{1 \leq k \leq |\partial v|} \cos^{-1} \left(1 - \frac{2r_k r_{k+1}}{(r_v + r_k)(r_v + r_{k+1})} \right) \quad (2.8)$$

where θ_k are the interior angles of the neighboring faces, r_0 is the central radius and $\{r_1, r_2, \dots, r_{|\partial v|}\}$ is the cycle of neighboring vertex radii. A radii label satisfying the angle sum condition for K is called a *circle packing label*.

A *circle packing geometry*, \mathbf{P} , then identifies a specific circle packing geometry in \mathbb{C} associated with the underlying combinatoric structure, K , and radii label, \mathbf{R} . We will denote the vertex positions by $\mathbf{Z} = \{z_v : v \in \mathcal{V}\}$. The faces of the resulting triangulation will be denoted by \mathbf{F} with the *carrier* of \mathbf{P} representing the union of all triangular faces of \mathbf{P} . We will use $d_{\vec{e}}$ and $\zeta_{\vec{e}} = d_{\vec{e}}/|d_{\vec{e}}|$ to denote directed edge displacement and direction respectively and in addition denote the *edge intersection points* located at the tangency points between neighboring circles by z_e .

It is well known that every simply connected simplicial 2-complex K has an essentially unique maximal packing that is one of: the *disc*, the *sphere*, or the *complex plane* as given in the following fundamental theorem for circle packings (Beardon and Stephenson, 1990).

Theorem 2.2.1. *Let K be a simply connected complex with label \mathbf{R} . Let \mathbb{G} be one of the sphere \mathbb{P} , the plane \mathbb{C} , or the disc \mathbb{D} , depending on the geometry of \mathbf{R} . Then there exists a maximal packing \mathbf{P} in \mathbb{G} determined by the radii label \mathbf{R} if and only if \mathbf{R} is a maximal packing label. The circle packing \mathbf{P} is unique up to isometries of \mathbb{G} .*

We will be primarily interested in the hyperbolic case where the maximal packing is a unit disc.

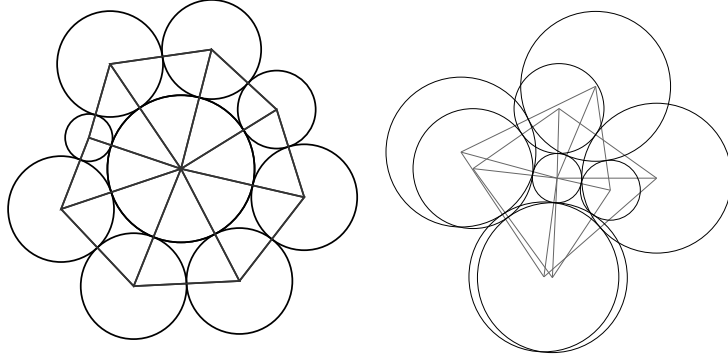


Figure 2.2: Circle Packing Flower or Cycle of Circles.

Shown (a) without branching, and (b) with a first order branch point at the central vertex.

2.3 Dual Packings

A circle packing is composed triangular faces determined by successive triples of radii (figure 2.3). This construction leads to a natural *dual circle packing* composed of the triangular face incircles. A basic proposition of Euclidean geometry states that a triangle incircle intersects the edges at the edge intersection points. The associated combinatoric dual geometric edge are perpendicular to their respective combinatoric geometric edges. We denote the edge displacement vectors and directions for the combinatoric dual geometric edges by $\delta_{\vec{e}}$ and $\eta_{\vec{e}}$ respectively for $\vec{e} \in \vec{\mathcal{E}}$. The vertexes of the dual circle packing, corresponding to the dual circle centers, will be denoted $\mathbf{W} = \{w_f : f \in \mathcal{F}\}$. We will take the convention that $\delta_{\vec{e}} = id_{\vec{e}}$ and $\eta_{\vec{e}} = i\zeta_{\vec{e}}$ and use the term *combinatorial dual* to denote the collection of a circle packings combinatoric dual geometric edges.

2.4 Circle Packing Quadrilaterals

It will be convenient to define a *circle packing quadrilateral* consisting of two neighboring faces in a circle packing, each sharing a common directed edge \vec{e} . We will take the notation $g \uparrow_{\vec{e}} f$ to indicate that the directed dual edge $\delta_{\vec{e}}$ is oriented towards the face g from the face f as in figure 2.4. This quadrilateral consists of four vertexes and contains five intersection points, including one along the common edge. A simple but useful proposition gives a geometric relation between the edge intersection points.

Proposition 2.4.1. *The edge intersection points on the boundary of a circle packing quadrilateral lie on a common circle.*

The proof relies on the fact that circles are preserved under Möbius maps and that the dual circles intersect the primary circles in a perpendicular fashion. This proposition can be

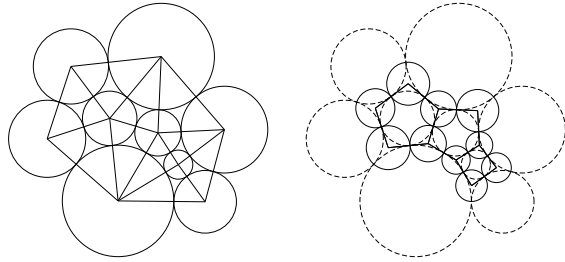


Figure 2.3: A Circle Packing and its Dual

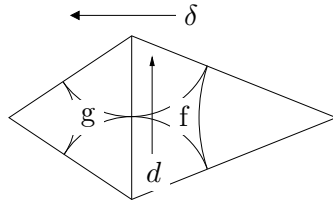


Figure 2.4: Circle Packing Quadrilateral
determined by $g \uparrow_e f$.

seen by translating the central edge intersection to the origin and then applying a Möbius mapping to obtain dual circles of equal radius so that the desired circle through the four boundary edge intersection points can then be constructed by symmetry as in figure 2.5.

2.5 Face Paths

Two faces f and $g \in \mathcal{F}$ are *neighboring*, denoted $f \sim g$, if they share a common edge. An *abstract face path*, $\Gamma = \{f_0, f_1, \dots, f_N\}$, in a triangulation K is a sequence of neighboring faces in \mathcal{F} so that $\Gamma = \{f_0, f_1, \dots, f_N\}$ with $f_{k-1} \sim f_k$ for $k = 1, \dots, N$; f_1, \dots, f_{N-1} are the *interior faces* of the abstract path Γ while f_0 and f_1 are the *terminal faces* of Γ . We next define a *face path* joining two specified points in the carrier of a given \mathbf{P} .

Definition 2.5.1 (Face Path). Let \mathbf{P} be a specified circle packing and let u and v be points in the carrier of \mathbf{P} , and let $\Gamma = \{f_0, f_1, \dots, f_N\}$ be an abstract face path with u contained in f_0 and v contained in f_1 . We define a *face path* in \mathbf{P} joining u and v along Γ to be the path $\gamma : [0, 1] \rightarrow \text{carrier}(\mathbf{P})$ constructed so that the trace of γ in an interior face f of Γ consists of the two geodesic arcs joining the dual circle center with the two bounding edge intersection points for f with respect to the Γ , and the trace on a terminal face consists of at most two geodesic arcs joining the terminal point with the respective edge intersection point (either a single geodesic segment joining the path endpoint to the terminal edge intersection point or having two geodesic segments joining the path endpoint, terminal face dual circle center and the respective edge intersection point). This *face path* $\gamma : [0 : 1] \rightarrow \text{carrier}(\mathbf{P})$ joining u and v with $\gamma(t)$ is parametrized proportional to the euclidean arc length in the carrier.

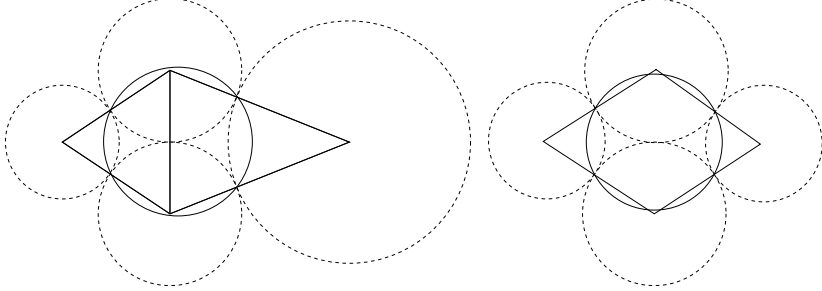


Figure 2.5: Circle Packing Quadrilateral Edge Intersection Circle.
Geometric construction of circle through quadrilateral edge intersection points.

A face path γ joining u and v is said to be a *minimal face path* when the arc length of γ is minimized in the appropriate metric (figure 2.6) among all face paths connecting u and v .

In the euclidean metric we can translate the image of γ so that $\gamma(0) = -\gamma(1)$ to obtain a *reference face path* joining u and v . In the hyperbolic case we can obtain a corresponding *reference hyperbolic face path* joining u and v by composition with an appropriate automorphism of the disc ϕ , where ϕ is chosen so that $0 < \phi \circ \gamma(0) = -\phi \circ \gamma(1)$.

Circle packing face paths differ from the classical paths of analytic function theory in that the paths are only differentiable in the interior of the faces comprising the carrier of \mathcal{P} , and that the minimal paths between two points are no longer classical geodesic paths (lines in the euclidean metric or arcs of circles in the hyperbolic setting). These differences will lead to some discretization effects which must be accounted for in a discrete analytic function theory. The following definition of *Euclidean and Hyperbolic Domain Path Directivity Measures* quantify the deviation of a circle packing minimal path joining two points from the traditional minimal path joining the same two points.

Definition 2.5.2 ((Euclidean/Hyperbolic) Domain Path Directivity Measure). Let $\gamma : [0, 1] \rightarrow \text{carrier}(\mathbf{P})$ be a path joining u and v in the carrier of the circle packing \mathbf{P} . The *domain path directivity measure* is given by $\cos(\theta_{max})$ where

$$\theta_{max} = \max_{\gamma} \arg \left(\frac{\gamma'}{v - u} \right).$$

In the hyperbolic metric we define a *hyperbolic domain path directivity measure* by considering $\tilde{\gamma} = \phi \circ \gamma$ where ϕ is a Möbius transformation chosen so that $(\phi \circ \gamma)(0) = -(\phi \circ \gamma)(1)$ with $\phi \circ \gamma$ having euclidean arc length 2ρ .

2.6 Interior Triangulations

A circle packing triangulation has a natural *interior triangulation* which will be useful in characterizing circle packing maps in terms of the dual packing circles. The *interior*

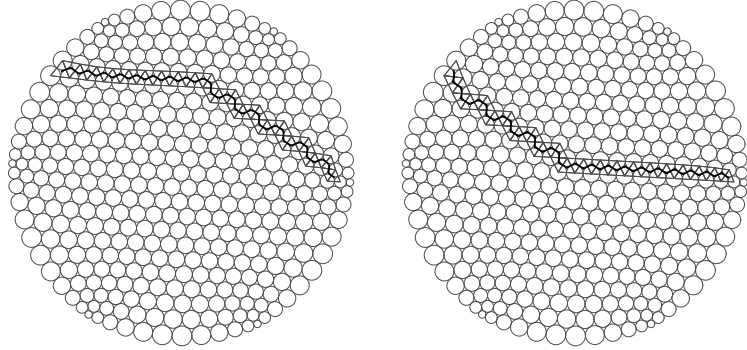


Figure 2.6: Circle Packing Minimal Paths.
 (a) Euclidean minimal path, and (b) Hyperbolic minimal path.

triangulation for a circle packing consists of the triangles formed by the three edge intersection points surrounding each face; the collection of interior faces will be denoted $\mathbf{T} = \{T_f : f \in \mathcal{F}\}$. The circle packing dual circles are the circumscribed circles about the interior triangular faces (figure 2.7).

2.7 Circle Packing Maps

A *circle packing map* is a mapping between circle packings having the same combinatoric structure. If \mathbf{P} and \mathbf{Q} are circle packings having the combinatoric structure K , then there is an induced circle packing map $F : \mathbf{P} \rightarrow \mathbf{Q}$ between them which we define in our context. Circle packing maps can be viewed at the lowest level as maps between vertexes, between the circle centers themselves. It is customary to extend this vertex mapping to an isomorphism between the carriers of the domain and range packings – we will choose a particular isomorphism which preserves the vertex and dual circle interior of the domain and range packings. In short, the dual circles (and their interiors) will be respectively mapped via an appropriate Möbius map; the dual circle maps will then be extended to the domain carrier in a straightforward fashion while ensuring that the vertex centers also correspond. The resulting map F then takes vertex circles onto vertex circles and dual circles onto dual circles. We will choose to specify this mapping by the dual circle maps since there is a unique Möbius mapping on each face between the corresponding edge intersection points of the interior triangulation.

Remark 2.7.1. Let F_0 and F_1 correspond to the faces of two (similarly oriented) triples of circles in \mathbb{C} and let μ be the (unique) Möbius mapping between their corresponding edge intersections. Then μ maps the vertex circle arcs on the interior of F_0 onto the corresponding vertex circle arcs of F_1 .

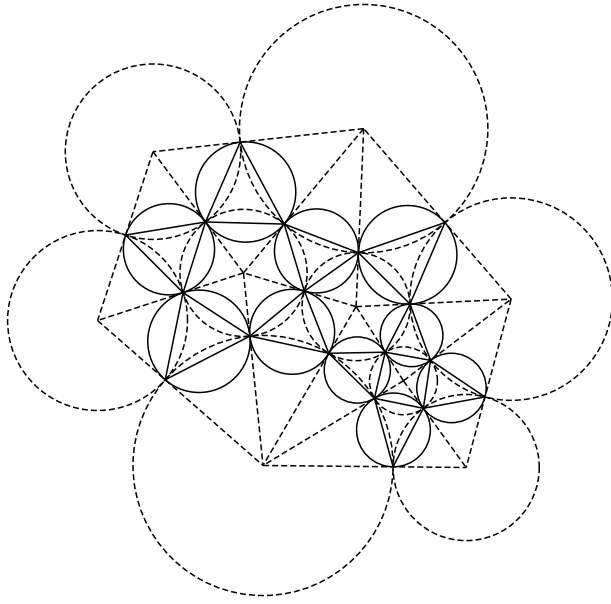


Figure 2.7: A Circle Packing Interior Triangulation.
Dashed lines indicate original circle packing and faces.

This fact follows from the definition of a circle packing and the fact that Möbius mappings preserve the incidence angle between intersecting circles.

Definition 2.7.2 (Face Möbius Mapping). A circle packing *face Möbius mapping* for \mathbf{P} is a face-wise assignment of Möbius maps $\mathbf{M} = \{M_f : f \in \mathcal{F}\}$ which take the edge intersection points of \mathbf{P} onto corresponding edge intersection points of a circle packing \mathbf{Q} sharing the same combinatoric structure.

Note that a face Möbius mapping for \mathbf{P} corresponds to a circle packing map $F : \mathbf{P} \rightarrow \mathbf{Q}$ but the definition is independent of the circle pack

Two immediate statements are in order.

Remark 2.7.3. Every circle packing map admits a unique face Möbius mapping,
and

Remark 2.7.4. A face Möbius mapping M on a circle packing \mathbf{P} maps the circular arcs of the domain circles onto the circular arcs of the image and maps the interior of the dual circles of the domain onto those of the range circle packing.

We will choose an extension $F : \mathbf{P} \rightarrow \mathbf{Q}$ on the carrier of \mathbf{P} which agrees with the face Möbius mappings on the dual circle interiors and also agrees on the vertex centers themselves. In the Euclidean case this can easily be accomplished by linearly extending F over the circular polygonal wedges about each vertex by using the interior face Möbius

on the dual circle boundary. It is clear that this particular isomorphism will agree on the interior edges of \mathbf{P} so that this extended F will be our chosen isomorphism between the domain and range carriers.

2.8 Matrix Representations of Möbius Maps and Circles

Möbius maps have a significant role in the study of circle packing maps. This is true not only because Möbius maps preserve the collection of circles (with lines serving as circles with infinite radius) but also because every circle packing map $F : \mathbf{P} \rightarrow \mathbf{Q}$ has a well defined face Möbius mapping M defined on each interior face for each circle packing map as remarked in 2.7.3.

Convenient algebraic methods for manipulating general linear transformations and their actions on circles have been developed. Schwerdtfeger's text on *The Geometry of Complex Numbers* presents one such example giving matrix representations in $PSL_2(\mathbb{C})$ for Möbius transformations, circles and expressions for the action of Möbius maps on circles (Schwerdtfeger, 1979). These matrix representation are based in projective geometry and provide a convenient algebraic representation of several circle manipulations employed in this thesis, in fact many of the observations were initially made as a consequence of Schwerdtfeger's representation, though the final proofs do not emphasize this representation. We next summarize this notation since it can serve as an alternative computational tool.

A Möbius transformation $m(z) = \frac{az+b}{cz+d}$ can be represented as an equivalence class in $PSL_2(\mathbb{C})$ by the coefficients

$$[m(z)] = \left[\begin{array}{c} az + b \\ cz + d \end{array} \right] \sim \left[\begin{array}{cc} a & b \\ c & d \end{array} \right].$$

The composition and inverse of a Möbius mapping can be easily computed using matrix arithmetic as in the following remark.

Remark 2.8.1. The composition of two Möbius mappings ϕ and ψ is represented by the matrix product

$$[\phi \circ \psi] \sim [\phi][\psi],$$

and the inverse Möbius mappings is obtained by the usual matrix inversion

$$[\phi^{-1}] \sim [\phi]^{-1}.$$

The matrix representations for (non constant) Möbius transformations can be expressed with unit determinant. Under this normalization, a Möbius map M falls into one of three types; for completeness we summarize the statements from Marden (2007).

M is *parabolic* if the three equivalent statements hold

- $\text{Tr}(M) = \pm 2$ and $M \neq \mathbb{I}$.
- M has exactly one fixed point in \mathbb{S} .
- M is conjugate to $z \mapsto z + 1$.

M is *elliptic* if the three equivalent statements hold

- $\text{Tr}(M) \in (-2, 2)$.
- M has exactly two fixed points, and the derivative of M has absolute value 1 at each of them.
- M is conjugate to $z \mapsto e^{2i\theta}z$, with $M \neq \mathbb{I}$.

M is *loxodromic* if the three equivalent statements hold

- $\text{Tr}(M) = \mathbb{C} \setminus [-2, 2]$.
- M has exactly two fixed points, one attracting and one repelling.
- M is conjugate to $z \mapsto \lambda^2 a$, with $|\lambda| > 1$.

Parabolic Möbius maps are the most significant in our development.

A circle in the complex plane can also be represented by its associated coefficients by taking

$$\begin{bmatrix} A & B \\ C & D \end{bmatrix} \sim [Az\bar{z} + Bz + C\bar{z} + D].$$

The circle $\mathcal{C}(\zeta, \rho) = \{z : |z - \zeta| = \rho\}$ then has a corresponding representation

$$\mathcal{C}(\zeta, \rho) = \{z : 0 = \bar{z}z - \bar{\zeta}z - \zeta\bar{z} + \bar{\zeta}\zeta - \rho^2\}$$

so that the circle centered at ζ with radius ρ is represented in $PSL_2(\mathbb{C})$ by

$$[\mathcal{C}(\zeta, \rho)] \sim \begin{bmatrix} 1 & -\bar{\zeta} \\ -\zeta & |\zeta|^2 - \rho^2 \end{bmatrix}. \quad (2.9)$$

For $[m] = \begin{bmatrix} a & b \\ c & d \end{bmatrix}$, we let $\mathcal{S} = \begin{bmatrix} d & -b \\ -c & a \end{bmatrix} \sim [m^{-1}]$, and with this notation, Schwerdtfeger gives a concise representation of the image of a circle under a Möbius map.

Remark 2.8.2. Let \mathcal{M} represent a Möbius mapping of a circle \mathcal{C} . The image circle \mathcal{C}' of \mathcal{C} is represented by the matrix product

$$\mathcal{C}' \sim \mathcal{S}' \mathcal{C} \bar{\mathcal{S}}. \quad (2.10)$$

2.9 Directed Möbius Edge Derivative

This section defines a key quantity in the analysis of circle packing maps as discrete analytic functions. The *directed Möbius edge derivative*, or *edge derivative*, is defined along each directed edge of the underlying complex in terms of the neighboring face Möbius maps. As a preliminary we will briefly discuss circle packing quadrilateral maps.

Let Q_0, Q_1 be two circle packing quadrilaterals with faces $g_0 \uparrow f_0$ and $g_1 \uparrow f_1$ respectively. There is then a pair of Möbius maps, μ_f and μ_g , on the associated face interior triangles (and the dual circles) that describe the mapping $F : Q_0 \rightarrow Q_1$.

The following proposition is a useful fact to have available.

Proposition 2.9.1. *Let Q be a circle packing quadrilateral with central edge intersection point z and central edge direction ζ and faces $g \uparrow f$. Let Q' be a second circle packing quadrilateral with faces $g' \uparrow f'$ having f' coincident with f . Let $\mu_0 = \mathbb{I}$ and define μ_1 to be the interior face Möbius mapping from $g \rightarrow g'$. Then the mapping μ_1 is equivalent to*

$$\mathbb{I} + \sigma \begin{bmatrix} z & -z^2 \\ 1 & -z \end{bmatrix}$$

with $\sigma = ic\bar{\zeta} = c\bar{\eta}$ for some $c \in \mathbb{R}$, where ζ and η are the edge and dual edge directions respectively.

PROOF: By hypothesis f and f' are coincident so that μ preserves the vertex circles along the central edge. In the case where the central edge intersection is zero ($z = 0$) we observe that the vertex circles under inversion become lines parallel to $i\bar{\zeta} = \bar{\eta}$. Hence μ_1 can be expressed as the composition of two inversions, \mathcal{I} , and a translation ϕ so that $\mu_1 = \mathcal{I} \circ \phi_{ic\bar{\zeta}} \circ \mathcal{I}$. This may be observed from the matrix expression:

$$[\mu_1] \sim \begin{bmatrix} 0 & 1 \\ 1 & 0 \end{bmatrix} \begin{bmatrix} 1 & ic\bar{\zeta} \\ 0 & 1 \end{bmatrix} \begin{bmatrix} 0 & 1 \\ 1 & 0 \end{bmatrix} \sim \begin{bmatrix} 1 & 0 \\ ic\bar{\zeta} & 1 \end{bmatrix} = \mathbb{I} + ic\bar{\zeta} \begin{bmatrix} 0 & 0 \\ 1 & 0 \end{bmatrix}.$$

When the central edge intersection $z \neq 0$, the image $\phi_{-z}(Q)$ has central edge intersection at zero so apply previous case to $\nu = \phi_{-z} \circ \mu \circ \phi_z$ which maps $\phi_{-z}(g)$ to $\phi_{-z}(g')$ and fixes zero. Expressing μ as $\phi_z \circ \nu \circ \phi_{-z}$ gives the desired result, In particular,

$$[\mu] \sim \begin{bmatrix} 1 & z \\ 0 & 1 \end{bmatrix} \left(\mathbb{I} + ic\bar{\zeta} \begin{bmatrix} 0 & 0 \\ 1 & 0 \end{bmatrix} \right) \begin{bmatrix} 1 & -z \\ 0 & 1 \end{bmatrix} = \mathbb{I} + ic\bar{\zeta} \begin{bmatrix} z & -z^2 \\ 1 & -z \end{bmatrix}. \quad \square$$

We would like to describe these face Möbius mappings in a manner independent of normalization, in particular we would like an expression that is invariant by post composition of an automorphism of the complex plane. The simplest such quantity for the directed edge

of the mapping F is

$$dM = \mu_0^{-1} \mu_1. \quad (2.11)$$

Definition 2.9.2 (Directed Möbius Edge Derivative). We define the (*directed Möbius edge derivative*) for a circle packing quadrilateral map $F : Q \rightarrow Q'$ to be the expression $dM_{\vec{e}} = \mu_f^{-1} \mu_g$ where f and g are the faces of Q with $g \uparrow_{\vec{e}} f$ and μ_f and μ_g correspond to the face Möbius mappings for F .

When representing dM in $PSL_2(\mathbb{C})$ we take the convention that $\det([dM]) = 1$ and $\text{Tr}([dM]) > 0$, in fact it turns out that the trace of dM is 2.

Using an argument similar to that in the previous proposition we get the following representative form for the edge derivative.

Proposition 2.9.3. *For any circle packing map, $F : \mathbf{P} \rightarrow \mathbf{P}'$, the edge derivatives have the form*

$$dM = \mathbb{I} + \sigma \begin{bmatrix} z & -z^2 \\ 1 & -z \end{bmatrix} \quad (2.12)$$

where z is the edge intersection point and σ is real proportional to the conjugate of the dual edge direction, $\sigma = ic\bar{\zeta} = c\bar{\eta}$ with $c \in \mathbb{R}$.

The proof is an immediate application of proposition 2.9.1.

2.10 Harmonic Functions and Circle Packing Weights

Discrete harmonic functions also have a significant role to play in the circle packing arena. We will take a variant of the definition used for the geometric embedding of more general meshes as in (Gortler and Craig Gotsman, 2006). Let $K = (\mathcal{V}, \mathcal{E}, \mathcal{F})$ be an oriented abstract graph (mesh) with \mathcal{V} , \mathcal{E} , and \mathcal{F} the sets of vertexes, edges and faces respectively. For each vertex $v \in \mathcal{V}$ let ∂v denote the cycle of vertexes about v , and for each face $f \in \mathcal{F}$ let ∂f denote the cycle of faces about f . For a function $F : \mathcal{V} \rightarrow \mathbb{C}$ let $\Delta_{\vec{e}} F = F(v) - F(u)$ where \vec{e} is the directed edge from u to v in K .

Definition 2.10.1 (Discrete Harmonic Function). A function $F : \mathcal{V} \rightarrow \mathbb{C}$ is said to be a *discrete harmonic function* if there exists an assignment of positive weights $w_{\vec{e}}$ on the directed edges $\vec{e} \in \vec{\mathcal{E}}$ such that

$$\sum_{\vec{e} \in \partial v} w_{\vec{e}} \Delta_{\vec{e}} F = 0 \quad (2.13)$$

for each interior vertex.

In the case of circle packings the weight assignments are specified on the undirected edges, $c : \mathcal{E} \rightarrow \mathbb{R}^+$; the directed edge weights are then expressed as

$$w_{\vec{e}} = \frac{c_e}{\sum_{e \in \partial v} c_e}, \quad (2.14)$$

taking the convention that $\vec{e} \in \partial v$ is outward pointing.

In Dubenko's study of random walks on circle packings he showed that the center function \mathbf{Z}_P is harmonic with respect to the *edge conductance weights* corresponding to the transition probabilities (Dubenko, 97). These *edge conductances* can be geometrically formed by taking the ratio of the dual edge length to the usual edge length. This result is summarized in our context as the following proposition.

Proposition 2.10.2. *Let $K = (\mathcal{V}, \mathcal{E}, \mathcal{F})$ be a simply connected triangulation of the disc with nonempty boundary ∂V . If \mathbf{P} is a circle packing with combinatoric structure K then the interior vertex positions \mathbf{Z}_o are harmonic with respect to the directed edge weights*

$$c_e = |\delta_e/d_e|. \quad (2.15)$$

The directed edge weights are then computed as above:

$$w_{\vec{e}} = \frac{c_e}{\sum_{e \in \partial v} c_e}.$$

The edge conductances and their relation to the vertex positions harmonic nature have a more geometric realization in that they are determined (up to normalization) by the centroids of the central circular sector lying in each face neighboring a given interior vertex.

Definition 2.10.3 (Geometric Centroid Weights). Let S be a circular sector with interior radius r and sector angle $2\alpha < \pi$. Let η_1 and η_2 denote the bounding ray directions, let ξ be the sector centroid and A the sector area. The *geometric centroid weights* w_1 and w_2 on the bounding rays are weights such that $w_1\eta_1 + w_2\eta_2 = A\xi$.

Definition 2.10.4 (Circle Packing Weights). The *circle packing direct edge weights* are the directed edge weights which correspond to the geometric centroid condition about each interior vertex. For each directed edge \vec{e} the circle packing weights are given by

$$w_{\vec{e}} = \frac{w_- + w_+}{|d_{\vec{e}}|}$$

where w_- and w_+ are the weights to the right and left of the directed edge in the notation above.

The above definition for the circle packing weights is justified by the following computation. If v is an interior vertex then, in the above notation,

$$0 = \frac{\sum_{f \in \partial v} \xi_f A_f}{\sum_{f \in \partial v} A_f} = \frac{\sum_{\vec{e} \in \partial v} (w_- + w_+) \frac{d_{\vec{e}}}{|d_{\vec{e}}|}}{\sum_{f \in \partial v} A_f}$$

so that

$$\sum_{\vec{e} \in \partial v} w_{\vec{e}} d_{\vec{e}} = 0.$$

We remark that since the bounding rays, η_1 and η_2 , have unit magnitude, symmetry ensures that $w_1 = w_2 = w$, where w has magnitude proportional to $\tan(\alpha)$ which allows the geometric centroid weights for a circle packing to be locally expressed as the ratios of the dual edge lengths to the edge lengths. In fact the geometric circle packing weights are an alternate interpretation of the *edge conductances* of Dubejko.

Proposition 2.10.5. *The edge conductances are locally equivalent (up to scale) to the circle packing weights.*

A direct computation of the center position based on the sector centroids and normalizing gives the edge conductance weights (a similar computation is given in the proof of the next proposition). This alternate interpretation of the edge conductances gives an immediate extension of Dubejko's observation, namely that the dual circle packing centers are harmonic with respect to the reciprocal circle packing weights.

Theorem 2.10.6. *Let $K = (\mathcal{V}, \mathcal{E}, \mathcal{F})$ be a simply connected triangulation of the disc with nonempty boundary ∂V . If \mathbf{P} is a circle packing of K with dual circle packing \mathbf{Q} then the interior vertex positions \mathbf{W}_o of the dual packing are harmonic with respect to the directed edge weights*

$$\kappa_e = 1/c_e = |d_e/\delta_e|. \quad (2.16)$$

The directed edge weights are then computed as above:

$$\omega_{\vec{e}} = \frac{\kappa_e}{\sum_{e \in \partial v} \kappa_e}.$$

PROOF: Let $f \in \mathcal{F}$ be an interior face in K with oriented neighboring faces f_1, f_2 and f_3 corresponding to the three edges of f namely e_1, e_2 and e_3 . Denote the central interior face circle by \mathcal{C} and the neighboring interior face circles $\mathcal{C}_1, \mathcal{C}_2$ and \mathcal{C}_3 , and the outward pointing segments joining \mathcal{C} to the neighboring circles by η_1, η_2 and η_3 . The central circle is thus divided into three sectors. The three sectors have areas A_k and centroids ζ_k so that the center of \mathcal{C} , ζ , is given by

$$\zeta = \frac{\sum A_k \zeta_k}{\sum A_k}. \quad (2.17)$$

We will express the terms on the right using the weights $\kappa_e = |d_e/\delta_e|$ – first considering the one the sector formed by η_1 and η_2 after scaling (and relabeling) so that the central circle has unit radius. After this scaling, the product $|A\xi| = \alpha \frac{2}{3} \frac{\sin(\alpha)}{\alpha}$ and is acting along the bisector, hence the components along the neighboring edges are given by $|A\xi|/\cos(\alpha)$ or $\frac{1}{3}\tan(\alpha)$. But the central radius was taken to be unit so that the component has magnitude $\frac{1}{3}r_{12}$ where r_{12} is the radius of the original vertex circle which is common to the faces f, f_1 and f_2 . Summing over all such components and applying a common scaling to all the weights gives the result. \square

As a final observation about the harmonic weights we note that again changing point of view and applying Huron's formula, the interior centers of a circle packing can be expressed in terms of the *film tension* on each face; here the film tension is computed by considering the ratio of the area of each face to its semi-perimeter. This observation is summarized in the following proposition.

Proposition 2.10.7. *Let \mathbf{P} be a circle packing and let $\mathcal{T} = \{\tau_f : f \in \mathcal{F}\}$ be the film tension $\tau_f = A_f/s_f$ where A_f and s_f are the area and semi-perimeter of the associated face f . Then, for each interior vertex v we have the vector sum*

$$\sum_{\vec{e} \in \partial v} (\tau_+ + \tau_-) \zeta_{\vec{e}} = 0,$$

where τ_+ and τ_- are the film tensions on the left and right neighboring faces of the directed edge \vec{e} , and $\zeta_{\vec{e}}$ is the unit outward pointing normal along the directed edge \vec{e} .

The condition of the previous proposition is distinctly different from a similar problem of minimizing the area to perimeter ratio studied in the physics of film tension – our condition is a vector force condition. This interpretation also gives a physical aspect that may be useful in proving the convergence of the computational circle packing algorithm presented in this thesis, though none is yet in hand.

2.11 Tutte's Theorem for Planar Graph Embeddings

The problem of obtaining a straight-line embedding of a planar graph has seen many proposed solutions. One of the most convenient graph embedding processes is *Tutte's* where any simply connected, oriented planar graph, $G = (\mathcal{V}, \mathcal{E})$ with finite boundary can be embedded in the plane as a solution to a discrete harmonic Dirichlet problem with arbitrary positive weights. Tutte's theorem states that positioning the boundary vertexes in the proper orientation around a convex boundary and assigning arbitrary positive edge weights, $C : \mathcal{E} \rightarrow \mathbb{R}^+$ to the edges is sufficient to ensure that the solution to the discrete harmonic function

$$\sum_{\vec{e} \in \partial v} w_{\vec{e}} \Delta_{\vec{e}} Z = 0 \tag{2.18}$$

(where $w_{\vec{e}} = \frac{c_e}{\sum_{e \in \partial v} c_e}$) is a planar straight-line embedding of G . The conditions of Tutte's theorem have been relaxed to allow for less restrictive boundary conditions and even permit its application to higher dimensional graph embedding applications (Gortler and Craig Gotsman, 2006).

This graph embedding process is straightforward with modern large scale linear algebra solvers – though the subjective question of graph geometric quality still remains.

Circle packings also provide their underlying complex with a planar geometry and in the case of univalent packings, as a traditional straight-line embedding of the graph (having line crossings only at vertexes). In this respect circle packing methods can serve to obtain a straight-line planar embedding of a graph. As circle packing computational performance increases there is beginning to be some interest in using the geometric appeal of circle packings to enhance the visual quality of graph embedding algorithms.

Coupling Tutte's method with the circle packing harmonic weights (specifically an approximate sequence of such weights) in an iterative manner leads to the new circle packing computational algorithm presented in this thesis.

2.12 General Triangulations and Circle Packing Geometries

The process of circle packing gives a natural method for obtaining a triangulation in the plane for a specified complex; we would like to quantify how well a given triangulation approximates to a circle packing triangulation. This section presents some error measures and a method for estimating an *effective radius* at a vertex of a given triangulation (not necessarily derived from a circle packing).

Given a generic triangle we can determine the three associated radii, one for each vertex by a simple computation. Namely, if the vertexes of the triangle are the triple (z_1, z_2, z_3) then twice the radius of the circle at vertex v_1 is obtained by summing the neighboring side lengths and subtracting the opposite side length. The radii for the remaining vertexes are similarly obtained.

We will need to modify the definition of angle sum in the generic triangulation case. For a general triangulation we will define the *angle sum* Θ_v for a vertex to be the sum of the interior face angles at the vertex. When the vertex v is interior, the angle sum will be a multiple of 2π as determined by the winding of the neighboring cycle about the vertex.

In addition we can define an *effective radius* at each vertex of a general triangulation, which plays a key role on the computational algorithm.

Definition 2.12.1 (Effective Radius). Let v be a vertex of a triangulation with angle sum Θ_v . Summing the interior circular sector areas of neighboring faces ($f \in \partial v$) gives the effective area at a vertex A_v . The *effective radius* at the vertex v is the equivalent radius which would give the same area, namely

$$r_{eff}(v) = \sqrt{\frac{2A_v}{\Theta_v}}. \quad (2.19)$$

When the desired circle packing representation is branched at the vertex v we can include

a winding factor where n is the winding number for the flower about the vertex:

$$r_{eff}(v) = \sqrt{\frac{2A_v}{n\Theta_v}}. \quad (2.20)$$

The *quadrilateral skew error* provides a practical measure of the deviation of a general triangulation from a circle packing. The simple computation makes it practical for use (see figure 2.8).

Definition 2.12.2 (Quadrilateral Skew Error). Let Q be a quadrilateral with boundary vertexes at z_1, z_2, z_3, z_4 and central edge joining vertexes at z_1 and z_3 . The *quadrilateral skew error* is the magnitude of the difference between the left and right sector radii across the central edge (either associated sector can be used). This error measure can be easily computed by summing the boundary edge lengths with alternating signs

$$E_{Quad} = ||z_2 - z_1| - |z_3 - z_2| + |z_4 - z_3| - |z_1 - z_4|| \quad (2.21)$$

The *normalized quadrilateral skew error* is taken to be $\hat{E}_{Quad} = E_{Quad}/d$ where d is the length of the common edge.. When \mathbf{Z} is an triangulation in \mathbb{C} for abstract triangulation K use the notation $E_{Quad}(e)$ and $\hat{E}_{Quad}(e)$ to specify the quadrilateral skew error associated with each interior edge of K .

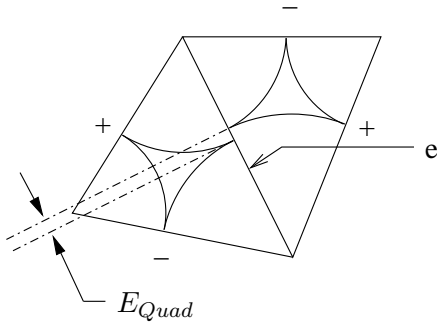


Figure 2.8: Quadrilateral Skew Error

Chapter 3

Functions on Circle Packings

3.1 Convergence on Compact Sets

Several authors have shown that a sequence of circle packings, under suitable refinement, converge uniformly on compact sets to the Riemann map as in (Rodin and Sullivan, 1987), (Stephenson, 1990), and (He and Schramm, 1996). We state the version from He and Schramm.

Theorem 3.1.1 (He - Schramm Theorem 1). *Let $D, \tilde{D} \subsetneq \mathbb{C}$ be two simply connected domains, and let p_0 be some point in D . For each n , let P^n be a disk packing in D , with all bounded interstices triangular, let \tilde{P}^n be an isomorphic packing in \tilde{D} , and let $f_n : \text{supp}(P^n) \rightarrow \text{supp}(\tilde{P}^n)$ be an isomorphism.*

Let δ_n be a sequence of positive numbers, tending to zero, and assume that the spherical diameters of the disks in every P^n are less than δ_n , and for each boundary disk P_v^n of P^n the spherical distance from it to ∂D and the spherical distance from ∂D to the corresponding disk $f_n(P_v^n)$ are less than δ_n . Suppose that for each n the point p_0 is contained in the support of P^n , and that the set $\{f_n(p_0) : n = 1, 2, \dots\}$ has compact closure in \tilde{D} . Then a subsequence f_n converges uniformly on compact subsets of D to a conformal homeomorphism $f : D \rightarrow \tilde{D}$.

He and Schramm further show that the first and second derivatives also converge uniformly on the restriction of compact sets of D to the dual circles and their interiors.

Theorem 3.1.2 (He - Schramm Theorem 2). *Let the situation be as in theorem 1 (3.1.1), and assume that f_n converges to f (rather than a subsequence, for simplicity of notation). Denote the union of the bounded interstices of P^n by I^n , and let g_n be the induced interstitial map. Then the restrictions of g'_n and g''_n to I^n converge uniformly on compacts of D to f' and f'' , respectively, that is, given any compact $K \subset D$ and $\epsilon > 0$ there is an N such that $|f'(z) - g'_n(z)| < \epsilon$ and $|f''(z) - g''_n(z)| < \epsilon$ hold for any $n > N$ and $z \in K \cap I^n$.*

In their proof of theorems 1 and 2 one lemma will be particularly useful for us; their clever proof is also presented since this observation is important to our main results.

Lemma 3.1.3 (He - Schramm Lemma). *Using the notation of theorems 1 and 2, g'_n is well defined and continuous.*

PROOF: Suppose that P_v^n and P_u^n are two tangent disks in P^n , and let q be their point of tangency. Let m_1 be the Möbius transformation that agrees with g_n on an interstice whose closure contains q , and let m_2 be the Möbius transformation that agrees with g_n in the other neighboring interstice. Clearly, all we need to prove is that $m'_1(q) = m'_2(q)$.

The Möbius transformation m_1 takes P_v^n onto \tilde{P}_v^n and takes P_u^n onto \tilde{P}_u^n , and the same is true for m_2 . Hence $m_2^{-1} \circ m_1$ takes P_v^n onto itself and P_u^n onto itself.

Now let $\phi(z) = q + \frac{1}{z-q}$. The ϕ is a Möbius transformation that takes q to ∞ and $\phi \circ \phi(z) = z$. The Möbius transformation $\phi \circ m_2^{-1} \circ m_1 \circ \phi$ then takes the line $\phi(\partial P_v^n)$ into itself and the line $\phi(\partial P_u^n)$ into itself. Hence, it must have the form $z \rightarrow z + b$, for some $b \in \mathbb{C}$. This means that $m_2^{-1} \circ m_1 = \phi(b + \phi(z))$, and so the derivative of $m_2^{-1} \circ m_1$ at q is 1. Therefore $m'_2(q) = m'_1(q)$, which proves the lemma. \square

It is important to note that in He and Schramm's second theorem, the uniform convergence of the first and second derivatives only applies on a subset of the carrier of the domain packing, in particular it holds on the dual circles themselves under the face Möbius mapping. For this reason we also state a version of the original Rodin-Sullivan theorem as formulated in (Stephenson, 2005b).

Theorem 3.1.4. *Let Ω be a simply connected bounded domain in the plane with distinguished points w_1, w_2 and let $F : \mathbb{D} \rightarrow \Omega$ be the unique conformal mapping with $F^{-1}(w_1) = 0$ and $F^{-1}(w_2) > 0$. Assume \mathcal{P}_n is a sequence of univalent circle packings in Ω which, along with their complexes K_n , satisfy the following conditions:*

1. $\text{Mesh}(\mathbf{P}_n) \rightarrow 0$ as $n \rightarrow \infty$.
2. The carriers of \mathbf{P}_n exhaust Ω .
3. There exists a uniform bound, d , on $\deg(K_n)$.
4. The sequence $\{K_n\}$ either is a nested sequence which exhausts a parabolic combinatorial disc or is asymptotically parabolic.

For each n , let $f_n : \mathcal{P}_{K_n} \rightarrow \mathbf{P}_n$ be the associated discrete conformal mapping, normalized by $f_n^{-1}(w_1) = 0, f_n^{-1}(w_2) > 0$. Then on compact subsets of \mathbb{D} , the f_n converge uniformly to F and their ratio functions $f_n^\#$ converge uniformly to $|f'|$.

This theorem gives convergence of the real valued ratio of corresponding circle radii to the magnitude of the derivative of the limiting conformal map (here the maps are extended affinely on each face), and differs from He-Schramm in that the uniform convergence of the derivative is not restricted to a portion of the domain carrier.

3.2 Linear Derivative

The classical derivative is the fundamental quantity of analytic function theory. The parallels between circle packing maps and analytic functions suggest a definition for complex valued derivative along the edges and their duals.

Circle packing literature has shown a relationship between the ratios of associated radii and the analytic derivative under successively refined packings. This real valued derivative-like quantity is denoted $F^\#$ and has been shown to converge uniformly (in magnitude) to the traditional derivative under a sequence of refined packings as in theorem 3.1.4.

The analytic derivative can be approximated in the circle packing discrete analytic function case by forming the complex valued ratios of the embedded edge and dual edge displacement vectors in the range and domain.

Definition 3.2.1 (Linear Edge Derivative). The *linear edge derivative* of a circle packing map $F : \mathbf{P} \rightarrow \mathbf{P}'$ is an edgewise assignment $F_d : \vec{\mathcal{E}} \rightarrow \mathbb{C}$ with $F_d(\vec{e}) = d'_{\vec{e}}/d_{\vec{e}}$, and *dual linear edge derivative* $F_\delta : \vec{\mathcal{E}} \rightarrow \mathbb{C}$ is similarly defined in terms of the dual edges, as $F_\delta(\vec{e}) = \delta'_{\vec{e}}/\delta_{\vec{e}}$.

The *linear edge derivative* and its dual are related in terms of the circle packing weights of the domain and range packings as given in the following proposition.

Proposition 3.2.2. *The ratios of the corresponding linear edge derivative and its dual at a directed edge \vec{e} correspond to the ratio of the domain and range circle packing weights c_e along the edge e (recall $c_{-\vec{e}} = c_{\vec{e}} = c_e$); in particular*

$$\frac{F_d(\vec{e})}{F_\delta(\vec{e})} = \frac{c_e}{c'_e} \quad (3.1)$$

These linear derivatives are defined edgewise but ultimately we would like a definition for the values to be given at the vertexes – these complex valued approximations can be estimated at vertexes by taking an appropriate weighted average using the circle packing weights. Of great interest would be a method for computing the anti-derivative of a circle packing though the problem is not well defined – this is an area with many potentially interesting results.

The weakness of the linear derivative is its limited invariance; the linear derivative is invariant only under translation of the range packing. This motivates the interest in a Möbius invariant derivative quantity for circle packings.

3.3 Schwarzian Derivative

The Schwarzian derivative was arrived at by seeking a differential operator which is invariant under Möbius maps (Nehari, 1975). The traditional definition of the Schwarzian derivative

for a meromorphic function $f(z)$ is

$$S_f = \left(\frac{f''}{f'} \right)' - \frac{1}{2} \left(\frac{f''}{f'} \right)^2, \quad (3.2)$$

with the term f''/f' called the pre-Schwarzian. We will construct a *discrete Schwarzian* quantity for circle packings which exhibits many of the key properties of the classical Schwarzian derivative.

Before continuing we would like to reiterate some of the common properties of the Schwarzian derivative which we would like to duplicate in the discrete setting. The function composition rule for the Schwarzian derivative is

$$S_{f \circ g} = (S_f \circ g)g'^2 + S_g. \quad (3.3)$$

If h is a general linear transformation then $S_h \equiv 0$, giving two special cases of the composition formula:

$$S_{f \circ h} = (S_f \circ h)h'^2 \quad (3.4)$$

$$S_{h \circ f} = S_f. \quad (3.5)$$

The simplest circle packing geometric quantity which is invariant under general linear transformations is the *directed Möbius edge derivative* $dM : \vec{\mathcal{E}} \rightarrow PSL_2(\mathbb{C})$ defined earlier.

Proposition 3.3.1. *The direct Möbius edge derivative is invariant under post composition of a general linear transformation.*

PROOF: Let $F : Q \rightarrow Q'$ be a circle packing quadrilateral map with $g \uparrow f$ and respective face Möbius maps μ_f and μ_g . Let H be a fixed general linear transformation and consider $G = H \circ F$ with $G : Q \rightarrow H(Q')$. The face Möbius maps of G are then $H \circ \mu_f$ and $H \circ \mu_g$ respectively, so that the edge derivative $dM_G = (H \circ \mu_f)^{-1} \circ (H \circ \mu_g) = \mu_f^{-1} \mu_g = dM_F$. \square

Proposition 3.3.2. *Let $F : \mathbf{P} \rightarrow \mathbf{P}'$ and $G : \mathbf{P}' \rightarrow \mathbf{P}''$ be circle packing maps. Let $M_F = \{\mu_F(f) : f \in \mathcal{F}\}$ and $M_G = \{\mu_G(f) : f \in \mathcal{F}\}$ be the respective face Möbius mappings. For any interior directed edge \vec{e} let $f_+ \uparrow_{\vec{e}} f_-$ be the two neighboring faces with $\mu_{F\pm}$ and $\mu_{G\pm}$ the respective Möbius maps corresponding to F and G . With this notation,*

$$dM_{G \circ F}(\vec{e}) = (\mu_{F-})^{-1} \circ dM_G \circ \mu_{F+},$$

where $dM_G = \mu_{G-}^{-1} \circ \mu_{G+}$.

PROOF: By direct computation

$$dM_{G \circ F} = (\mu_{G-} \circ \mu_{F-})^{-1} (\mu_{G+} \circ \mu_{F+}) = (\mu_{F-})^{-1} \circ dM_G \circ \mu_{F+}. \square$$

We now summarize the composition formulas for H a constant Möbius circle packing map.

$$d(H \circ M) \sim dM \quad (3.6)$$

$$d(M \circ H) \sim [H]^{-1}[dM][H] \quad (3.7)$$

The face Möbius maps of neighboring faces share a coupled geometry as shown in the following lemma.

Lemma 3.3.3. *Let F be a circle packing map and Q a circle packing quadrilateral in the domain with $F : Q \rightarrow Q'$. Then,*

1. *The face Möbius maps μ_f, μ_g each map the central vertex circles \mathcal{C}_0 and \mathcal{C}_1 (at vertexes of the common central edge) of the domain quadrilateral onto the central circles \mathcal{C}'_0 and \mathcal{C}'_1 of the image quadrilateral.*
 2. *The directed Möbius edge derivative $dM = \mu_f^{-1} \circ \mu_g$ maps the central vertex circles of the domain quadrilateral, \mathcal{C}_0 and \mathcal{C}_1 , onto themselves, and*
 3. *The directed Möbius edge derivative corresponds to a parabolic Möbius transformation of the form*
- $$dM = \mathbb{I} + \sigma \begin{bmatrix} z_{\vec{e}} & -z_{\vec{e}}^2 \\ 1 & -z_{\vec{e}} \end{bmatrix},$$
- where z is the edge intersection point of the common directed edge of Q .*
4. *The edge derivative matrix representation in $PSL_2(\mathbb{C})$ can be chosen to have $Tr(dM) = 2$ and $\det(dM) = 1$.*

PROOF: The first two statements were previous remarks and we have shown that the form of dM is as given. To show that dM is a parabolic Möbius map we observe that $\det(dM) = (1 + \sigma z_{\vec{e}})(1 - \sigma z_{\vec{e}}) + \sigma^2 z_{\vec{e}}^2 = 1$ and $Tr(dM) = 2$. The final statement is equivalent. \square

We can now define the *discrete Schwarzian* which will be shown to be related to the integral of the classical Schwarzian derivative.

Definition 3.3.4. Let $dM_{\vec{e}}$ be the directed Möbius edge derivative associated with \vec{e} , so that

$$dM_{\vec{e}} = \mathbb{I} + \sigma \begin{bmatrix} z_{\vec{e}} & -z_{\vec{e}}^2 \\ 1 & -z_{\vec{e}} \end{bmatrix}$$

with $z = z_{\vec{e}}$ the edge intersection point along e . We call σ the *discrete Schwarzian* along the directed edge \vec{e} , denoted $\sigma_{\vec{e}}$.

Definition 3.3.5 (Valid Discrete Schwarzian Assignment). Let $K = (\mathcal{V}, \mathcal{E}, \mathcal{F})$ be a triangulation of the disc. A *valid discrete Schwarzian assignment* on K is a function $\sigma : \vec{\mathcal{E}} \rightarrow \mathbb{C}$ such that there exists domain and range circle packings \mathbf{P} and \mathbf{Q} and associated circle packing map $F : \mathbf{P} \rightarrow \mathbf{Q}$ having edge derivatives of the form

$$dM_{\vec{e}} = \mathbb{I} + \sigma(\vec{e}) \begin{bmatrix} z_e & -z_e^2 \\ 1 & -z_e \end{bmatrix},$$

where z_e is the edge intersection point corresponding to the edge e .

Proposition 3.3.6. *Let $dM_{\vec{e}}$ and $\sigma_{\vec{e}}$ be the directed Möbius edge derivative and discrete Schwarzian along \vec{e} , then the following identities hold.*

1. $dM_{-\vec{e}} \sim (dM_{\vec{e}})^{-1}$, and

2. $\sigma_{-\vec{e}} = -\sigma_{\vec{e}}$.

PROOF: Let $g \uparrow_{\vec{e}} f$ be the neighboring faces of \vec{e} and let μ_f and μ_g be the corresponding face Möbius maps. By definition $dM_{-\vec{e}} = \mu_g^{-1}\mu_f = (\mu_f^{-1}\mu_g)^{-1} = dM_{\vec{e}}^{-1}$, and direct computation gives:

$$dM_{\vec{e}}^{-1} \sim \mathbb{I} + \sigma_{\vec{e}} \begin{bmatrix} -z_{\vec{e}} & z_{\vec{e}}^2 \\ -1 & z_{\vec{e}} \end{bmatrix} \sim \mathbb{I} - \sigma_{\vec{e}} \begin{bmatrix} z_{\vec{e}} & -z_{\vec{e}}^2 \\ 1 & -z_{\vec{e}} \end{bmatrix}.$$

Hence $\sigma_{-\vec{e}} = -\sigma_{\vec{e}}$. \square

The next proposition quantifies composition rules when H is a translation or a scaling.

Proposition 3.3.7. *Suppose M is the face Möbius mapping for a circle packing function F with $dM = \mathbb{I} + \sigma \begin{bmatrix} z_{\vec{e}} & -z_{\vec{e}}^2 \\ 1 & -z_{\vec{e}} \end{bmatrix}$. For H a translation, $H \sim H(z) = z + a$, then*

$$d(M \circ H) \sim \mathbb{I} + \sigma \begin{bmatrix} w_{\vec{e}} & -w_{\vec{e}}^2 \\ 1 & -w_{\vec{e}} \end{bmatrix}, \quad (w = z - a) \tag{3.8}$$

and for H a scaling $H \sim H(z) = \alpha z$, then

$$d(M \circ H) \sim \mathbb{I} + \alpha \sigma \begin{bmatrix} w_{\vec{e}} & -w_{\vec{e}}^2 \\ 1 & -w_{\vec{e}} \end{bmatrix}, \quad (w = z/\alpha) \tag{3.9}$$

PROOF: The expressions follow by direct computation taking $[H]$ to be $\begin{bmatrix} 1 & a \\ 0 & 1 \end{bmatrix}$ and $\begin{bmatrix} \alpha & 0 \\ 0 & 1 \end{bmatrix}$ respectively. \square

The previous proposition shows that the magnitude of the discrete Schwarzian is invariant under pre-composition of rotations and translations. We will later show an invariance under isomorphisms of the unit disc domain.

Previous authors have expressed relationships between the Schwarzian derivative and best fit Möbius maps. Using the notation $M(f; z)$ to represent the best fit Möbius for an analytic function f at the point z , Thurston (Marden, 2007) showed that for any $v \neq 0 \in \mathbb{C}$,

$$vS_f(z_0) = v \left(\left(\frac{f''}{f'} \right)' - \frac{1}{2} \left(\frac{f''}{f'} \right)^2 \right)_{z_0} = \frac{\partial^2}{\partial z^2} M(f; z)^{-1} M(f; z + tv)|_{t=0; z=z_0}. \quad (3.10)$$

Martio and Sarvas expressed the Schwarzian derivative indirectly in terms of a limit expression; their theorem states that there is a unique Möbius transformation h such that

$$\lim_{z \rightarrow z_0} \frac{(h \circ f)(z) - z}{(z - z_0)^3} \quad (3.11)$$

is finite, and the limit is equal to $S_f(z_0)/6$.

The relationship between the discrete Schwarzian σ_e and the traditional Schwarzian derivative is suggested by the following computational proposition concerning the best fit Möbius mapping for an analytic function $f(w)$ at a point $w = z$.

Proposition 3.3.8. *Let $f(w)$ be analytic at a point z in the domain of f , then, the best fit Möbius map with determinant 1 at z is given by*

$$M_z \sim \begin{bmatrix} 1/h - fkh/2 & fh - z/h + fkhz/2 \\ -kh/2 & h + khz/2 \end{bmatrix} \quad (3.12)$$

where $k = f''/f'$ and $h = 1/\sqrt{f'}$. Moreover the derivative of M_z at z is related to the Schwarzian derivative by

$$\frac{\partial}{\partial z} M_z = -\frac{h}{2} S_f \begin{bmatrix} f & -zf \\ 1 & -z \end{bmatrix}. \quad (3.13)$$

This result follows by direct computation and shows that for functions with $f'(z) = 1$, the Schwarzian derivative can be computed by the derivative of the (2,1) entry in the matrix representation of M_z , suggesting a natural relationship between the (2,1) element of the edge derivative dM for a circle packing map, which indeed is the case.

COMPUTATION: Let $f(z)$ be an analytic function; we wish to find the best fit Möbius :

$$M = \frac{Az + B}{Cz + D} \sim \begin{bmatrix} A & B \\ C & D \end{bmatrix}$$

For a fixed z , $M(z)$ need to satisfy $M(z) = f(z)$, $M'(z) = f'(z)$ and $M''(z) = f''(z)$.

Restating in terms of the coefficients these conditions become

$$\begin{aligned} Az + B &= (Cz + D)f \\ AD - BC &= (Cz + D)^2 f' \\ -2C(AD - BC) &= (Cz + D)^3 f'' \end{aligned}$$

Since $\det(M) = 1$ we have $AD - BC = 1$. For notation, let $k = f''/f'$ and $h = 1/\sqrt{f'}$. Dividing the last two equations then gives

$$D = -C(2/k + z)$$

and substituting $Cz + D = \frac{-2C}{k}$ back into the third gives

$$C = -\frac{kh}{2}$$

up to an unknown sign, we pick a convenient representative. This computation leads to an expression for the (determinant) normalized best fit Möbius map for a locally univalent analytic function $f(z)$.

$$M_z \sim \begin{bmatrix} A & B \\ C & D \end{bmatrix} = \begin{bmatrix} 1/h - fkh/2 & fh - z/h + fkhz/2 \\ -kh/2 & h + khz/2 \end{bmatrix}.$$

The above can be derived by solving the system

$$\begin{aligned} AD - BC &= 1 \\ Az + B &= (Cz + D)f = \frac{-2Cf}{k} = fh \end{aligned}$$

or equivalently solving

$$\begin{pmatrix} D & -C \\ z & 1 \end{pmatrix} \begin{bmatrix} A \\ B \end{bmatrix} = \begin{bmatrix} 1 \\ fh \end{bmatrix}.$$

Since $D + Cz = -2C/k = h$ we have

$$\begin{bmatrix} A \\ B \end{bmatrix} = \begin{pmatrix} 1 & C \\ -z & D \end{pmatrix} \begin{bmatrix} 1/h \\ f \end{bmatrix} = \begin{pmatrix} 1 & -1 \\ -z & z + 2/k \end{pmatrix} \begin{bmatrix} 1/h \\ fkh/2 \end{bmatrix}.$$

Now taking derivatives gives the relationship to the Schwarzian derivative. In particular $\frac{\partial}{\partial z} \frac{kh}{2} = \frac{1}{2} [k'h + kh']$ but $h' = -\frac{1}{2}kh$ so that $\frac{\partial}{\partial z} \frac{kh}{2} = \frac{h}{2} (k' - \frac{1}{2}k^2) = \frac{h}{2} S_f$. Similar relations to the Schwarzian derivative hold for other coefficients and are in summary (taking $M =$

$$\begin{bmatrix} A & B \\ C & D \end{bmatrix})$$

$$\frac{\partial A}{\partial z} = -\frac{fh}{2} S_f \quad (3.14)$$

$$\frac{\partial B}{\partial z} = \frac{fhz}{2} S_f \quad (3.15)$$

$$\frac{\partial C}{\partial z} = -\frac{h}{2} S_f \quad (3.16)$$

$$\frac{\partial D}{\partial z} = \frac{hz}{2} S_f \quad (3.17)$$

or

$$\frac{d}{dz} M_z = -\frac{h}{2} S_f \begin{bmatrix} f & -zf \\ 1 & -z \end{bmatrix}. \quad \square$$

3.4 Face Linear Systems

Face linear systems will play a significant role in studying zero's of circle packing functions and the formulation of univalence criteria.

Definition 3.4.1 (Face Linear System). Let \mathbf{P} be a circle packing for a complex K with faces \mathcal{F} . A *face linear system*, \mathbf{A} , on \mathbf{P} is an assignment of linear functions to each circle packing face,

$$\mathbf{A} = \{A_f(z) = az + b : f \in \mathcal{F}; a, b \in \mathbb{C}\}$$

which satisfies the following face condition across each interior edge: Let $f \sim g$ be two neighboring faces having edge intersection point z_e , then

$$A_f(z_e) = A_g(z_e).$$

It will be useful to have an alternate definition when working in a projective geometry. A *projective face linear system*, \mathcal{A} , is a pair (A, \mathcal{S}) where A is a face wise assignment of linear functions to each circle packing face and \mathcal{S} , called the *character* of \mathcal{A} , is an edge-wise sign (± 1) assignment.

$$\mathbf{A} = \{A_f(z) = az + b : f \in \mathcal{F}; a, b \in \mathbb{C}\} \quad (3.18)$$

$$\mathcal{S} = \mathcal{S} : \mathcal{E} \rightarrow \{+1, -1\} \quad (3.19)$$

which satisfies the following condition across each interior edge: Let $f \sim g$ be two neighboring faces with common directed edge \vec{e} having edge intersection point z_e then,

$$A_f(z_e) = \mathcal{S}(e) A_g(z_e).$$

A face linear system is called *regular* if no face linear mapping has zero derivative (i.e. $a_f \neq 0$ for each $f \in \mathcal{F}$). Some examples of face linear systems on a regular hexagonal combinatoric domain are illustrated in figures 3.1 and 3.2.

Using these definitions we next present a fundamental theorem for circle packing maps. In the context of circle packings, we can consider the Möbius mappings on each face, or more specifically on the interior triangulation corresponding to the dual circles. A Möbius mapping on a circle packing face is the quotient of two linear maps on the interior triangulation and we will distinguish the numerator and denominator linear transformations in the following proposition.

Theorem 3.4.2. *Let $F : \mathbf{P} \rightarrow \mathbf{P}'$ be a circle packing map and let $M : \mathcal{F} \rightarrow PSL_2(\mathbb{C})$ be the face Möbius mappings corresponding to F with unit determinant. If A and B are the face wise linear mappings corresponding to the numerators and denominators of M , respectively, then A and B are projective face linear systems having the same character.*

PROOF: Let $f \sim g$ be two adjacent faces in K . Let z and ζ represent the edge intersection point and the common edge direction and $m_f = \begin{bmatrix} a & b \\ c & d \end{bmatrix}$, $m_g = \begin{bmatrix} \alpha & \beta \\ \gamma & \delta \end{bmatrix}$ the respective Möbius transformations. By hypothesis since F is a circle packing map we have $m_f(z) = m_g(z)$ and, by 2.9.3,

$$m_g \sim m_f \left(\mathbb{I} + \sigma \begin{bmatrix} z & -z^2 \\ 1 & -z \end{bmatrix} \right) = \begin{bmatrix} a & b \\ c & d \end{bmatrix} + \sigma \begin{bmatrix} az + b & -z(az + b) \\ cz + d & -z(cz + d) \end{bmatrix}.$$

Direct computation verifies that the numerator and denominator form a projective face linear system (with similar character determined by choice of representatives in $PSL_2(\mathbb{C})$). \square .

An alternate proof is given by using the lemma of He-Schramm. Let $f \sim g$ be two adjacent faces in K . Let z and ζ represent the edge intersection point and the common edge direction and $m_f = \begin{bmatrix} a & b \\ c & d \end{bmatrix}$, $m_g = \begin{bmatrix} \alpha & \beta \\ \gamma & \delta \end{bmatrix}$ the respective Möbius transformations. By hypothesis since F is a circle packing map we have $m_f(z) = m_g(z)$ and by He-Schramm lemma 3.1.3, $m'_f(z) = m'_g(z)$. Direct computation then shows that

$$\frac{1}{(cz + d)^2} = \frac{1}{(\gamma z + \delta)^2}, \quad (3.20)$$

so that $cz + d = s(\gamma z + \delta)$ for some sign $s = \pm 1$, and it follows that $az + b = s(\alpha z + \beta)$ for the same s . \square

A circle packing map is said to have *constant projective character* if the associated face linear systems have constant character. Experiments show that branched packing maps result in projective face linear systems but the question of characterizing those circle packing maps which yield projective face linear systems is still open.

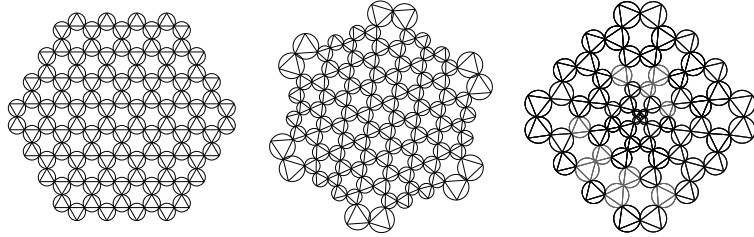


Figure 3.1: Example face linear Systems.

From left to right: regular hexagonal combinatoric domain interior triangulation, example face linear system, example projective face linear system (reflections shown in gray).

3.5 Path Mappings and Deformation Metrics

Let $F : \mathbf{P} \rightarrow \mathbf{P}'$ be a circle packing map and γ a face path in the domain packing joining u and v in the carrier of \mathbf{P} . We can construct the trace of $F(\gamma)$ in a natural fashion when both u and v lie in the closed interior of a dual circle in the domain as the image of γ under the face Möbius mappings. When one endpoint does not lie in a dual circle the image is not as well defined. We will be able to phrase what we need in terms of the first case, taking both endpoints to be contained in the dual graph.

We will next define a general *deformation metric* in both euclidean and hyperbolic geometry which will be used in studying the zeros and hence univalence properties of circle packing maps.

For the following definitions we suppose that a domain packing \mathbf{P} and a face path γ in the domain with at least one interior face are given. Let $f : \gamma \rightarrow \mathbb{C}$ be any complex valued function, typically taken to be the restriction to γ of some $f : \mathbf{P} \rightarrow \mathbb{C}$.

The face path γ can be partitioned into segments bounded by the dual centers belonging to the interior faces of γ . Let \mathcal{S}_γ be the collection of such segments s ; we identify s by the edge intersection point it contains. Under this partitioning scheme, each segment s of γ contains exactly one edge intersection point belonging to γ . Using this notation we define the *euclidean and hyperbolic deformation metrics*.

In the discussions that follow we will need to have an established parametrization for γ . In the euclidean setting we will take the parametric representation to be symmetric with respect to the euclidean arc length of γ ; specifically, let the euclidean length of the path γ be 2ρ and choose the parametrization by arc length $\gamma(t)$ with $t \in [-\rho, \rho]$. In the hyperbolic setting we will take the parametric representation to be symmetric with respect to either the hyperbolic or pseudo-hyperbolic arc length of γ , the choice to be specified in context.

Definition 3.5.1 (Euclidean Deformation Metric). The *euclidean deformation metric* of f

along the path γ is defined to be

$$EDM_\gamma(f) = \max_{s \in \mathcal{S}_\gamma} \left(\frac{|\tilde{f}|^2 \int_{\gamma|_s} |dz|}{\int_{\gamma|_s} |f|^2 |dt|} \right)$$

where $w(t) = \gamma|_s(t)$ represents the segment s of γ using the original parametrization by arc length along the path and the maximum is taken over the segments $s \in \mathcal{S}_\gamma$ meeting the edge intersection point \tilde{z} in the interior of γ with the notation \tilde{f} representing the function value at the face boundary point \tilde{z} of the segment s . For a circle packing $F : \mathbf{P} \rightarrow \mathbf{P}'$ define $EDM(f) = \sup EDM_\gamma(f)$ over all minimal paths γ of the domain packing \mathbf{P} .

We similarly define the hyperbolic deformation metric for a function f whose domain is contained in the unit disc.

Definition 3.5.2 (Hyperbolic Deformation Metric). The *hyperbolic deformation metric* of f with respect to the path γ is defined as

$$HDM_\gamma(f) = \frac{1}{2} \max_{s \in \mathcal{S}_\gamma} \left(\frac{\frac{|\tilde{f}|^2}{1-|\tilde{z}|^2} \int_{\gamma|_s} \frac{2|dz|}{1-|z|^2}}{\int_{\gamma|_s} \frac{|f|^2 |dt|}{(1-t^2)^2}} \right)$$

where $w(t) = \gamma|_s(t)$ represents the segment s of γ using the original parametrization by arc length along the path and the maximum is taken over the segments $s \in \mathcal{S}_\gamma$ meeting the edge intersection point \tilde{z} in the interior of γ with the notation \tilde{f} representing the function value at the face boundary point \tilde{z} of the segment s . For a circle packing with hyperbolic geometry define $HDM(f) = \sup HDM_\gamma(f)$ over all minimal hyperbolic paths γ of the domain packing \mathbf{P} .

For both the euclidean and hyperbolic deformation metrics, we take the deformation metric to have value 1 when the path γ contains no interior faces.

Before continuing, we remark that for a projective face linear system and given path γ there is a well defined piecewise linear system along the path that can be constructed by use of the character of the projective face linear system. With this in mind, the above definitions can be applied with the convention that the sign of particular linear map for each face in the face path is chosen in a consistent fashion. This convention will be used throughout the remainder of this thesis to simplify notation.

3.6 Functions with Specified Schwarzian Derivative

It is a useful fact that meromorphic functions with specified Schwarzian derivative are given as the ratio of two linearly independent solutions to the second order differential equation

$$y'' + p(z)y = 0 \tag{3.21}$$

where $p(z) = S_f(z)/2$. This fact is fundamental to the initial studies of zero's of analytic functions and subsequent studies of univalence by Nehari. A construction to reproduce this result in the circle packing context will be presented with the *discrete Schwarzian* serving as the quantity p above.

The fundamental objects under consideration in the following construction are the face Möbius maps underlying a circle packing map $F : \mathbf{P} \rightarrow \mathbf{Q}$. By a previous proposition we showed that the face Möbius maps are the quotients of two *projective face linear systems* on \mathbf{P} having the same projective character. We will show that each of the projective face linear systems satisfies a discrete difference interpretation of 3.21, giving a relation with the face Möbius mappings of F .

First we make a few remarks about solutions to the differential equation 3.21.

Remark 3.6.1. If u and v are two solutions of 3.21, then the expression

$$u'v - uv'$$

is constant.

PROOF: By direct computation

$$\frac{d}{dz}(u'v - uv') = u''v + u'v' - u'v' - uv'' = -p(uv - uv) = 0. \square$$

Proposition 3.6.2. Let $f(z)$ be analytic on Ω with $p(z) = S_f(z)/2$, and let u and v be two linearly independent solution of 3.21 with $f(z) = u(z)/v(z)$ and $u'v - uv' = 1$. Then, the best fit Möbius map M_0 at a point $z_0 \in \Omega$ is given by

$$M_0(z) \sim \begin{bmatrix} u'_0 & u_0 - u'_0 z \\ v'_0 & v_0 - v'_0 z \end{bmatrix}.$$

(where $u_0 = u(z_0)$, $u'_0 = u'(z_0)$ etc.)

PROOF: Using the notation in the proposition, let $\mu = \begin{bmatrix} u'_0 & u_0 - u'_0 z \\ v'_0 & v_0 - v'_0 z \end{bmatrix}$. Then, since u and v are linearly independent with $u'v - uv' = 1$ we have

$$\det(\mu) = u'_0(v_0 - v'_0 z) - v'_0(u_0 - u'_0 z) = u'_0 v_0 - v'_0 u_0 = 1.$$

Also $f(z_0) = (u/v)(z_0) = \mu(z_0)$, $f'(z_0) = (u/v)'(z_0) = (\frac{u'v - uv'}{v^2})(z_0) = \frac{1}{v_0^2} = \mu'(z_0)$ and since since $d(u'v - uv') = 0$, we also have $f''(z_0) = -\frac{2}{v_0^3} = \mu''(z_0)$. \square

The above proposition was noted after the circle packing results to follow were discovered. This relationship between the differential equation 3.21 and Möbius maps provides a strong parallel with the circle packing construction.

3.7 Circle Packing Quotient Theorem

In the following discussions we will need to clarify the meaning of the difference operator acting across a directed edge on a projective face linear system. By our definition, the projective face linear system has a *character* $\mathcal{S} : \mathcal{E} \rightarrow \{\pm 1\}$. We will interpret the discrete difference operator to account for the character of the edge of interest. In particular, if $g \uparrow_{\vec{e}} f$ then the discrete difference operator $\Delta_{\vec{e}}$ will act on the neighboring linear expressions A_f and A_g in the following fashion: the discrete difference is computed by considering the quantity associated with $\mathcal{S}(e)A_g$ and subtracting the quantity associated with A_f . The finite difference expressions in this thesis are written with this convention in mind.

Theorem 3.7.1 (Circle Packing Quotient Theorem). *Let \mathbf{P} be a circle packing over a complex K and let $\sigma_{\vec{e}}$ be a valid discrete Schwarzian assignment on the directed edges of K . Then if $\mathbf{A} = \{A_f(z) = a_f z + b_f : f \in \mathcal{F}; a_f, b_f \in \mathbb{C}\}$, $\mathbf{B} = \{B_f(z) = c_f z + d_f : f \in \mathcal{F}\}$ are two projective face linear systems with the same projective character and which are linearly independent solutions to the discrete difference system:*

$$\Delta \begin{pmatrix} a \\ b \end{pmatrix} = \sigma_{\vec{e}} A_f(z_e) \begin{pmatrix} 1 \\ -z_e \end{pmatrix}, \quad (3.22)$$

with the difference across each directed edge \vec{e} then there is a constant λ such that the face wise Möbius mapping $M = \frac{\lambda \mathbf{A}}{\mathbf{B}}$ is a determinant normalized face Möbius map for \mathbf{P} . Moreover, every circle packing map $F : \mathbf{P} \rightarrow \mathbf{P}'$ over K is given by such a quotient.

PROOF: Suppose that \mathbf{A}, \mathbf{B} are two linearly independent solutions under the conditions of the theorem. Since the two solutions are linearly independent, there is a face for which the quotient $\begin{bmatrix} a_f & b_f \\ c_f & d_f \end{bmatrix}$ has determinant $1/\lambda$. Form the face quotient map $M = \lambda \mathbf{A}/\mathbf{B}$ (we may scale \mathbf{A} to ensure $\lambda \equiv 1$ since inspection shows that scalar multiples of solutions are also solutions to the difference system). Let $f \in \mathcal{F}$ be a face such that $\det(\mu_f) = 1$ and let $f \sim g$ be two faces of \mathbf{P} , ordered by the convention $g \uparrow_{\vec{e}} f$, and compute $dM_{\vec{e}} = \mu_f^{-1} \mu_g$. By construction we can denote

$$\mu_f = \begin{bmatrix} a & b \\ c & d \end{bmatrix}$$

with

$$\mu_g = \mu_f + \sigma_{\vec{e}} \begin{bmatrix} A_f(z_e) & -zA_f(z_e) \\ B_g(z_e) & -zB_g(z_e) \end{bmatrix}.$$

Now

$$dM = \mu_f^{-1} \mu_g \sim \mathbb{I} + \sigma_{\vec{e}} \begin{bmatrix} d & -b \\ -c & a \end{bmatrix} \begin{bmatrix} A_f(z_e) & -zA_f(z_e) \\ B_f(z_e) & -zB_f(z_e) \end{bmatrix}$$

$$= \mathbb{I} + \sigma_{\vec{e}} \begin{bmatrix} dA_f - bB_f & -z(dA_f - bB_f) \\ -cA_f + aB_f & -z(-cA_f + aB_f) \end{bmatrix}$$

but $A_f(z_e) = az_e + b, B_f(z_e) = cz_e + d$ so that

$$dM = \mathbb{I} + \det(\mu_f)\sigma_{\vec{e}} \begin{bmatrix} z & -z^2 \\ 1 & -z \end{bmatrix} = \mathbb{I} + \sigma_{\vec{e}} \begin{bmatrix} z & -z \\ 1 & -z \end{bmatrix}.$$

Note that $\det(dM) = 1$ with single fixed point z (since $\text{trace}(dM) = 2$ giving a parabolic Möbius map) when $\sigma_{\vec{e}} \neq 0$. Since $\sigma_{\vec{e}}$ is a valid discrete Schwarzian assignment the quotient face map then corresponds to a circle packing.

Moreover, let M be a circle packing map for K normalized with determinant 1, then the numerators and the denominators form protective face linear systems with the same character by theorem 3.4.2. We reproduce the computation here in this context. If \mathbf{A}, \mathbf{B} are the numerator and denominators of the unit determinant face Möbius mappings, then we claim that \mathbf{A}, \mathbf{B} satisfy the discrete difference systems 3.22. Direct computation shows that for appropriate choice of representatives across a directed edge

$$\begin{aligned} \Delta M &= \sigma_{\vec{e}} \begin{bmatrix} a & b \\ c & d \end{bmatrix} \begin{bmatrix} z & -z^2 \\ 1 & -z \end{bmatrix} \\ &= \sigma_{\vec{e}} \begin{bmatrix} az + b & -z(az + b) \\ cz + d & -z(cz + d) \end{bmatrix}. \end{aligned}$$

In particular

$$\Delta \begin{pmatrix} a \\ b \end{pmatrix} = \sigma_{\vec{e}} A_f(z_e) \begin{pmatrix} 1 \\ -z_e \end{pmatrix} \quad \text{and} \quad \Delta \begin{pmatrix} c \\ d \end{pmatrix} = \sigma_{\vec{e}} B_f(z_e) \begin{pmatrix} 1 \\ -z_e \end{pmatrix}. \quad \square$$

Remark 3.7.2. Solutions to the discrete difference system 3.22 can be expressed as face linear solutions to the discrete difference system

$$\Delta y' - \sigma y = 0. \tag{3.23}$$

where the difference is across the directed edges of an underlying circle packing \mathbf{P} .

The above theorem states that the numerators and denominators belonging to the face Möbius mapping between two circle packings of K are geometrically realized as projective face linear systems. Figure 3.2 illustrate an underlying hexagonal combinatoric structure with the numerator-denominator pairs for two circle packing maps (corresponding to the maximal packing map and an approximation to $z \mapsto z^2$ respectively).

We next give a corollary that emphasizes the parallels of the circle packing theory with the classical analytic function theory.

Corollary 3.7.3. *Let u and v be linearly independent solutions of 3.23 then*

$$\Delta(u'v - v'u) = 0.$$

PROOF: Since u and v are face linear systems they can be represented on a fixed face by $u(z) = u'z + u_0$ and $v(z) = v'z + v_0$. Then

$$0 = \Delta(\det([u/v])) = \Delta(u'v_0 - v'u_0) = \Delta(u'(v'z + v_0) - v'(u'z + u_0)) = \Delta(u'v - v'u). \square$$

Corollary 3.7.4. *Let \mathbf{P} be a circle packing of a complex K and let $\sigma_{\vec{e}}$ be a valid discrete Schwarzian assignment. Then if \mathbf{u}, \mathbf{v} are two projective face linear systems with the same projective character which are linearly independent solutions to the discrete difference system 3.23, then if \mathbf{M} is the unit determinant face Möbius mapping determined by the quotient \mathbf{u}/\mathbf{v} then the map F on domain \mathbf{P} corresponding to M is a circle packing map. Moreover every circle packing map $F : \mathbf{P} \rightarrow \mathbf{P}'$ having combinatoric structure K is given by such a quotient.*

PROOF: The proof is a restatement using the above remark. \square .

3.8 A Discrete Hille Condition

Following the formulations of Hille, we multiply the discrete difference system 3.23 by \bar{y} and sum over a chain of neighboring edge intersections to arrive at a discrete analog of the Green's function condition used by Hille in the study of zeros to solutions of 3.21. We introduce some notation first. Let y be a face linear system (face wise linear and continuous at the edge intersection points). For indexing take the sequence of faces (f_0, \dots, f_N) and edges intersections as illustrated schematically as

$$f_0 \mid_{z_1} f_1 \mid_{z_2} \dots \mid_{z_{N-1}} f_{N-1} \mid_{z_N} f_N.$$

Now summing over the N edge intersection points, $\{z_1, z_2, \dots, z_N\}$ gives

$$\sum \bar{y} \Delta y' - \sum \sigma |y|^2 = 0. \quad (3.24)$$

The slope of the face linear system on face f_k is denoted y'_k or a_k , while the value at edge intersection point z_k is denoted y_k . The discrete difference Δy and $\Delta y'$ have the usual meaning across an edge intersection point, $\Delta_k y = y_k - y_{k-1}$ and $\Delta_k y' = a_k - a_{k-1}$.

Let γ be an edge terminated non degenerate face path, joining edge e_0 and edge e_N .

Summing by parts, using the expression

$$\sum_m^n a_k b_k = A_{n,m} b_n - \sum_m^{n-1} A_{k,m} (b_{k+1} - b_k), \quad (A_{k,m} = \sum_{j=k}^m a_j)$$

over γ gives the left sum as

$$\begin{aligned} S &= \sum_1^N \bar{y} \Delta y' = \bar{y}_N (y'_N - y'_0) - \sum_1^{N-1} (y'_k - y'_0) \Delta_{k+1} \bar{y} \\ &= \bar{y}_N y'_N - \sum_1^{N-1} (y'_k) \Delta_{k+1} \bar{y} - y'_1 \left(\bar{y}_N - \sum_1^{N-1} \Delta_{k+1} \bar{y} \right) \\ &= \bar{y}_N a_N - \bar{y}_1 a_0 - \sum_1^{N-1} (y'_k) \Delta_{k+1} \bar{y}. \end{aligned} \tag{3.25}$$

Then the expression $\sum \bar{y} \Delta y' - \sum \sigma |y|^2 = 0$ can be written

$$\bar{y}_N a_N - \bar{y}_1 a_0 - \sum_1^{N-1} (y'_k) \Delta_{k+1} \bar{y} - \sum \sigma |y|^2 = 0 \tag{3.26}$$

An alternate expression in terms of the interior face (incircle) radii, ρ_k , the dual edge directions η_k and the face linear slopes a_k is

$$\bar{y}_N a_N - \bar{y}_1 a_0 - \sum_1^{N-1} (y'_k) \rho_k \bar{a}_k (\bar{\eta}_{k+1} - \bar{\eta}_k) - \sum \sigma |y|^2 = 0 \tag{3.27}$$

This expression will yield the discrete Hille condition mentioned above.

Lemma 3.8.1 (Discrete Hille Identity). *Let F be a face linear system on K and γ be a face path joining two zeros, w_0 and w_N , of F . Then*

$$\int_{\gamma} |y'|^2 dz = - \sum_{\mathcal{E}(\gamma)} \sigma_{\vec{e}} |y|^2.$$

PROOF: The proof is accomplished by elimination of the boundary terms of 3.27. As above use the face labeling notation

$$f_0 |_{z_1} f_1 |_{z_2} \dots |_{z_{N-1}} f_{N-1} |_{z_N} f_N.$$

The lemma states that the discrete sum is equal to the usual integral over the piecewise linear function. Let y_k denote the function value at an edge intersection and a_k denote the derivative on face k . (For notation take the k^{th} face to be to the right of the k^{th} edge.) With

this notation, since $w_0 \in f_0$, we have $y_1 = a_0(z_1 - w_0)$, and similarly $y_N = -a_N(z_N - w_N)$. Computing the integral $\int_{\gamma} |y'|^2$ gives

$$\int_{\gamma} |y'|^2 \overline{dz} = \int_{w_0}^{z_1} |y'|^2 \overline{dz} + \sum_1^{N-1} \int_{z_k}^{z_{k+1}} |y'|^2 \overline{dz} + \int_{z_N}^{w_N} |y'|^2 \overline{dz}$$

so that

$$\sum_1^{N-1} |a_k|^2 \rho_k (\bar{\eta}_{k+1} - \bar{\eta}_k) = \int_{\gamma} |y'|^2 \overline{dz} - \left(\int_{w_0}^{z_1} |y'|^2 \overline{dz} + \int_{z_N}^{w_N} |y'|^2 \overline{dz} \right)$$

Substituting into Hille's condition (3.27) gives

$$\bar{y}_N a_N - \bar{y}_1 a_0 - \left(\int_{\gamma} |y'|^2 \overline{dz} - \left(\int_{w_0}^{z_1} |y'|^2 \overline{dz} + \int_{z_N}^{w_N} |y'|^2 \overline{dz} \right) \right) - \sum \sigma |y|^2 = 0.$$

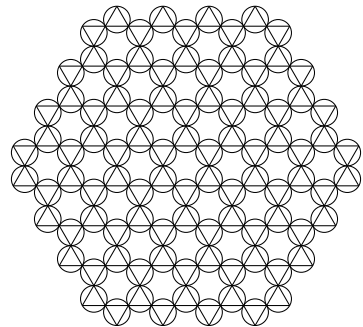
but $\bar{y}_1 a_0 = \int_{w_0}^{z_1} |y'|^2 \overline{dz}$, and $\bar{y}_N a_N = - \int_{z_N}^{w_N} |y'|^2 \overline{dz}$ so that

$$\int_{\gamma} |y'|^2 \overline{dz} = - \sum \sigma |y|^2. \quad \square$$

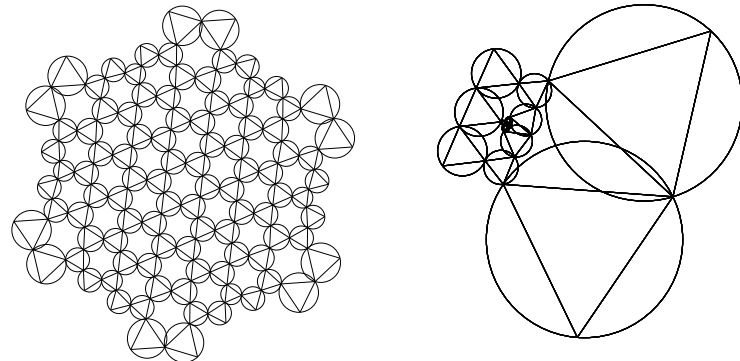
For comparison, Hille's original analytic condition is given by

$$\int_{z_0}^{z_1} |y'|^2 \overline{dz} = \int_{z_0}^{z_1} p |y|^2 dz.$$

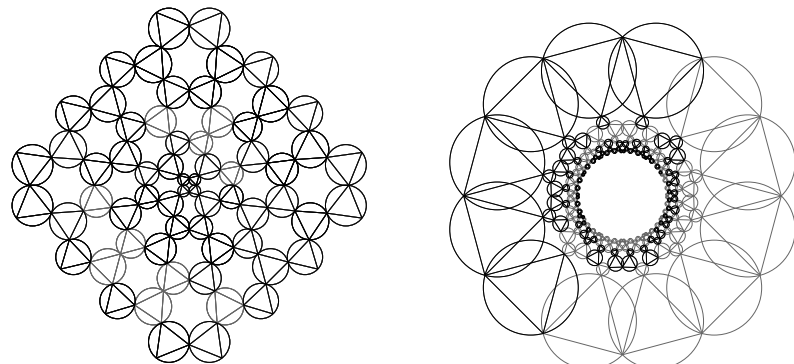
where y is a solution to $y'' + p(z)y = 0$ with zeros at z_0 and z_1 .



(a) Hexagonal Lattice Domain



(b) Example Face Linear Systems



(c) Example Projective Face Linear System

Figure 3.2: Example Interior Face Linear Systems.

Figure (a) shows the underlying regular hexagonal combinatoric triangulation, (b) shows *face linear systems* on the regular hexagonal combinatoric structure for the Möbius mapping numerator and denominator for the maximal packing map, while (c) shows *projective face linear systems* for a circle packing approximation of $z \mapsto z^2$.

Chapter 4

Univalence Results

4.1 Zeros of Circle Packing Maps

A circle packing map preserves the orientation of the packing's vertex triples by construction. This leads to the following conclusions about the zeros of circle packings maps.

Proposition 4.1.1. *Let $F : \mathbf{P} \rightarrow \mathbf{Q}$ be a circle packing map with face Möbius mapping $M = A/B$ where A and B are projective face linear systems for \mathbf{P} . Then*

1. *The image of the dual circles of \mathbf{P} under B does not contain the origin.*
2. *If w lies in a dual circle of \mathbf{P} then $A(w) = 0$ if and only if w is a zero of F .*

PROOF: The face Möbius mapping M is an isomorphism from the dual circle interiors of \mathbf{P} onto those of \mathbf{Q} . First suppose $B(w) = 0$ for some $w \in \mathcal{C}^o$ where \mathcal{C} is a closed dual circle of \mathbf{P} (w does not lie in the boundary of the dual circle since the image of the dual circle boundary is a usual circle and not a line). If $A(w) \neq 0$ then $M|_{\mathcal{C}}$ is an inversion contradicting the orientation of the cycle of edge intersection points about the face containing \mathcal{C} ; therefore conclude $A(w) = 0$. Now A and B are then linear with common zero on the same face, hence they are scalar multiples so that the image of the corresponding dual circle collapses to a point – a contradiction. Therefore we conclude that the image of the dual circles under B excludes the origin. Next, let w be a zero of F (taking the usual Möbius extension on the dual circles) lying in a closed dual circle of \mathbf{P} . Since $B(w) \neq 0$, $F(w) = A(w)/B(w)$ implies $A(w) = 0$. The converse is immediate: for z in a dual circle of \mathbf{P} , $A(z) = 0$ implies $F(z) = 0$. \square .

As in the case of Hille's characterization, the zeros of a circle packing map are precisely given by the zeros of the face Möbius map numerators. This relation coupled with a discrete criteria on zeros allows Nehari's univalence results to be stated for circle packings. First let us restate the discrete version of Hille's characterization of zeros for solutions to the Schwarzian differential equation 3.21.

By lemma 3.8.1, if y is a face linear map with interior face path $\gamma : [0, 1] \rightarrow \text{carrier}(\mathbf{P})$ with $y(\gamma(0)) = y(\gamma(1)) = 0$, then

$$\int_{\gamma} |y'|^2 \overline{dz} = - \sum_{\gamma} \sigma |y|^2. \quad (4.1)$$

This statement gives a fundamental equality for studying the zeros of solutions to the discrete difference system 3.23 and hence for circle packing maps in general.

4.2 Zeros and Univalence

This section sets up the discussion of schlicht circle packing maps following the approach Nehari took in his paper. We begin with some definitions.

Definition 4.2.1 (Interior Carrier). The *interior carrier* for a complex K is defined to be the interior of the abstract dual of K . We similarly define the *interior carrier* of a univalent circle circle packing \mathbf{P} to be the closure of the interior portion of the dual carrier of \mathbf{P} , specifically the *interior carrier* is the closure of the union of the unbounded components of the *carrier*(\mathbf{P}) when partitioned by the dual edges of \mathbf{P} .

Definition 4.2.2 (Univalent Circle Packing Map). We say that a circle packing map $F : \mathbf{P} \rightarrow \mathbf{Q}$ is *univalent* if the restriction of F to the interior carrier of the domain packing \mathbf{P} is univalent.

The following remarks are evident since circle packing maps take oriented circle packing quadrilaterals to oriented circle packing quadrilaterals – taking an *interstice* to be the circular polygon about an interior vertex bounded by the packing dual circles.

Remark 4.2.3. Let \mathbf{P} be a circle packing in the disc or plane with neighboring interstices I_1 and I_2 . If $F : \mathbf{P} \rightarrow \mathbf{Q}$ is a circle packing map then the images of I_1 and I_2 are disjoint.

Remark 4.2.4. Let \mathbf{P} be a circle packing in the disc or plane with neighboring interstices I_1 and I_2 which share a common cycle of dual circles then $I_1 \equiv I_2$, i.e. both correspond to the same vertex of the underlying complex.

Remark 4.2.5. Let \mathbf{P} be a circle packing in the disc or plane and let z_1 and z_2 be interior points of neighboring faces. If $F : \mathbf{P} \rightarrow \mathbf{Q}$ is a circle packing map then $F(z_1) \neq F(z_2)$.

We are interested in expressing conditions on circle packing univalence by construction of a path γ in the domain packing joining two distinct points with a common image. The next proposition in effect shows that we may suppose the initial and terminal points each lie in a dual circle of the domain packing.

Proposition 4.2.6. *Let $F : \mathbf{P} \rightarrow \mathbf{Q}$ be a non-univalent circle packing map then there are points z_1 and z_2 each lying on the dual edges of \mathbf{P} .*

PROOF: Let F be non-univalent so that there are points z_1 and z_2 in the interior carrier of \mathbf{P} with $F(z_1) = F(z_2)$; since F is a circle packing map the points cannot lie in a common vertex interstice. There are three cases: (1) both z_1 and z_2 lie on dual edges of \mathbf{P} , (2) both lie in a vertex interstice, and (3) one of the z_1 or z_2 lies on the dual edge of \mathbf{P} and the other in a vertex interstice. We may exclude case (1). For case (2), let Ω_1 and Ω_2 be the vertex interstices containing z_1 and z_2 respectively. Since $\partial\Omega_1 \cap \partial\Omega_2 = \emptyset$ we have $\partial\Omega_1 \subset \Omega_2 \subset \partial\Omega_1$ a contradiction. For case (3), suppose z_2 lies on a dual edge of \mathbf{P} and suppose $z_1 \in \Omega_1$ for some vertex interstice. Let D be the union of the dual edges of \mathbf{P} . Since the D is connected we then have $D \subset \Omega_1 \subset \partial\Omega_1$ a contradiction. \square

Nehari's 1948 paper on *The Schwarzian Derivative and Schlicht Function* (Nehari, 1949) presented a then new approach to the study of univalent functions. Nehari's paper follows up the work of Einar Hille (Hille, 1922) and exploits two of Hardy, Littlewood and Polya's once obscure inequalities from their compilation in G. H. Hardy (1934). Nehari used the approach of Hille in studying the zeros of solutions to the differential equation

$$y'' + py = 0 \quad (4.2)$$

since it was known that analytic functions with Schwarzian derivative $2p$ are the ratios of two such linearly independent solutions. Nehari derived his univalence results by application of two integral inequalities for real valued differentiable functions.

The proofs of these integral inequalities presented in the original paper assume differentiability over the interval of definition however they also hold for piecewise differentiable functions as in the following remarks.

Remark 4.2.7. Let $u(x)$ be continuous, piecewise differentiable on the interval $[\pi/2, \pi/2]$ with zeros of the first order at $\pm\pi/2$ then

$$\int_{-\pi/2}^{\pi/2} u^2 dx \leq \int_{-\pi/2}^{\pi/2} u'^2 dx \quad (4.3)$$

with equality for $y(x) = c \cos(x)$.

Remark 4.2.8. Let $y(x)$ be a continuous, piecewise differentiable function defined on the interval $[-1, 1]$ with zeros of the first order at $x = \pm 1$, then

$$\int_{-1}^1 \frac{u^2 dx}{(1-x^2)^2} < \int_{-1}^1 u'^2 dx \quad (4.4)$$

with strict inequality.

For our applications we will need a change of variables for each of the above inequalities.

With the change of variables $x \mapsto (\pi/2\rho)r$ the inequality 4.3 becomes

$$\int_{-\rho}^{\rho} u^2 dr \leq \frac{4\rho^2}{\pi^2} \int_{-\rho}^{\rho} u'^2 dr, \quad (4.5)$$

and with the change of variables $x \mapsto \rho x$ the inequality 4.4 becomes

$$\rho^2 \int_{-\rho}^{\rho} \frac{u^2 dx}{(\rho^2 - x^2)^2} < \int_{-\rho}^{\rho} u'^2 dx. \quad (4.6)$$

Before continuing we will consider two results concerning the zeros of circle packing maps.

4.3 Some Results on Zeros of Circle Packing Maps

In the statements that follow, when u is a function on the carrier of a circle packing \mathbf{P} we will use the notation \tilde{u} to represent the value of the function u on the appropriate edge intersection point of \mathbf{P} .

Lemma 4.3.1. *Let u be a solution to 3.23 for a maximal packing of the disc having two distinct zeros lying on the combinatoric dual of the domain, z_0 and z_1 . If γ is a minimal face path connecting z_0 and z_1 with euclidean domain path directivity measure k then for some edge intersection point and neighboring segment s of γ the discrete Schwarzian parameter σ satisfies the inequality*

$$|\sigma_e| \geq \frac{k\pi^2}{4} \frac{\int_{\gamma|_s} |u|^2 dt}{|\tilde{u}|^2} \quad (4.7)$$

PROOF: Suppose u is a face linear solution to 3.23 for a maximal packing of the disc with two zeros, z_0 and z_1 , lying on the combinatoric dual of the domain, and further suppose that the inequality

$$|\sigma_e| < \frac{k\pi^2}{4} \frac{\int_{\gamma|_s} |u|^2 dt}{|\tilde{u}|^2} \quad (4.8)$$

holds at each edge intersection point of γ . By construction we have

$$k \int_{\gamma} |u'|^2 |\overline{dz}| < \left| \int_{\gamma} |u'|^2 \overline{dz} \right| = \left| \sum \sigma |u|^2 \right| \leq \sum |\sigma| |u|^2.$$

Supposing 4.8 holds we have

$$\begin{aligned} k \int_{\gamma} |u'|^2 |\overline{dz}| &< \sum \frac{k\pi^2}{4} \int_{\gamma|_s} |u|^2 dt = \frac{k\pi^2}{4} \int_{\gamma} |u|^2 dt \\ &\leq k\rho^2 \int_{-\rho}^{\rho} |u'|^2 dt \leq k \int_{-\rho}^{\rho} |u'|^2 dt. \end{aligned}$$

This is a contradiction of 4.5 since we may consider the real and imaginary components of u separately.

Lemma 4.3.2. *Let u be a solution to 3.23 for a maximal packing of the disc having two distinct zeros lying on the combinatoric dual of the domain, z_0 and z_1 . If γ is a minimal face path connecting z_0 and z_1 with euclidean domain path directivity measure k and euclidean length less than 2 then for some edge intersection point and neighboring geodesic segment s of γ the discrete Schwarzian parameter σ satisfies the inequality*

$$|\sigma_{\bar{e}}| \geq k \frac{\int_{\gamma|_s} |u|^2 \frac{dt}{(1-|t|^2)^2}}{|\tilde{u}|^2}. \quad (4.9)$$

PROOF: Suppose u is an face linear solution to 3.23 for a maximal packing of the disc with two zeros, z_0 and z_1 , lying on the combinatoric dual of the domain, and further suppose that the inequality

$$|\sigma_{\bar{e}}| < k \frac{\int_{\gamma|_s} |u|^2 \frac{dt}{(1-|t|^2)^2}}{|\tilde{u}|^2}. \quad (4.10)$$

holds at each edge intersection point of γ . By construction we have

$$k \int_{\gamma} |u'|^2 |\overline{dz}| < \left| \int_{\gamma} |u'|^2 \overline{dz} \right| = \left| \sum \sigma |u|^2 \right| \leq \sum |\sigma| |u|^2.$$

By 4.10 we have

$$k \int_{\gamma} |u'|^2 |\overline{dz}| < k \int_{\gamma} |u|^2 \frac{dt}{(1-|t|^2)^2} \leq k \rho^2 \int_{-\rho}^{\rho} \frac{|u|^2 dt}{(\rho^2 - t^2)^2} \leq k \int_{-\rho}^{\rho} |u'|^2 dt$$

contradicting 4.6.

We now apply the above lemmas to obtain equivalent statements for circle packing maps.

Theorem 4.3.3. *Let $F : \mathbf{P} \rightarrow \mathbf{P}'$ be a circle packing map for a maximal packing of the disc having two distinct zeros lying on the combinatoric dual of the domain, z_0 and z_1 and let F have face Möbius mapping \mathbf{u}/\mathbf{v} . If γ is a minimal path connecting z_0 and z_1 with euclidean domain path directivity measure k then for some edge intersection point and neighboring segment s of γ the discrete Schwarzian σ of F satisfies the inequality*

$$|\sigma_{\bar{e}}| \geq \frac{k\pi^2}{4} \frac{\int_{\gamma|_s} |u|^2 dt}{|\tilde{u}|^2} \quad (4.11)$$

PROOF: Let F be a circle packing map for a maximal packing having face Möbius map

$\mathbf{M} = \mathbf{u}/\mathbf{v}$. Then by hypothesis u satisfies the conditions of lemma 4.3.1 and

$$|\sigma_{\vec{e}}| \geq \frac{k\pi^2}{4} \frac{\int_{\gamma|_s} |u|^2 dt}{|\tilde{u}|^2}$$

for some edge intersection point along γ .

Theorem 4.3.4. *Let $F : \mathbf{P} \rightarrow \mathbf{P}'$ be a circle packing map for a maximal packing of the disc having two distinct zeros lying on the combinatoric dual of the domain, z_0 and z_1 and let F have face Möbius mapping \mathbf{u}/\mathbf{v} . If γ is a minimal hyperbolic path connecting z_0 and z_1 with euclidean domain path directivity measure k and euclidean length less than 2 then for some edge intersection point and neighboring segment s of γ the discrete Schwarzian σ of F satisfies the inequality*

$$|\sigma_{\vec{e}}| > k \frac{\int_{\gamma|_s} |u|^2 \frac{dt}{(1-|t|^2)^2}}{|u_{\vec{e}}|^2}. \quad (4.12)$$

PROOF: Let F be a circle packing map for a maximal packing having face Möbius map $\mathbf{M} = \mathbf{u}/\mathbf{v}$. Then by hypothesis u satisfies the conditions of lemma 4.3.2 and

$$|\sigma_{\vec{e}}| \geq k \frac{\int_{\gamma|_s} |u|^2 \frac{dt}{(1-|t|^2)^2}}{|u_{\vec{e}}|^2}$$

for some edge intersection point along γ . \square

We would like to extend these results to statements about the univalence of circle packing maps; a particular goal is to quantify the discretization effects that impact a circle packing equivalent of Nehari's univalence proofs.

4.4 The Results of Nehari

Nehari's paper presented three results namely which we would like to frame in the circle packing setting – these results are presented using his original notation with $\{w, z\}$ representing the Schwarzian derivative of w with respect to z .

Theorem 4.4.1. *In order that the analytic function $w = f(z)$ be schlicht in $|z| < 1$, it is necessary that*

$$|\{w, z\}| \leq \frac{6}{(1 - |z|^2)^2}$$

and sufficient that

$$|\{w, z\}| \leq \frac{2}{(1 - |z|^2)^2}.$$

Theorem 4.4.2. *If*

$$|\{w, z\}| \leq \pi^2/2$$

in $|z| < 1$, then $w = f(z)$ is schlicht in the unit disc. The constant $\pi^2/2$ is the best possible.

Corollary 4.4.3. *The radius of univalence of the function $w = f(z)$ is at least equal to the smallest positive root ρ_0 of the equation*

$$\rho^2 M(\rho) = \pi^2/2, \quad (4.13)$$

where

$$M(\rho) = \max_{|z|=\rho} |\{w, z\}|. \quad (4.14)$$

Discrete analytic results are presented for the sufficiency conditions of Nehari's results as well as an analog of the radius of univalence corollary.

The discrete Schwarzian like the traditional Schwarzian derivative has an invariant in the hyperbolic metric. It is well known that if $f : \mathbb{D} \rightarrow \Omega$ is an analytic function on the unit disc with

$$|S_f(z)| < \frac{2}{(1 - |z|^2)^2}$$

then for any automorphism of the disc, h the same inequality holds for $f \circ h$, namely

$$|S_{f \circ h}(w)| < \frac{2}{(1 - |w|^2)^2}$$

with $z = h(w)$. We now show a similar result for circle packings.

Lemma 4.4.4. *Let $F : \mathbb{D} \rightarrow \mathbf{P}$ be a circle packing map whose domain is a maximal packing of the disc, let H be an automorphism of the disc and let $G = F \circ H$. Let $\sigma_F : \vec{\mathcal{E}} \rightarrow \mathbb{C}$ and $\sigma_G : \vec{\mathcal{E}} \rightarrow \mathbb{C}$ be the discrete Schwarzian for the circle packing maps F and $G = F \circ H$ respectively. If M is a positive constant such that*

$$|\sigma_F(z)| \leq \frac{M}{1 - |z|^2}$$

along each directed edge \vec{e} at the corresponding edge intersection $z = z_e$, then if $w = w_e = H^{-1}(z_e)$ the discrete Schwarzian of G satisfies

$$|\sigma_G(w)| \leq \frac{M}{1 - |w|^2}$$

where $z = H(w)$.

PROOF: Let $F : \mathbb{D} \rightarrow \mathbf{P}$ be a circle packing map. The task is to find an invariant form relating to the discrete Schwarzian. Consider the composed mapping

$$\mathbb{D} \xrightarrow{\phi} \mathbb{D} \xrightarrow{F} \mathbf{P}$$

where H is an automorphism of the disc with matrix representation $[H]$. Let $G = F \circ H$, we

need to express the discrete Schwarzian of G in terms of H and dM_F . Using this notation we get the edge derivatives of G

$$dM_G = [H]^{-1} dM_F[H].$$

It is a well known fact that every automorphism of the disc can be expressed as the composition of two rotations, $w = kz(|k| = 1)$, and a general linear transformation of the form $w = (\beta - z)/(1 - \beta z)$ with real valued β in the interval $(-1, 1)$. There are then two cases to consider

$$H(z) = kz, \quad |k| = 1$$

and

$$H(z) = \frac{\beta - z}{1 - \beta z}, \beta \in (-1, 1).$$

In the first case (with $H(z) = kz, |k| = 1$) taking $w = H(z)$ we get

$$dM_G \sim \mathbb{I} + c_F \begin{bmatrix} 1/k & 0 \\ 0 & 1 \end{bmatrix} \begin{bmatrix} z & -z^2 \\ 1 & -z \end{bmatrix} \begin{bmatrix} k & 0 \\ 0 & 1 \end{bmatrix}$$

$$dM_G \sim \mathbb{I} + c_F \begin{bmatrix} 1/k & 0 \\ 0 & 1 \end{bmatrix} \begin{bmatrix} kz & -z^2 \\ k & -z \end{bmatrix}$$

$$dM_G \sim \mathbb{I} + c_F \begin{bmatrix} z & -z^2/k \\ k & -z \end{bmatrix}$$

$$dM_G \sim \mathbb{I} + c_F k \begin{bmatrix} w & -w^2 \\ 1 & -w \end{bmatrix}$$

with $w = H(z) = z/k$. and in the second case (with $H(z) = \frac{\beta - z}{1 - \beta z}, \beta \in (-1, 1)$),

$$dM_G \sim (1 - \beta^2)\mathbb{I} + c_F \begin{bmatrix} -1 & \beta \\ -\beta & 1 \end{bmatrix} \begin{bmatrix} z & -z^2 \\ 1 & -z \end{bmatrix} \begin{bmatrix} -1 & \beta \\ -\beta & 1 \end{bmatrix}$$

$$dM_G \sim (1 - \beta^2)\mathbb{I} + c_F \begin{bmatrix} -1 & \beta \\ -\beta & 1 \end{bmatrix} \begin{bmatrix} -z(1 - \beta z) & z(\beta - z) \\ -(1 - \beta z) & \beta - z \end{bmatrix}$$

$$dM_G \sim (1 - \beta^2)\mathbb{I} + c_F \begin{bmatrix} -(\beta - z)(1 - \beta z) & (\beta - z)^2 \\ -(1 - \beta z)^2 & (1 - \beta z)(\beta - z) \end{bmatrix}$$

$$dM_G \sim (1 - \beta^2)\mathbb{I} - c_F(1 - \beta z)^2 \begin{bmatrix} w & -w^2 \\ 1 & -w \end{bmatrix}$$

$$\sim \mathbb{I} - c_F \frac{(1-\beta z)^2}{1-\beta^2} \begin{bmatrix} w & -w^2 \\ 1 & -w \end{bmatrix}$$

with $w = H(z) = \frac{\beta-z}{1-\beta z}$.

The claim is evident in the first case ($\phi(z) = kz$ with $|k| = 1$). For the second case let $w = H^{-1}(z) = \frac{\beta-z}{1-\beta z}$, $\beta \in (-1, 1)$ so that

$$\begin{aligned} |\sigma_G| &= \left| \sigma_F \frac{|1-\beta z|^2}{1-\beta^2} \right| \leq \left| \frac{M}{|1-|\frac{\beta-w}{1-\beta w}|^2|} \frac{|1-\beta \frac{\beta-w}{1-\beta w}|^2}{1-\beta^2} \right|. \\ &= \left| \frac{M}{1-\beta^2} \frac{(1-\beta w) - \beta(\beta-w)}{|1-\beta w|^2 - |\beta-w|^2} \right| = \left| \frac{M}{1-\beta^2} \frac{|1-\beta^2|^2}{|1-\beta w|^2 - |\beta-w|^2} \right| \\ &= M \left| \frac{|1-\beta^2|}{|1-\beta w|^2 - |\beta-w|^2} \right| = M \left| \frac{|1-\beta^2|}{(1-\beta w)(1-\beta \bar{w}) - (\beta-w)(\beta-\bar{w})} \right| \\ &= \frac{M}{1-|w|^2}. \quad \square \end{aligned}$$

4.5 Some Notes on Schlicht Circle Packing Maps

The methods of the previous section demonstrate the applicability of Nehari's method in the circle packing setting but the a full statement of his results in the context of circle packings are not yet available.

The discretization errors inherent in the circle packing construction can be quantified for our purposes by the *domain path directivity measure* and the *euclidean and hyperbolic deformation metrics* encountered previously. We do however need to clarify two aspects of the definitions. In the hyperbolic setting the domain path directivity measure will correspond to the domain path directivity measure of the normalized hyperbolic path having endpoints located symmetrically with respect to the origin. In addition we are in need of a definition for the deformation metric of a circle packing map.

Let $F : \mathbf{P} \rightarrow \mathbf{Q}$ be a circle packing map, with \mathbf{P} a maximal packing of the disc. We need to specialize the definition of the hyperbolic deformation metric to the circle packing map. For each pair of points z_0 and z_1 in the combinatoric dual of \mathbf{P} there is an automorphism of the disc $\phi(w) = \frac{w-\alpha}{1-\bar{\alpha}w}$, with α the hyperbolic midpoint of the geodesic through the two points which maps z_0 and z_1 symmetrically about the origin. Let $G(w) = (F-F(z_0)) \circ \phi^{-1}$, having face Möbius mapping M acting on $\phi(\mathbf{P})$ with numerator face linear system \mathbf{u}_G . For each such a system \mathbf{u} we can compute the hyperbolic deformation metric $HDM_{\phi \circ \gamma}(\mathbf{u}_G)$. We define the hyperbolic deformation metric of \mathbf{P} to be the supremum $B = \sup_{(z_0, z_1)} HDM_{\phi \circ \gamma}(\mathbf{u}_G)$ over all pairs of points z_0 and z_1 on the combinatoric dual of \mathbf{P} and whose minimal paths contain an interior face.

Formulations of circle packing univalence criterion can be stated using these definitions

however further work is needed to exclude boundary cases where the euclidean directivity metric is small or even zero along some paths and also to improve the computation of the supremum above. Future efforts will focus on establishing a discrete difference inequality which will remove the difficulty with the directivity metric k and improving the deformation metric constants which appear in the formulations. The essence of the theorems and proofs are expected to be similar to that of theorems 4.3.3 and 4.3.4.

Chapter 5

Linearized Circle Packing Algorithm

5.1 Abstract

This section presents a geometric algorithm for computing radii and centers for univalent circle packings on the sphere. This algorithm proceeds by iterating the solution to a sparse linear system determined by the underlying combinatoric structure with the parameters at each iterate determined by the current estimated circle packing radii. In practice the algorithm achieves a first order convergence providing significant improvement over previous methods. This method presupposes the availability of an efficient sparse linear solver for non-symmetric systems, and these are now common in the computing environment.

5.2 Introduction

We will use the previous definition of circle packing as a configuration of circles with a specified pattern of tangencies; in our case the tangency pattern will be a triangulation of the disc or the sphere (Stephenson, 2005b). It is important to distinguish between the *combinatoric* structure given by the triangulation and the *geometric* structure which is inherited from an associated circle packing. The underlying combinatoric structure by $K = \{\mathcal{V}, \mathcal{E}, \mathcal{F}\}$ is a collection of vertexes, undirected edges and interior triangular faces, whose graph triangulates a topological disc or sphere so that K is a simplicial 2-complex – there is no inherent geometric structure in the combinatoric data itself. However there are natural geometries that are inherited from circle packings. Several examples of circle packings are shown in figures 5.1 and 5.2

A circle packing in this context is said to be *univalent* if the interiors of all vertex circles are disjoint. A *maximal packing* for K , denoted \mathcal{P}_K , is a circle packing so that all boundary circles are interior and tangent to the unit circle or, in the spherical triangulation case, the

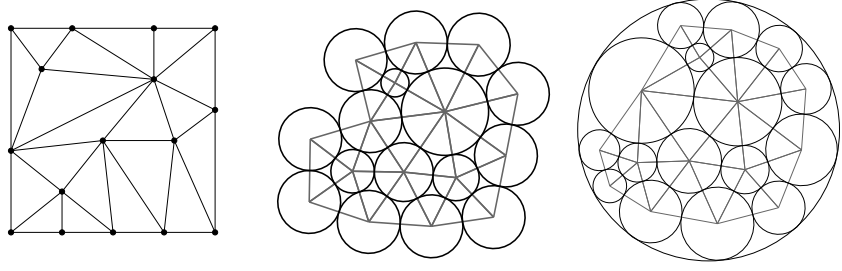


Figure 5.1: Triangulation and Circle Packings.
A triangulation of disc with two associated circle packings.

circles univalently pack the surface of the sphere. The existence of such packings are guaranteed by the Koebe-Andreav-Thurston Theorem (Stephenson, 2005b). Each combinatoric structure, K , has an associated essentially unique *maximal packing*, with uniqueness up to Möbius transformations of the sphere or disc (figure 5.3).

Theorem 5.2.1. *Let K be a combinatorial sphere (disc). Then there exists an essentially unique univalent circle packing \mathcal{P}_K for K on the Riemann sphere, \mathbb{S} , (disc, \mathbb{D}).*

We will distinguish the sets of interior and boundary vertexes by the notation V_0 and V_∂ respectively and denote the degree of a vertex by $d(v)$. The notation $u \sim v$ and $v \sim f$ will indicate that the vertexes u and v form an edge of K , and, that the vertex v lies on the boundary of the face f , respectively. The notation ∂V will denote the cycle of boundary vertexes for the complex K by $\{v_k\}_1^{|V_\partial|}$ with counter-clockwise orientation around the border. Since ∂V is a cycle we take the convention that $v_{|V_\partial|+1} \equiv v_1$. Similarly, ∂v will denote the cycle (or chain) of vertexes about an interior vertex (boundary vertex) traversed in counter-clockwise order.

A *radii label*, $\mathbf{R} : V \rightarrow \mathbb{R}^+$, for the triangulation K , is a putative radii assignment for each vertex of K which may or may not correspond to a circle packing. We say that a radii label is a *circle packing label* whenever the radii label satisfies the appropriate *angle sum condition* at each interior vertex, namely that the neighboring circles radii are such that their corresponding circles can be realized with the specified tangencies. An *embedding*, $\mathbf{Z} : V \rightarrow \mathbb{C}$ (or \mathbb{C}_∞ in spherical geometry), for the combinatoric triangulation K is an embedding of the associated graph into the disc or sphere (figure 5.3);

Circle packings of many varieties have been around since the time of Apollonius and there are several variations of interest to current research (Bobenko and Springborn, 2003). The existence and essential uniqueness of the circle packings described above is well established and these packings have been shown to exhibit near conformal (κ -quasiconformal) behaviour. In fact, the conformal nature of circle packings was a primary modern motivation for studying circle packings – Thurston conjectured that appropriately refined circle packings converge in the limit to conformal maps and his assertion was subsequently proven

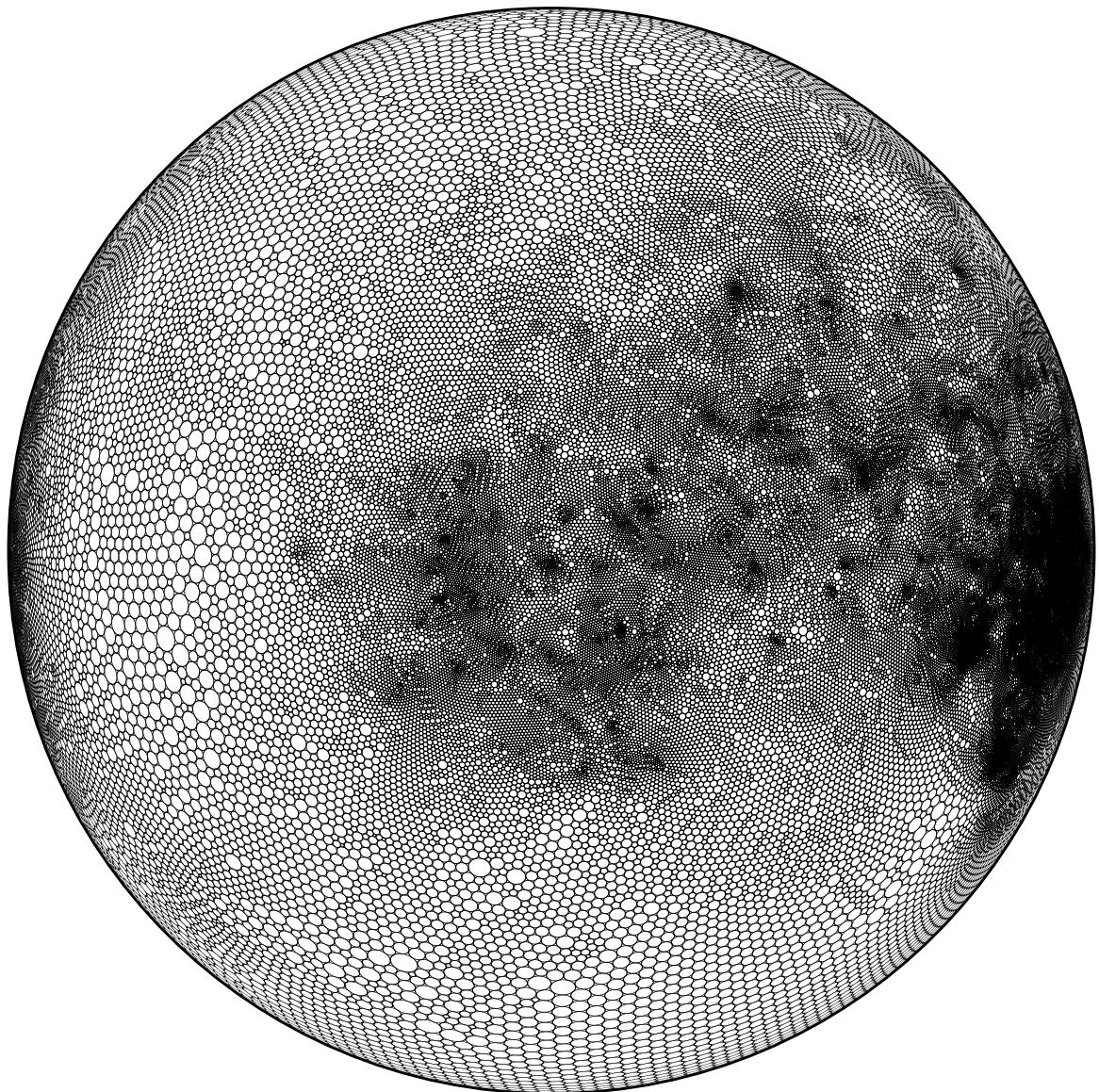


Figure 5.2: Spherical circle packing image of MRI data.
Figure produced using the techniques of this paper and reference data from (Hurdal et al., 2009).

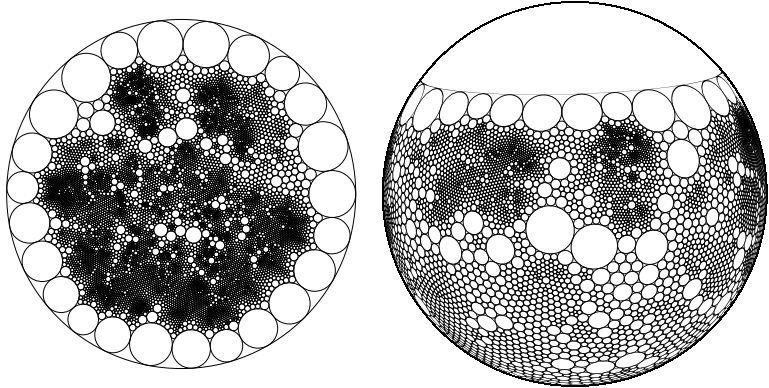


Figure 5.3: Maximal packings of the disc and the sphere.

by Sullivan(Thurston, 1985)(Rodin and Sullivan, 1987).

Circle packings and their related geometry have since found a wide variety of applications such as the conformal tilings of Floyd and Perry (Cannon and W. J. Floyd, 2001), sonar sensor placement (ling Lam and hui Liu, 2007), and brain imaging via cortical flattening (Hurdal et al., 2009). The aim of this section is to present an efficient algorithm for computing maximal packings of a complex K . The method currently in use iterates circle packing labels \mathbf{R} , to estimate a circle packing label which satisfies the local *packing condition*, namely that the angle sum about every interior vertex is 2π in the non-branched case (Collins and Stephenson, 2003). The new method presented here instead alternately estimates new radii iterates and the geometry of an associated modified Tutte-type straight line embedding. Alternate estimation of these quantities lead to significant improvements in computational efficiency. In addition, the new algorithm gives an associated embedding that approximates the true circle packing geometry at each stage giving a real time aspect which would be useful in applications such as cortical brain flattening (Hurdal et al., 2009). For example, the packing of figure 5.2 with about 150,000 vertexes takes several hours to compute using local radii refinement, whereas the new algorithm performs the computations in under 3 minutes on a laptop with a visually useful approximate packing after the first iteration (about 15 seconds). The dual nature of the current algorithm thus addresses the *layout problem* for packings; previous methods relied solely on highly accurate radii to determine the associated geometry. However, for intricate packings, such as those derived from the complex structures revealed by medical MRI scan data, the error accumulation leads to significant computational difficulties during the layout process; the use of a Tutte-like embedding at each stage effectively eliminates this difficulty.

This algorithm makes consistent use of the dual association between triangles and triples of radii which allows the alternating computation of vertex radii and vertex position and enables the computational efficiency of the algorithm.

This basic geometric observation allows an intuitive interpretation of circle packing

construction. Any circle packing label associated with a triangulation K determines a triangle for each face; circle packing labels have the property that these resulting faces and their interior arcs can be positioned in a consistent fashion. Upon placement, the interior arcs for neighboring faces form the circles of the packing itself (figure 5.4.1). Alternately, a similar consideration can be made in reverse beginning with an arbitrary approximate embedding of the triangulation; in this case, the radii of the interior circular sectors do not necessarily match across the edge boundaries (as they would if the vertexes corresponded to the circle centers in a circle packing) (figure 5.4.2). Given any embedding, circle packing or not, we can then assign an *effective radius* to each vertex, namely the radius which would contribute an equivalent effective area about each vertex through the same angular extent (2π for interior vertexes in the univalent case).

The dual processes of determining circle packing labels, \mathbf{R} , and approximate embeddings, \mathcal{Z} , lead to dual notations which distinguish between the abstract unrealized circle packing based on the label \mathcal{R} and a concrete embedding \mathcal{Z} . In particular we take θ_{vf} to denote the abstract interior angle at a vertex v of the face f as determined by the label \mathcal{R} , and, ϕ_{vf} to be the interior angle of the face f neighboring the vertex v in the embedding \mathcal{Z} . The abstract angles θ_{vf} are determined by individually constructing the triangles determine by the vertex radii according the label \mathcal{R} , whereas the embedded angle ϕ_{vf} is determined directly from the geometry of the embedding. Each interior face angle of an embedding has an associated radius, r_{vf} , so that the area of the interior embedded face sector is given by $A_{vf} = \phi_{vf}r_{vf}^2/2$.

The notation Θ_v and Φ_v will denote the total angle sum in the context of the abstract triangulation according to the label \mathcal{R} and embedding, \mathcal{Z} , respectively.

The embedded angle sum at a vertex v is

$$\Phi_v = \sum_{f \sim v} \phi_{vf},$$

so that the effective radius at v is then

$$\tilde{r}_v = \sqrt{\frac{\sum_{f \sim v} A_{vf}}{\Phi_v/2}} = \sqrt{\frac{\sum_{f \sim v} \phi_{vf} r_{vf}^2}{\Phi_v}}.$$

An effective radius can be assigned to each vertex of any non-degenerate (each triangular face having non-zero area) embedding of the underlying complex K in the plane.

From an analytic geometric view, when a collection of faces realizes the geometry of a circle packing for K , the position of a central vertex v satisfies a centroid relation with respect to the interior circular sectors surrounding v ,

$$z_v = \frac{\sum_{f \sim v} \bar{u}_f A_{vf}}{\sum_{f \sim v} A_{vf}},$$

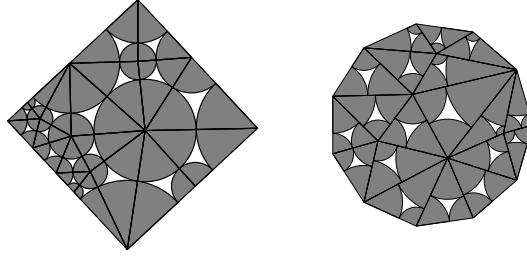


Figure 5.4: Triangular Face Matching.

- (1) Matched faces of circle packing triangulation, (2) Mismatched across edges for an arbitrary embedding.

where \bar{u}_f denotes the area centroid of an interior face sector neighboring the vertex v .

This centroid position can be expressed in terms of the two unit vectors along the abstract interior face sector bounding edges as determined by the radii label (figure 5.5.2) by noting that the geometric centroid of a circular sector of angle $\theta = 2\alpha$ and radius r is located along the axis of symmetry at a radial distance of $\frac{2r \sin \alpha}{3}$ (see figure 5.5.1). A symmetric trigonometric computation yields the abstract coordinates

$$\bar{u} = z_0 + \frac{r_0 \tan \alpha}{3} (\hat{e}_1 + \hat{e}_2),$$

where r_0 and z_0 are the central circle packing radius and vertex position at the interior vertex v and the unit sectors \hat{e}_1 and \hat{e}_2 bound the sector. These abstract coordinates can be superimposed on the embedding \mathcal{Z} as illustrated in figure 5.5.2, with the unit vectors \hat{e}_1 and \hat{e}_2 expressed in terms of the embedded vertex positions z_0, z_1 , and z_2 as

$$\hat{e}_1 = \frac{z_1 - z_0}{|z_1 - z_0|}, \quad \text{and } \hat{e}_2 = \frac{z_2 - z_0}{|z_2 - z_0|}.$$

As a consequence, the relative local position of an interior vertex can be expressed in terms of the neighboring vertex positions. Summing the terms of this centroid expression based on the embedded positions and the analytic centroid relations gives a linear expression for any interior vertex position in the form

$$z_v = \sum_{w \in \partial v} \eta_{vw} z_w,$$

where the weights η_{vw} , for fixed v , satisfy $\sum_{v \neq w \in V} \eta_{vw} = 1$, $\eta_{vv} = -1$, and $\eta_{vw} = 0$ for all non-neighbor vertexes w ($w \notin \partial v$). With this notation, for each interior vertex v

$$\sum_{w \in \mathcal{V}} \eta_{vw} z_w = 0.$$

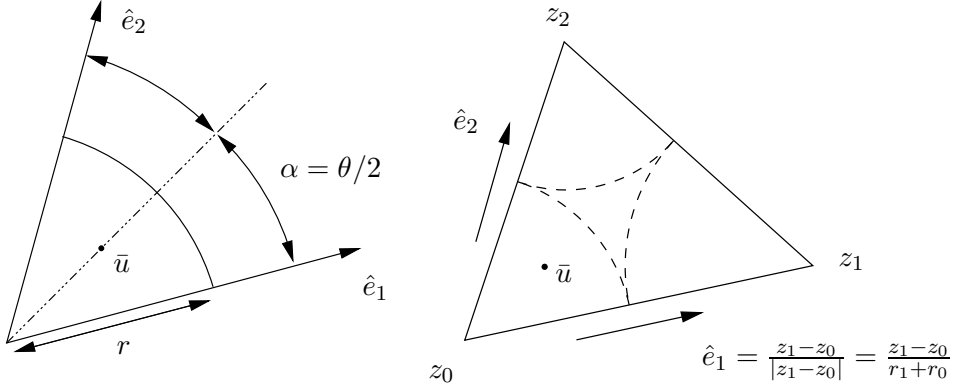


Figure 5.5: Circular Sector Centroids.

- (1) Sector centroid, \bar{u} ,
- (2) Embedded relative centroid coordinates in terms of neighboring vertex positions.

The weights η_{vw} can be expressed in terms of the abstract interior angles of each of the faces at an interior vertex. The values of the *centroid weights* about an interior vertex v with respect to a neighboring vertex $w \in \partial v$ is given by

$$\eta_{vw} = \frac{\frac{1}{r_v+r_w} [\tan(\theta_{vw}^+/2) + \tan(\theta_{vw}^-/2)]}{\sum_{u \in \partial v} \frac{1}{r_v+r_u} [\tan(\theta_{vu}^+/2) + \tan(\theta_{vu}^-/2)]}$$

with θ_{vw}^+ and θ_{vw}^- indicating the abstract interior face angles at the vertex v to the right and left of the combinatoric edge $\{v, w\}$ as determined by the radii label. For boundary vertexes v we define $\eta_{vv} = 1$, and $\eta_{vw} = 0$ for all $w \neq v$. Alternate geometric interpretations include the *edge conductances* encountered in the study of random walks on circle packings.

In the case of a circle packing, the centroid relations give local relative expressions for each interior vertex in terms of the neighboring vertex positions. An additional global geometric boundary condition needed is given by the maximal packing geometry which will allow the construction of an approximate circle packing embedding.

5.3 Fundamental Global Maximal Packing Geometry

Recall that the underlying circle packing combinatoric structure has no inherent geometry since it is specified only as an abstract triangulation K . However a circle packing associated with the given triangulation does provide a geometric context for K . This section will discuss the global features of the circle packing geometry for a given complex and will focus on the geometry of maximal packings in the disc. This case will be sufficient since triangulations of the sphere can be modified to equivalent triangulations of the disc by puncturing any vertex or face of the spherical complex. Puncturing the spherical complex at a vertex, v , gives a corresponding triangulation of the disc having $d(v)$ boundary vertexes (figure 5.6); while

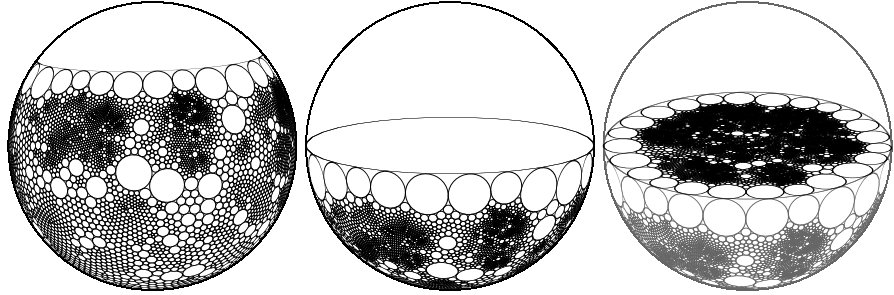


Figure 5.6: Puncturing a Spherical Maximal Packing.

- (1) Spherical maximal packing, (2) Isometric packing on the sphere, (3) Punctured packing in the disc.

puncturing the complex at a face results in a triangulation of the disc having exactly three boundary vertexes. In either case the computed maximal packing can then be projected to the Riemann sphere and the missing vertex circle can be restored.

Let K be a triangulation of the disc with boundary vertex cycle ∂V . The boundary circles for any given proper circle packing label in the maximal packing can be positioned up to rotation by univalently inscribing the cycle of boundary circles inside and tangent to the unit circle obeying the tangency relations given by the combinatorics as in figure 5.7.1.

Once a proper maximal packing label is known, the process of laying out the vertexes, edges and faces of the complex is a straightforward application of a modified Tutte embedding with weights derived from the local centroid relations. This application is not the usual Tutte embedding since the boundary vertexes (the centers of the boundary circles) are not necessarily on a convex boundary – this said, the associated embedding given by a Tutte-type system for a proper circle packing label will give the correct layout since the system is determined in a geometric fashion from circular sector centroids (see figure 5.7.2). For a proper circle packing label, the resulting vertex positions will correspond to the circle centers as in figure 5.7.3. When the proper label is not known the distinction is important since the convexity requirement for Tutte’s method is not met; as a result, an arbitrary label is not guaranteed to give a proper embedding with the centroid weights determined by an arbitrary label (as described in the following section) unless the boundary centers form a convex region. This convexity condition is always met when the boundary has exactly three boundary vertexes so that this is not a true limitation of our method – any spherical or disc triangulation can modified to have three boundary vertexes.

Any combinatoric triangulation of the disc can be converted (by resorting to a “combinatoric Riemann Sphere”) to an equivalent triangulation of the disc with exactly three boundary vertexes in a fashion similar to the sphere puncturing illustrated in figure 5.8. This is accomplished by adding an ideal vertex at ∞ and then puncturing any combinatorial face of the resulting triangulation. The desired maximal disc packing can be recovered from the maximal packing of this equivalent triangulation by projection to the Riemann sphere,

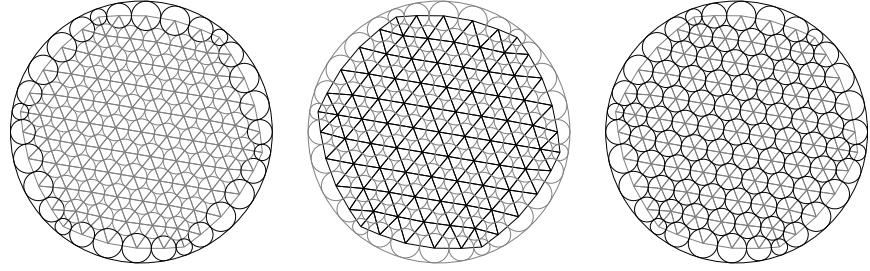


Figure 5.7: Maximal Packing Geometry.

- (1) Maximal packing boundary layout, (2) Maximal packing embedded graph, (3) Maximal packing.

applying a spherical Möbius transformation and then puncturing the inserted ideal vertex.

5.4 Linearized Circle Packing Algorithm

The maximal packing algorithm takes as its input a triangulation of the disc (after conversion in the spherical case) and an arbitrary positive and nonzero label \mathcal{R} , typically $\mathcal{R}_v \equiv 1$ for all vertexes v . The algorithm proceeds in three iterated steps, each step used the current iterated radii label in place of the as yet unknown circle packing label. The steps in sequence are:

1. STEP 1: Position the boundary circle centers (figure 5.9.1). The boundary circles are positioned by inscribing these circles into the interior of the unit disc while obeying the tangency requirements of the complex.(A scaling of the radii label may be necessary to accomplish this layout.)
2. STEP 2: Position the interior circle centers (figure 5.9.2). The interior circle centers are positioned by producing an embedding in the disc by using the centroid weights which result from the current iterated radii label and solving the sparse linear system formed by the local relative positions giving approximate interior circle centers.
3. STEP 3: Compute new effective radii at each vertex (giving an updated label) (figure 5.9.3). The updated effective radius at each vertex is determined in terms of the embedded angle sum at a vertex (2π for interior vertexes) and area contributions from the interior circular sectors from each neighboring triangular face.

An iterated sequence for an example packing is shown in figure 5.10 and each step is detailed below. It should be noted that the simple combinatoric structure of the given example allows its maximal packing to be more efficiently solved by the previous method of iterating the radii label alone; for more intricate circle packings the new algorithm improves performance by orders of magnitude.

5.4.1 STEP 1: Boundary Layout

The first step is to determine the boundary circle centers z_v for each $v \in \partial V$ (figure 5.9.1) as determined by the current radii label. Let $\{r_j\}$ and $\{z_j\}$ be the cycle of radii and center positions for the boundary circles associated with the vertexes ∂V . These boundary circles can then be sequentially located interior and tangent to some circle of unknown radius R , given by the positive solution to the (monotonic) angle sum condition

$$\sum_{j=1}^{|v_\partial|} \theta_j = 2\pi, \quad \text{where } \theta_j = \cos^{-1} \left(1 + \frac{2r_j r_{j+1}}{(R+r_j)(R+r_{j+1})} \right),$$

over the interior angles formed by the origin and two successive neighboring circles with radii r_j and r_{j+1} corresponding to the successive boundary vertexes (figure 5.11). After appropriately scaling the label \mathcal{R} in its entirety the circumscribed circle can be taken to have radius $R = 1$. This boundary layout construction gives approximate boundary circle positions for the maximal packing based on the current radii label up to a rotation by fixing one circle interior and tangent to the unit circle and successively placing the remainder of the boundary cycle as in figure 5.9.1.

5.4.2 STEP 2: Interior Layout

The second step consists of determining the relative local positions and solving an associated sparse linear system for the interior circle center positions. Let $\{r_j\}$ and $\{z_j\}$ represent the radius and center for the circle at each vertex; taking the convention that the interior circles are indexed first followed by the boundary circles. The current radii label determines a sparse linear system with positive weights (the centroid weights) expressing the local relative position of each interior vertex with respect to neighboring vertexes by imposing the centroid condition based on the current radii label. Since the radii label may not actually be a circle packing we resort to an *abstract face* determined by the corresponding triple of radii in the label. The centroid of an interior circular sector at a vertex of the abstract face can be expressed as before and used to determine the next approximate circle packing weights, η .

The centroid weights are constructed by considering the angles formed on the abstract faces – for each interior vertex, v , the weights $\eta_{vw}, w \in \partial v$ are given by

$$\eta_{vw} = \frac{\frac{1}{r_v+r_w} [\tan(\theta_{vw}^+/2) + \tan(\theta_{vw}^-/2)]}{\sum_{u \in \partial v} \frac{1}{r_v+r_u} [\tan(\theta_{vu}^+/2) + \tan(\theta_{vu}^-/2)]}$$

and using the notation of figure 5.5.3

$$\theta_{vw}^\pm = \cos^{-1} \left(1 - \frac{2(r_{w\pm})(r_w)}{(r_v + r_{w\pm})(r_v + r_w)} \right).$$

Given the boundary vertex positions from STEP 1, the interior positions satisfy the linear relations

$$\sum_{w \in \partial v} \eta_{vw} z_w = 0$$

for each interior vertex v . Using the notation \mathcal{Z}_0 and \mathcal{Z}_∂ to indicate the centers for interior and boundary vertexes respectively, we can express the linear system given by the above weights in terms of

$$\mathbb{W} = (\eta_{vw}) = \begin{bmatrix} \mathbf{A}_o & \mathbf{A}_\partial \\ 0 & \mathbf{I}_{N_\partial} \end{bmatrix}, \quad \text{and} \quad \mathcal{B} = \begin{bmatrix} \mathbf{0} \\ \mathcal{Z}_\partial \end{bmatrix},$$

so the linear system $\mathbb{W}\mathcal{Z} = \mathcal{B}$ can be expressed as

$$\begin{bmatrix} \mathbf{A}_o & \mathbf{A}_\partial \\ 0 & \mathbf{I}_{N_\partial} \end{bmatrix} \begin{bmatrix} \mathcal{Z}_o \\ \mathcal{Z}_\partial \end{bmatrix} = \begin{bmatrix} \mathbf{0} \\ \mathcal{Z}_\partial \end{bmatrix}.$$

The approximate interior circle centers are then solutions to the linear system

$$\mathbf{A}_0 \mathcal{Z}_0 = -\mathbf{A}_\partial \mathcal{Z}_\partial,$$

which completes a geometric embedding of the complex K determined by the current label, giving an approximate circle packing geometry to K which will be used to further refine the radii label.

5.4.3 STEP 3: Effective Radii

The final iterative step consists of updating the radii label by computing an effective radius at each vertex (interior and boundary). The embedding given by STEP 2 is partitioned into triangles, each of which has a natural circular sectors associated with each vertex. The effective area, A_v , of a vertex is the sum of the adjacent interior circular sector areas over each neighboring face in the current embedding (figure 5.12); the embedded angle sum, Φ_v , at each vertex is the sum of the interior angles of neighboring faces. The effective radius at vertex v is then computed as

$$\tilde{r} = \sqrt{\frac{A_v}{\phi_v/2}},$$

which gives a new effective radius label for each vertex of the complex K . The resulting iterated sequence of radii labels converges in practice to a proper maximal packing label.

5.4.4 Discussion of Convergence

The algorithm was presented in an intuitive fashion but convergence may not necessarily guaranteed in the case where there are more than three vertexes, partly because the Tutte

embedding conditions include a convexity requirement – this difficulty in itself is not a true limitation since every triangulation of the disc always has an equivalent three boundary triangulation by resorting to the Riemann sphere. This limitation can often be overcome in practice without resorting to the three boundary vertexes by (1) choosing a “nice” starting label and (2) modifying STEP 3 to limit the relative incremental change in the boundary radii labels at each iteration. These modifications still yield significantly improved convergence over older methods with the added advantage of a straightforward implementation. As mentioned above, limiting the boundary to three vertexes avoids the convexity problem and also leads to other simplifications. For the three boundary case it is not necessary to modify the boundary radii or positions since they can be taken to be constant as in figure 5.13. In this case then, STEP 1 is unnecessary and STEP 3 can be modified to only compute effective radii for interior vertexes.

Though no proper proof of convergence is in hand as yet, we expect that there is such a convergence proof for the maximal packing algorithm for arbitrary positive initial radii label in the three boundary case. The computations of the effective radii at the boundary in some cases lead to instability of the iterated process for complicated boundary combinatorics. These difficulties can be minimized in practice by controlling the rate at which the boundary vertex radii can adjust at each iteration.

5.4.5 Error Estimation

The iterative algorithm approximates the maximal packing radii and geometry for the complex K at each iteration. There are several methods to measure the error at each iteration between the current label and embedding to that of a proper maximal packing, two methods in common use are listed below.

Angle Sum Error

For each interior vertex v_0 compare the angle sum based on the radii label to 2π for the univalent case (see figure 5.14.1). Let v_1, v_2, \dots, v_d denote the cycle of vertexes ∂v_0 . The angle sum, $\Theta(v_0)$, at the vertex v_0 realized by the label \mathcal{R} is then given by

$$\Theta(v_0; \mathcal{R}) = \sum_1^d \cos^{-1} \left(1 - \frac{2r_j r_{j+1}}{(r_0 + r_j)(r_0 + r_{j+1})} \right), \quad (5.1)$$

so that the angle sum error at v_0 with respect to the label \mathcal{R} is

$$E_\Theta(v; \mathcal{R}) = |2\pi - \Theta(v_0; \mathcal{R})|. \quad (5.2)$$

Quadrilateral Skew Error

For each interior quadrilateral of the embedding formed by two adjacent faces (having one edge in common) compare the radius error across the common edge (see figure 5.14.2). Let $\{v, w\}$ be an interior edge of K , with v an interior vertex, and take the quadrilateral, Q_e , formed by the two faces with common edge $e = \{v, w\}$ with embedded vertexes z_v, z_w, z_{v+} , and z_{v-} . Each of the adjacent faces (z_v, z_{v-}, z_w) and (z_v, z_w, z_{v+}) have associated radii for the vertexes v and w ; the absolute difference of either two corresponding radii give the *skew error* for the quadrilateral. The two interior sector radii at v associated with the two faces are given by

$$r_v = \frac{1}{2}[|z_{v+} - z_v| + |z_w - z_v| - |z_{v+} - z_w|]$$

and

$$r'_v = \frac{1}{2}[|z_{v-} - z_v| + |z_w - z_v| - |z_{v-} - z_w|]$$

respectively. The *quadrilateral skew error* for the edge $\{v, w\}$ realized by the embedding \mathcal{Z} is then given by

$$E_Q(e; \mathcal{Z}) = \frac{1}{2}||z_{v-} - z_v| - |z_w - z_{v-}| + |z_{v+} - z_w| - |z_v - z_{v+}||. \quad (5.3)$$

The geometric nature of the quadrilateral Skew Error make it the preferred error measure for the iterated embeddings.

5.5 Geometry and Weights

The geometric centroid weights for a circle packing arrived at by considering the analytic geometric centroid of the interior circular sectors of the face triangles about an interior vertex can be expressed up to local scale as the ratio of the perpendicular dual edge, and proper edges of the embedding as shown in figure 5.15. The relationship with the geometric centroid weights is evident after scaling the radii label at a vertex to have unit radius so that the portion of the perpendicular dual edge lying in each neighboring face corresponds to the $\tan(\theta_{\pm}/2)$ terms. This observation gives an alternate geometric interpretation of the weights in the proper circle packing case, namely as the ratio of the sum of the incircle radii of the two neighboring faces and the original edge length (figure 5.15). This relationship simplifies the implementation of this maximal packing algorithm since the effective radii need never be computed for the interior vertexes – only the boundary effective radii need be computed if there are more than three boundary vertexes. This simplification is accomplished by the geometric identity for the incircle radius of a triangle, namely, if a, b , and c are the triangle side lengths and $s = (a + b + c)/2$ is the semi-perimeter, then the incircle radius is given by $\rho = \sqrt{\frac{s(s-a)(s-b)(s-c)}{s}}$ ($= k/s$ where k is the triangle area).

These *circle packing weights* have been related curvature flow in conformal mappings of circle packing literature (Collins et al., 2003).

5.6 Conclusion

This section presented an algorithm for computing maximal packings in the unit disc (hence for the sphere) for an arbitrary triangulation of the disc or sphere. The method iterates the solution of a sparse linear system with varying parameters, essentially determining the boundary centers and using approximate local relative coordinates to determine the new interior centers at each stage. This is reminiscent of Tutte's method for drawing planar graphs in a convex region (Tutte, 1962). The relationship with Tutte's theorem may yield a proof of convergence. The essential differences in our case are: for more than three boundary vertexes the boundary circle centers do not necessarily remain on a convex boundary during the iteration process, and, the local coordinate weights vary at each stage of the iteration.

Minor modifications to this algorithm yield a method of efficiently laying out the pattern of circles associated with any radii assignment; in particular a circle pattern layout can be found given circle packing radii computed by some other algorithm. This layout procedure is generic in that any simply connected circle packing (not necessarily a maximal packing of the disc and possibly branched) can be geometrically realized provided a sufficiently accurate radii label is known. This layout method can also be iterated to further refine the starting label in some cases though the conditions for convergence are even less understood.

These methods have also been used to empirically solve for circle packings with various smooth and polygonal boundary conditions. The methods are most successful in the case of a convex boundary but have been applied for more general shapes. A few examples are shown in figure 5.16.

This algorithm and the various individual components have been implemented as part of the CirclePack geometry suite developed by Ken Stephenson (Stephenson, 2005a) which is available from the CirclePack website, www.math.utk.edu/~kens/CirclePack.

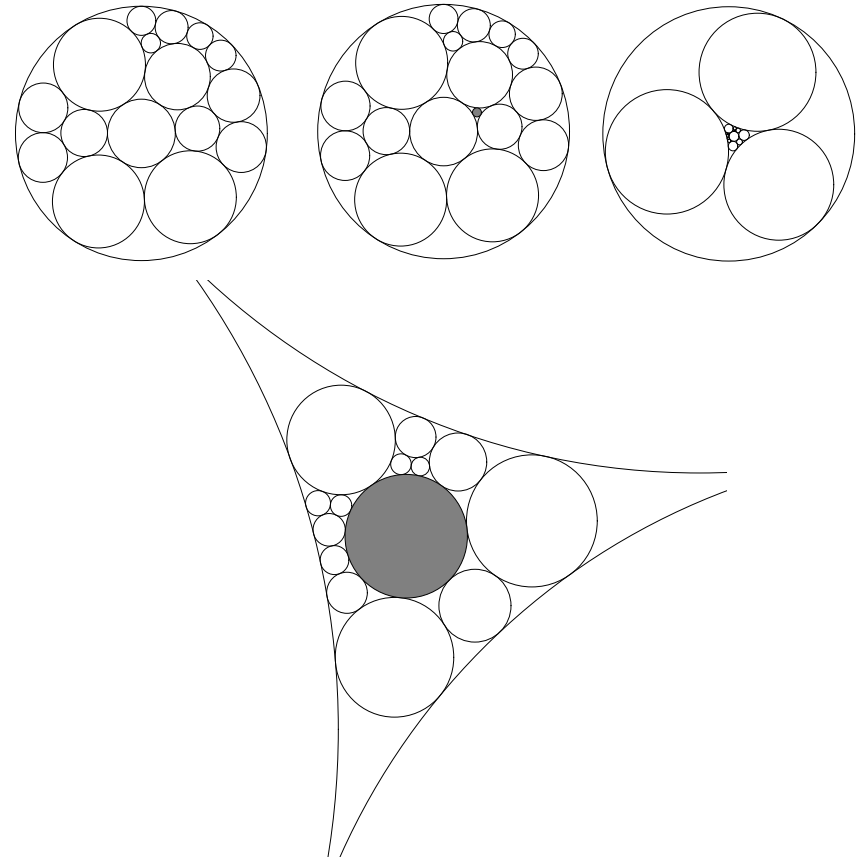


Figure 5.8: Modification of Disc Packing Combinatorics.

- (1) Maximal packing in the unit disc, (2) Insertion of interstitial vertex, (3) Equivalent maximal packing on the sphere (viewed on disc), (4) Magnified interstice to show orientation with the initial ideal vertex shaded.

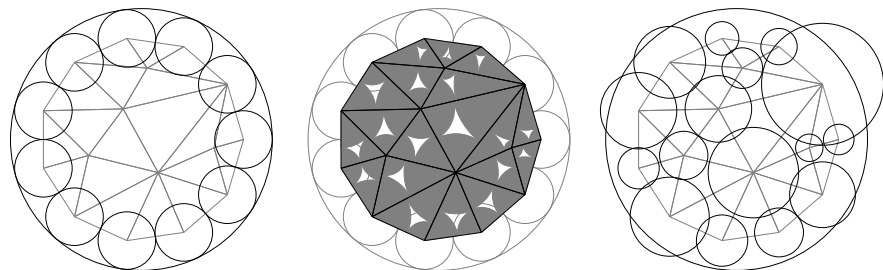


Figure 5.9: Circle Packing Algorithm.

- (1) Boundary layout, (2) Interior layout, (3) Effective radii.

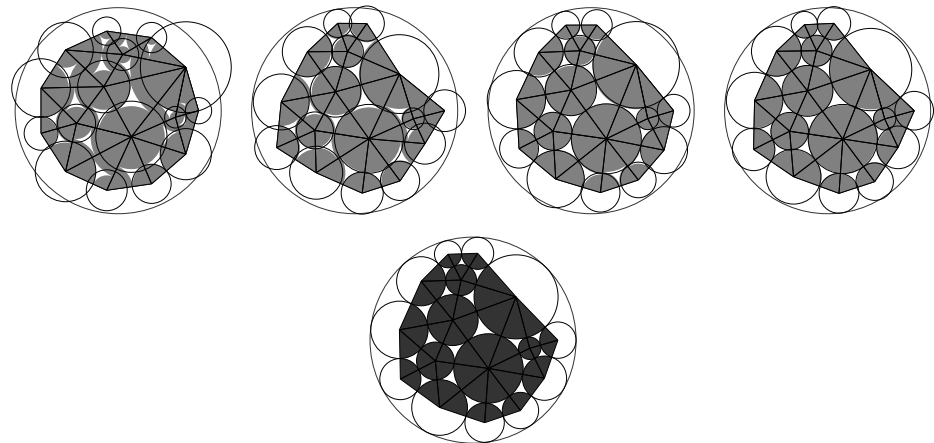


Figure 5.10: Example Maximal Packing Sequence.
The centers and effective radii are shown at the completion of the 1st, 2nd, 3rd, 4th, and 20th iterations.

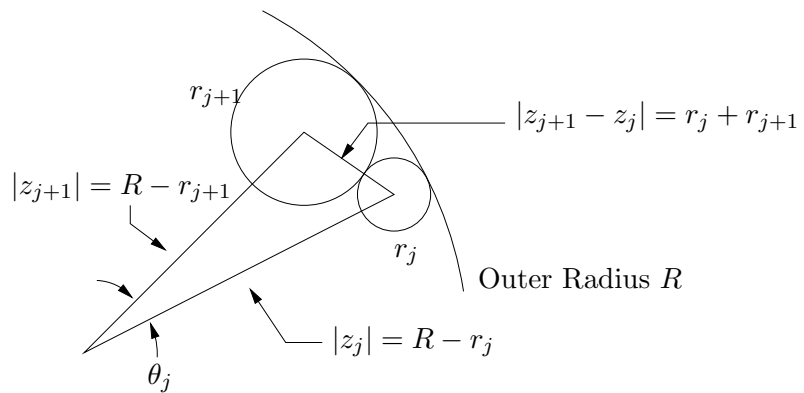


Figure 5.11: Inscribing Boundary Circles.

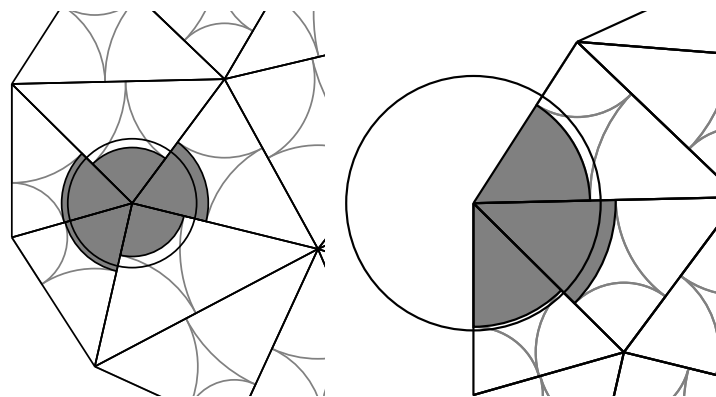


Figure 5.12: Effective Radii Computation.
(1) For an interior vertex ($\Phi_v = 2\pi$), (2) For a boundary vertex ($\Phi_v = \sum \phi_{vf}$).

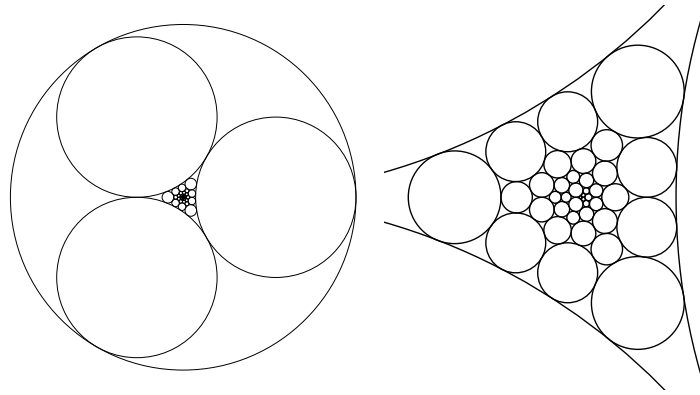


Figure 5.13: Fixed Boundary Conditions for Three Boundary Vertices.

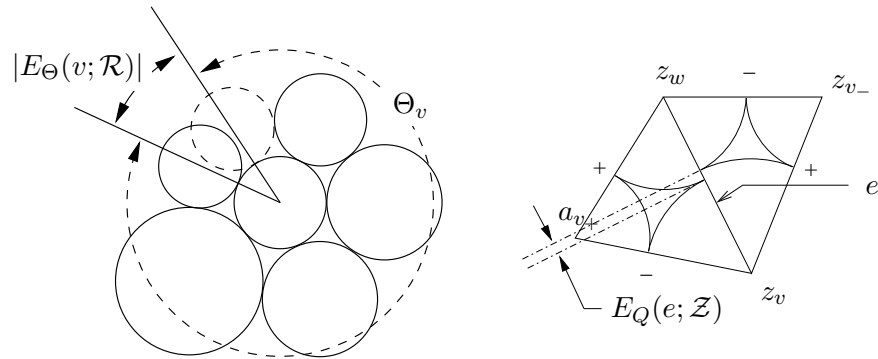


Figure 5.14: Circle Packing Error Measurement.

- (1) Angle sum error for radius label \mathcal{R} ,
- (2) Quadrilateral skew error for embedding \mathcal{Z}
(note the sign assignments for quadrilateral edges for computation of E_Q).

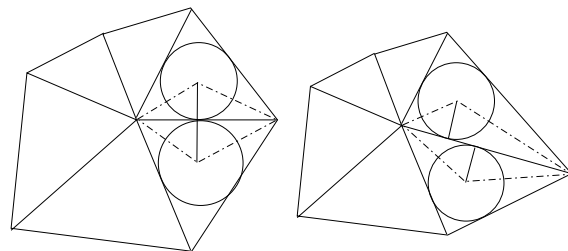
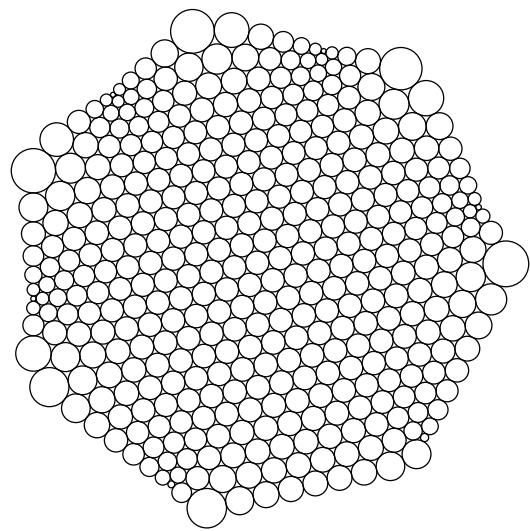
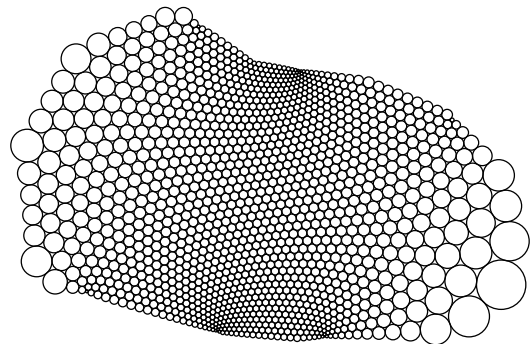


Figure 5.15: Alternate Circle Packing Weight Construction.

- (1) Perpendicular dual edges align for matched circle packing faces,
- (2) Misaligned perpendicular dual edges in generic case.



(a) Septagonal Boundary



(b) General Path Boundary

Figure 5.16: Packings with Generic Boundary.

Chapter 6

Experiments

6.1 Circle Packing Function Approximation

This chapter presents circle packing experiments which employ *circle packing approximations* to traditional analytic functions. This section defines the notion of circle packing approximation that we will use.

Let K be a complex with domain packing \mathbf{P} . The usual circle packing function is a map $F : \mathbf{P} \rightarrow \mathbf{P}'$ onto a range circle packing but which range packing is a good choice to approximate a specified analytic function $f(z)$? The following technique gives a reasonable choice for our purposes though other schemes may be reasonable. Our basic method considers the map of the carrier embedding in the domain packing and its image (by vertexes) into the range. This mapping is illustrated in figure 6.1 for the exponential and sine functions as well as the Koebe function.

The carrier image in the range for these functions were computed by finding the circle packing whose boundary circle radii were determined by specifying the $F^\#$ at each boundary vertex by the function derivative at the domain vertex center. With this notion of function approximation we can go on to experiment with the circle packing interpretations of the derivative and Schwarzian derivative.

The domain packing is not restricted to regular geometric structure as in figure 6.1 but we do expect the circle packing numerical approximations depend on the domain geometry and combinatoric structure as we will see below. Figure 6.4 shows the domain and range circle packings for the exponential over a maximal packing. This function approximation method can also be modified to accommodate functions with branch points in the domain.

6.2 Schwarzian Derivative

This section will illustrate the relationship between the circle packing discrete Schwarzian and the the traditional Schwarzian derivative. The experiments suggest a strong relation

between the two which has not been fully quantified. The approach will be to consider three familiar analytic functions and their respective Schwarzian derivatives, namely the exponential, sine and Koebe functions.

The common thread in the following computations is the relationship between the derivative of the best fit Möbius map and the value of the Schwarzian derivative at a point. From proposition 3.3.8, the Schwarzian derivative is related to the best fit Möbius map coefficients by

$$S_f(z) = 2\sqrt{f'(z)}C'(z) \quad (6.1)$$

where the best fit Möbius map $M(z)$ (with unit determinant) is $\begin{bmatrix} A(z) & B(z) \\ C(z) & D(z) \end{bmatrix}$. When $f'(z) = 1$ this expression gives a straightforward interpretation of the Schwarzian as twice the derivative of the coefficient C . Intuitively this case corresponds to considering the edge derivatives dM_e instead of the Möbius maps themselves; this assertion will be justified in a later remark.

All of the necessary quantities can be interpreted in the circle packing geometry, in particular we have the face Möbius maps and discrete dual edge derivatives. This sets us up for our first experiment.

Experiment 6.2.1. *Approximate the Schwarzian derivative for the complex exponential function at each edge intersection point.*

Let $F : \mathbf{P} \rightarrow \mathbf{P}'$ approximate the exponential as in section 6.1.

The exponential function $f(z) = e^z$ has constant Schwarzian derivative $-1/2$ since $f''/f' \equiv 1$. For a first observation, we compute and estimate of the Schwarzian derivative at each edge intersection by using the expression from the best fit Möbius for an analytic function:

$$S_f(z) = 2\sqrt{f'} \frac{\partial}{\partial z} \frac{-kh}{2} = 2\sqrt{f'} \frac{\partial}{\partial z} M_C(z) \quad (6.2)$$

where $k = f''/f'$ and $h = 1/\sqrt{f'}$ and $M_C(z) = -kh/2$ is the $(2,1)$ coefficient of $M(z)$. In our case we have $k(z) = 1$ and $h = e^{-z/2}$ so that $S_f(z) \equiv -1/2$, a nice check. Now we would like to interpret 6.2 in terms of circle packing quantities. Since the face maps are defined at dual vertexes we choose the dual edge derivative to represent f' , $f' \approx \delta'_e/\delta_e$. The final derivative expression can be estimated by using the face Möbius map coefficients at the face incircle centers.

$$\frac{\partial}{\partial z} M_C(z) \approx \frac{\Delta C}{\delta_e} \quad (6.3)$$

where ΔC is difference of the $(2,1)$ coefficient from appropriate the face Möbius maps, and δ the dual edge displacement. This gives a circle packing interpretation

$$S_F(z) = 2 \frac{\Delta c}{\delta_e} \sqrt{\frac{\delta'_e}{\delta_e}}. \quad (6.4)$$

Figure 6.5 shows the magnitude of the computed approximation. Some observations can be made – at first glance there are obvious combinatoric/geometric effects in that some values are double the expected values. This can be seen as a discretization effect due to the underlying combinatorics; observations show that the larger respective values occur when the dual edge is “aligned” with the gradient of the $(2, 1)$ Möbius coefficient. Such behaviour is not necessarily unexpected since as we shall see below, the complex valued discrete approximation above has argument dependent on the edgewise orientation of the domain dual embedding.

The directionality of the estimated quantities suggest averaging the values about each face to obtain a face estimate of the Schwarzian derivative. Figure 6.6(a) shows the face averaged edge Schwarzian from the maximal packed domain – the values approximate the analytic expected value in the interior where the geometric structure is nearly uniformly hexagonal, with the approximation degrading towards the boundary. For illustration we also show the real part of the face averaged Schwarzian approximation in 6.6(b). A look at the second figure illustrates why geometric/combinatorial are not surprising; the face centers of the domain carrier are arranged (in regular hex combinatorics) in a two on, one off fashion. The edges corresponding to the gaps (of the face center points) are the typical points where computed edge Schwarzian approximations are exaggerated.

6.3 Alternate Schwarzian Approximation

This section presents an alternative method for approximating the Schwarzian derivative along a circle packing edge which employs the (Möbius) edge derivative of earlier sections.

Adjacent face Möbius maps are related by the edge derivative $dM = \mathbb{I} + \sigma \begin{bmatrix} z & -z^2 \\ 1 & -z \end{bmatrix}$. If the first face map μ_0 is given and the edge derivative is known, then the change in the coefficient C needed above is given by

$$\Delta C = \sigma(Cz + D),$$

(since $\mu_1 = \mu_0 dM$), but using the formal expressions for the best fit Möbius map for an analytic function we have $C = -kh/2$ and $D = h + khz/2$. Combining these expressions gives $\Delta C = h\sigma$. We then have the following remark.

Remark 6.3.1. The discrete Schwarzian derivative approximation $S_F(z)$ can be computed in terms of the edge derivative $dM = \mu_0^{-1}\mu_1 = \mathbb{I} + \sigma \begin{bmatrix} z & -z^2 \\ 1 & -z \end{bmatrix}$ as

$$S_F(z) \approx -2\frac{\sigma}{\delta} = -2\frac{|\sigma|}{|\delta|}\bar{\eta}^2 \quad (6.5)$$

since by remark 2.9.1 the discrete Schwarzian has argument proportional to the dual edge direction $\sigma = s\bar{\eta}$ for some $s \in \mathbb{R}$.

The above remark shows that the circle packing edge Schwarzian approximations (using these constructions) will not converge to the analytic version, in particular, the argument of the circle packing edge Schwarzian approximation will have argument determined strictly by the dual edge direction in the domain packing.

6.4 The Sine Function

Experiment 6.4.1. *Approximate the Schwarzian derivative for the sine function on each face by computing the average of the bounding edge derivatives then compute the error in the magnitude with the analytic value.*

Figure 6.7 shows the relative error between the circle packing approximation and analytic values of the Schwarzian on the faces. A sequence of images over the discs $0.001\mathbb{D}$, $0.01\mathbb{D}$ and $0.1\mathbb{D}$ is shown. This sequence displays improved approximation as the density in the domain increases. The domain packing is an appropriately scaled version of the domain of figure 6.5; the range packings are not shown since the deviation from the regular hex domain is not significant enough to be visible in a figure.

6.5 The Koebe Function

Experiment 6.5.1. *Approximate the Schwarzian derivative for the Koebe function on each face by computing the average of the bounding edge derivatives then compute the error in the magnitude with the analytic value.*

The domain for the map was taken again to be the regular hexagonal combinatoric packing, scale to the disc $0.7\mathbb{D}$. Figure 6.8 shows the range packing for the Koebe map considered; the original domain is first shown, then a scaled version used for the computations.

Figure 6.9 shows the relative error between the circle packing approximation and analytic values of the Schwarzian on the faces.

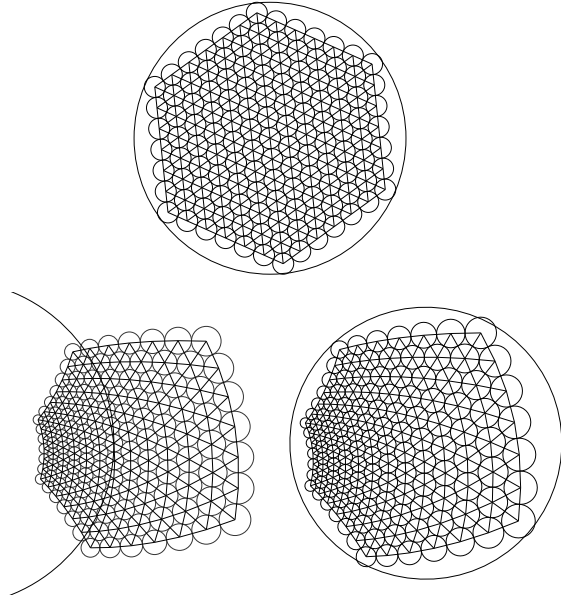


Figure 6.1: Function Approximation for the Exponential function
 Example circle packing approximation for $f(z) = \exp(z)$ on a hexagonal domain. Domain packing is shown with unit circle; Carrier image is shown with approximate vertex radii; and, a representative circle packing range is shown.

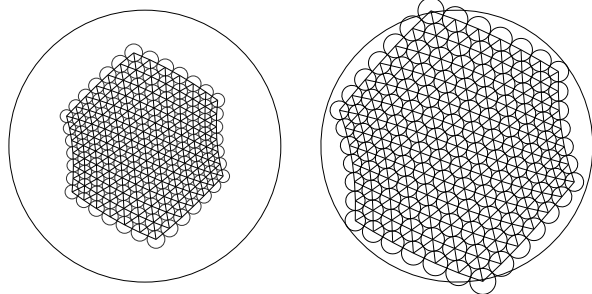


Figure 6.2: Function Approximation for the Sine function
 $f(z) = \sin(z)$

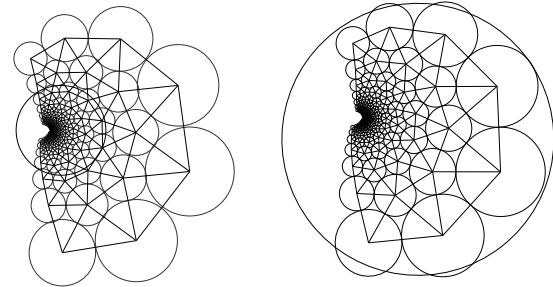


Figure 6.3: Function Approximation for the Koebe function
 $f(z) = \frac{z}{(1-z)^2}$

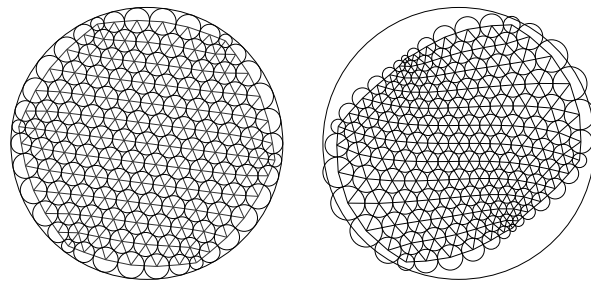
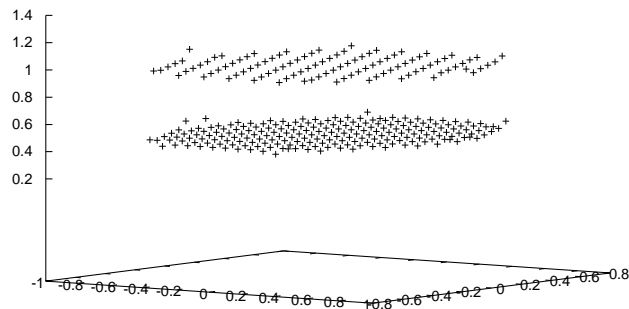
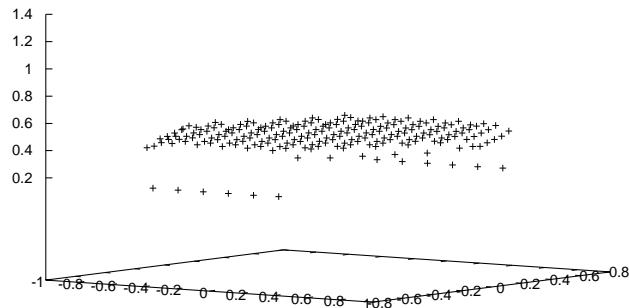


Figure 6.4: Function Approximation over a maximal packing
 $f(z) = \sin(z)$

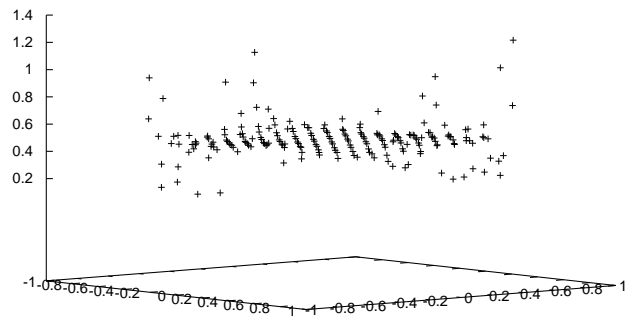


(a) Edge Schwarzian Approximation (Magnitude)

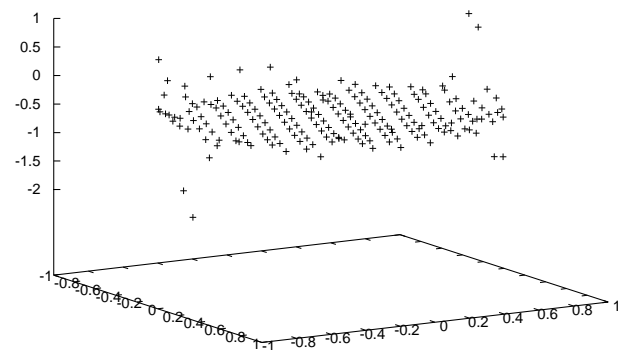


(b) Face Averaged Edge Schwarzian (Magnitude)

Figure 6.5: Edge Schwarzian Approximation for Exponential Map over a regular hexagonal domain.

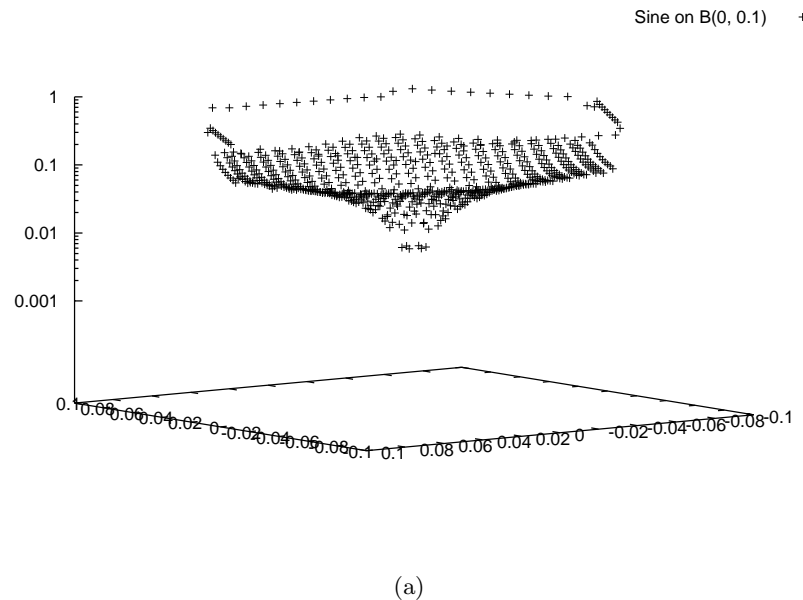


(a) Face Averaged Edge Schwarzian (Magnitude)

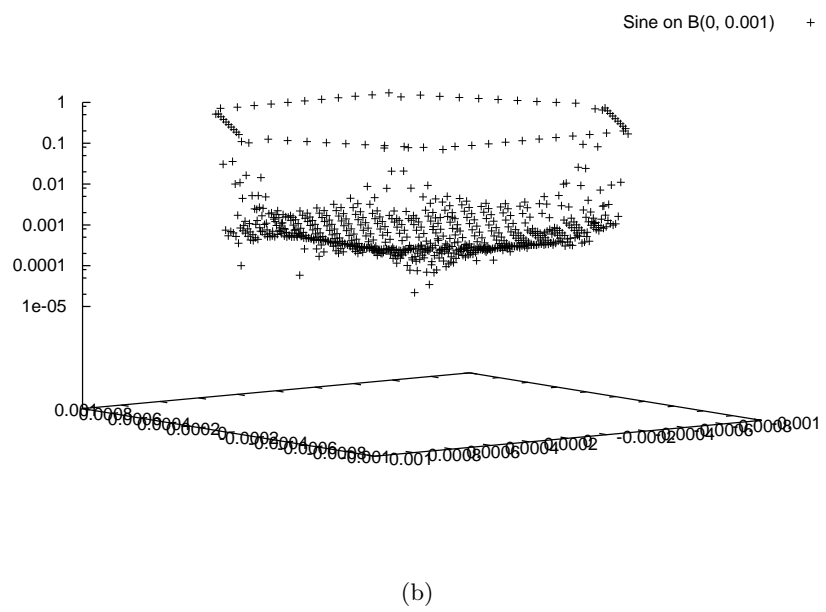


(b) Face Schwarzian (Real component)

Figure 6.6: Exponential Map over Disc Domain



(a)



(b)

Figure 6.7: Face Averaged Schwarzsian Approximation for the Sine Function.
 Relative error between analytic Schwarzsian derivative is shown for discs of radius (a) 0.1
 and (b) 0.001.

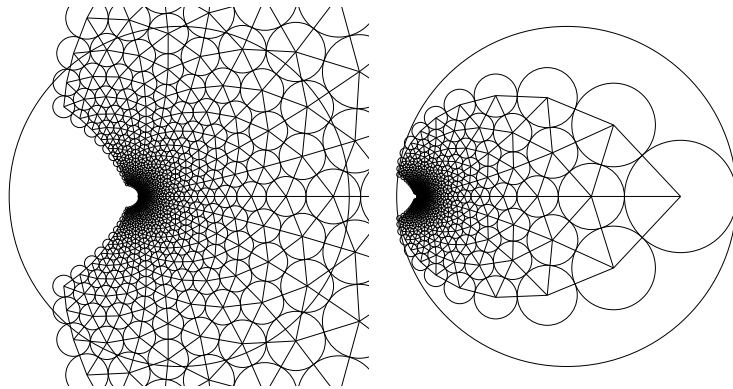


Figure 6.8: Koebe Map Range over Hexagonal Domain.

- (a) Shows the range of the Koebe function and (b) shows the scaled version used for computations.

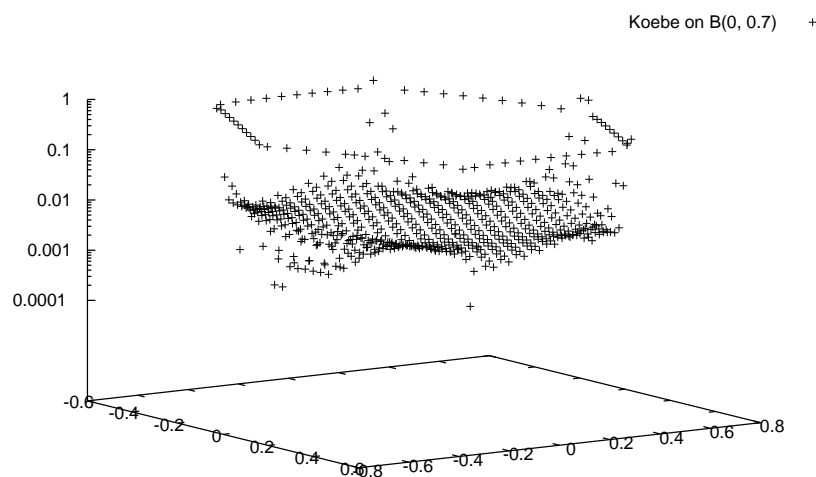


Figure 6.9: Face Averaged Schwarzian Approximation for the Koebe Function.
Relative error between analytic Schwarzian derivative is shown for the disc of radius 0.7.

Chapter 7

Maximal Packing Convergence

This chapter presents some empirical convergence data for the new circle packing algorithm. Example combinatoric structures were chosen to represent typical oriented triangulations of the disc encountered in practice.

7.1 Measures of Convergence

The primary measure of convergence in this section is the *angle sum* error. The covergens rates of the example packings were compiled by measuring the angle sum error after each iteration. Data is compiled for two conditions. In the first set of computations, the angle sum error's were tabulated after the completion of each iteration using the given combinatoric structure. In the second, the combinatoric structure was modified to an equivalent three boundary vertex case. Figure 7.1 shows an example conversion to the three boundary case for hexagonal combinatorics.

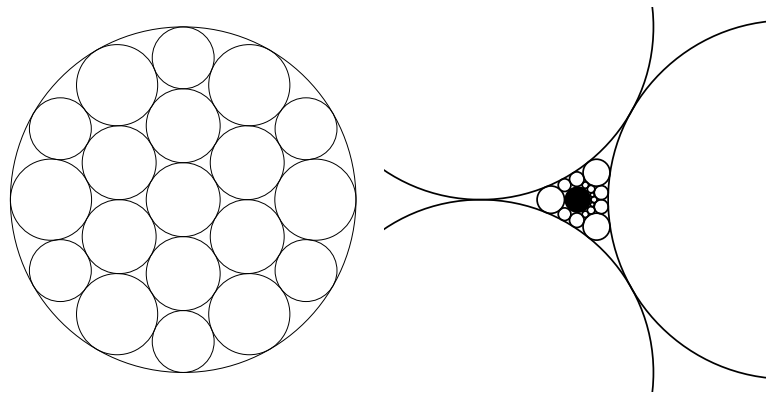


Figure 7.1: Example Three Boundary Conversion.
The added ideal vertex is marked for reference.

Experiments show that the error decrease approaches a linear factor for each iteration. The factor is expected to be dependent on the number of boundary vertexes and the interior

combinatoric structure – no theoretical estimates are known.

7.2 Example Packings

The example packings include various hexagonal and seven-degree packings as well as a few pseudo-random packings and a typical brain image data set. The example packings are shown in figure 7.2.

7.3 Convergence Data

The convergence data for the unmodified circle packing combinatorics are shown in figures 7.3 and the convergence data for the three boundary modified packings are shown in 7.4. The convergence examples demonstrate a reasonably clear dependence on the boundary vertex count.

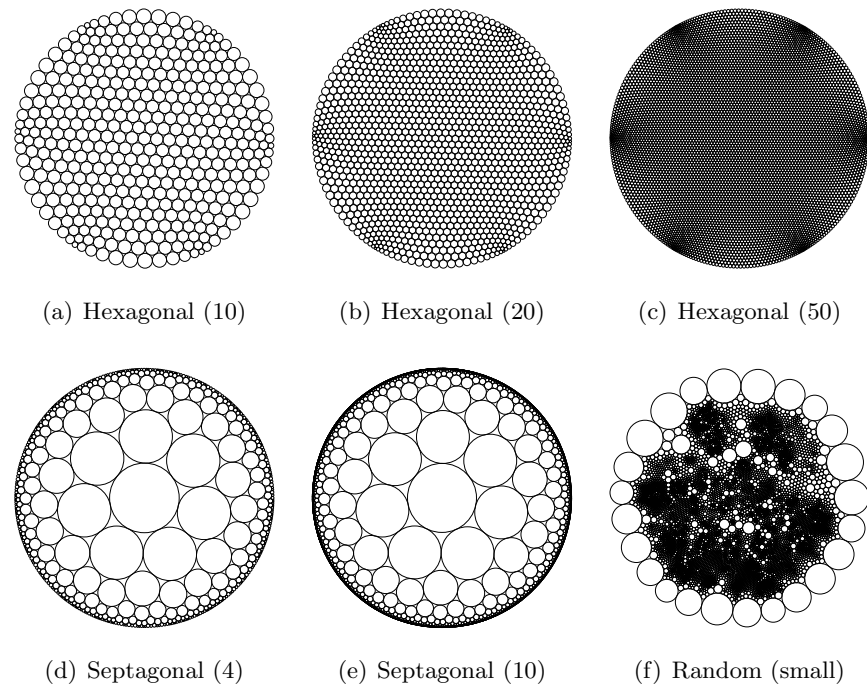


Figure 7.2: Example Circle Packings for Convergence Test.
(Large Random Packing and Brain Scan Packing not shown)

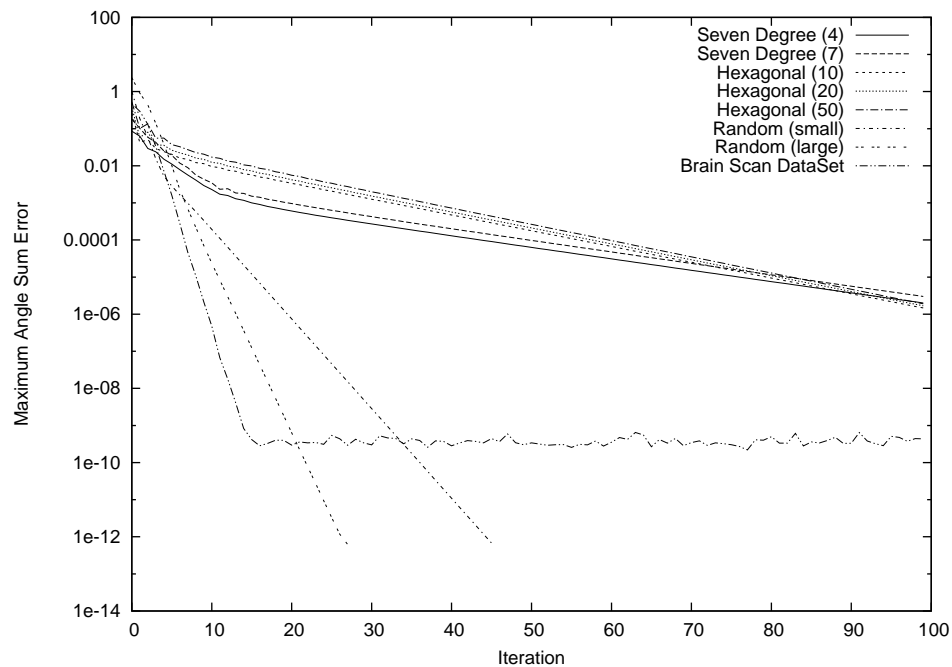


Figure 7.3: Convergence Data for Example Packings

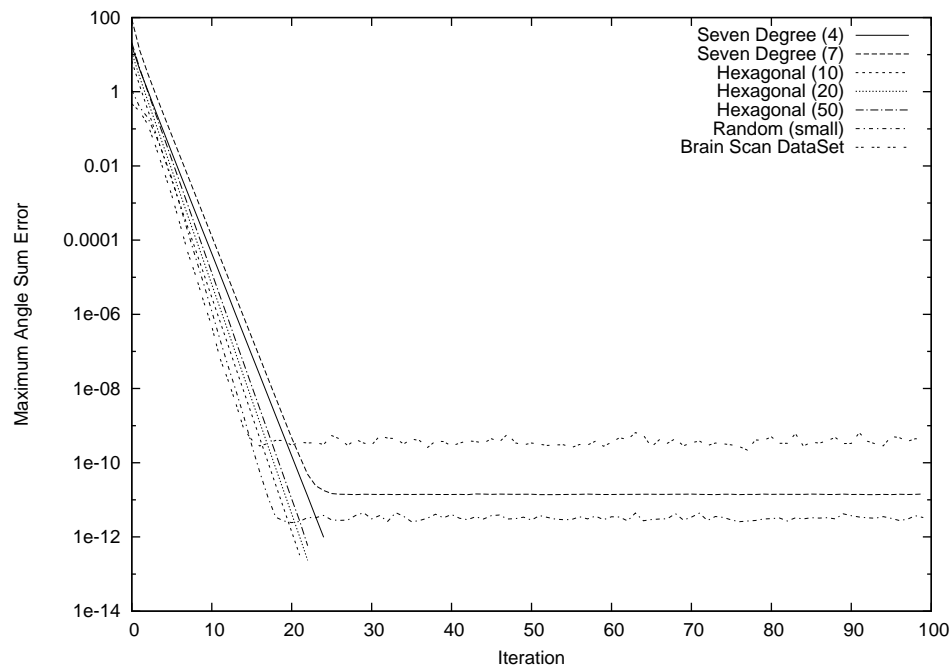


Figure 7.4: Convergence Data for Modified Example Packings

Bibliography

- Beardon, A. F. and Stephenson, K. (1990). The uniformization theorem for circle packings. *Indiana Univ. Math. J.*, 39:1383–1425.
- Beyer, W. H. (1987). *Standard Mathematical Tables*. Chemical Rubber Company, Florida.
- Bobenko, A. I. and Springborn, B. A. (2003). Variational principles for circle patterns and Koebe’s theorem. *Trans. Amer. Math. Soc.*, 356:659–689.
- Cannon, J. W. and W. J. Floyd, R. W. P. (2001). Finite subdivision rules. *Conformal Geometry and Dynamics*, 5:153–196.
- Collins, C. R., Driscoll, T. A., and Stephenson, K. (2003). Curvature flow in conformal mapping. *Comput. Methods Funct. Theory*, 3(1):325–347.
- Collins, C. R. and Stephenson, K. (2003). A circle packing algorithm. *Computational Geometry: Theory and Applications*, 25:233–256.
- Dubejko, T. (1993). *Branched Circle Packings, Discrete Complex Polynomials, and the Approximation of Analytic Functions*. PhD thesis, University of Tennessee, Knoxville (advisor: Kenneth Stephenson). Dissertation for the Universit of Tennessee, Knoxville.
- Dubejko, T. (1996–97). Circle-packing connections with random walks and a finite volume method. *Sémin. Théor. Spectr. Géom.*, 15:153–161.
- Dubejko, T. and Stephenson, K. (1995). Circle packing: Experiments in discrete analytic function theory. *Experimental Mathematics*, 4(4):307–348.
- G. H. Hardy, J. E. Littlewood, G. P. (1934). *Inequalities*. Cambridge, Cambridge.
- Gortler, S. and Craig Gotsman, D. T. (2006). Discrete one-forms on meshes and application to 3d mesh parameterization. *Elsevier Computer Aided Geometric Design* 23, 83-112.
- He, Z.-H. and Schramm, O. (1996). On the convergence of circle packings to the riemann map. *Inventiones mathematicae*, 125:285–305.
- Hille, E. (1922). *Americal Mathematical Society*, 28.

- Hurdal, M. K., Bowers, P. L., Stephenson, K., Sumners, D. W. L., Rehm, K., Schaper, K., and Rottenberg, D. A. (1999). Quasi-conformally flat mapping the human cerebellum. In Taylor, C. and Colchester, A., editors, *Medical Image Computing and Computer-Assisted Intervention - MICCAI'99*, volume 1679 of *Lecture Notes in Computer Science*, pages 279–286. Springer, Berlin.
- Hurdal, M. K. and Stephenson, K. (2004). Cortical cartography using the discrete conformal approach of circle packings. volume 23, Supplement 1, pages S119–S128.
- Hurdal, M. K., Stephenson, K., Bowers, P. L., Sumners, D. W. L., and Rottenberg, D. A. (2009). Cortical surface flattening: A quasi-conformal approach using circle packings.
- ling Lam, M. and hui Liu, Y. (10-14 April 2007). Heterogeneous sensor network deployment using circle packings. *Robotics and Automation, 2007 IEEE International Conference on*.
- Marden, A. (2007). *Outer Circles*. Cambridge, Cambridge.
- Nehari, Z. (1949). The schwarzian derivative and schlicht functions. *American Mathematical Society*, pages 545–551.
- Nehari, Z. (1975). *Conformal Mapping*. Dover Publications, inc., New York.
- Rodin, B. and Sullivan, D. (1987). The convergence of circle packings to the Riemann mapping. *J. Differential Geometry*, 26:349–360.
- Schwerdtfeger, H. (1979). *Geometry of Complex Numbers*. Dover Publications, inc., New York.
- Stephenson, K. (1990). Circle packings in the approximation of conformal mappings. *Bulletin, Amer. Math. Soc. (Research Announcements)*, 23, no. 2:407–415.
- Stephenson, K. (1992-2005a). *CirclePack* software. <http://www.math.utk.edu/~kens>.
- Stephenson, K. (2005b). *Introduction to Circle Packing*. New York.
- Thurston, W. (March 1985). The finite riemann mapping theorem. invited talk, an international symposium at purdue university on the occasion of the proof of the bieberbach conjecture.
- Tutte, W. T. (1962). Convex representations of graphs. *Proceedings London Mathematical Society*, 10(38):304–320.

Vita

Gerald Lee Orick Jr. was born in Painesville, Ohio. After completing his high school work he entered Park's College of St. Louis University, Missouri. He received a Bachelor of Science in Aerospace Engineering in April, 1990. After serving seven years in the United States Navy as a Submarine Warfare Office he then returned to the University of Missouri at Rolla to obtain a Masters of Science in Applied Mathematics in December, 2000. After a brief intermission he applied to the graduate school at the University of Tennessee at Knoxville and completed his graduate studies in May, 2010.